

1  
2  
3  
4  
5  
6  
7  
8  
9  
10  
11  
12  
13  
14  
15  
16  
17  
18  
19  
20  
21  
22  
23  
24  
25  
26  
27  
28  
29  
30  
31  
32  
33  
34  
35  
36  
37  
38  
39  
40  
41  
42  
43  
44  
45  
46  
47  
48  
49  
50  
51  
52  
53  
54  
55  
56  
57  
58  
59  
60

# Synthesis and Biological Evaluation of *N*-((1-(4-(Sulfonyl)piperazin-1-yl)cycloalkyl)methyl)benzamide Inhibitors of Glycine Transporter-1

Christopher L. Cioffi,<sup>\*,†,&</sup> Shuang Liu,<sup>\*,†,¥</sup> Mark A. Wolf,<sup>†</sup> Peter R. Guzzo,<sup>†,¥</sup> Kashinath Sadalpure,<sup>§,||</sup> Visweswaran Parthasarathy,<sup>§</sup> David T. J. Loong,<sup>§,#</sup> Jun-Ho Maeng,<sup>§</sup> Edmund Carulli,<sup>§</sup> Xiao Fang,<sup>§</sup> Karunakaran A. Kalesh,<sup>§</sup> Lakshman Matta,<sup>§</sup> Sok Hui Choo,<sup>§</sup> Shailijia Panduga,<sup>§</sup> Ronald N. Buckle,<sup>†</sup> Randall N. Davis,<sup>†</sup> Samuel A. Sakwa,<sup>†</sup> Priya Gupta,<sup>§</sup> Bruce J. Sargent,<sup>†</sup> Nicholas A. Moore,<sup>†,x</sup> Michele M. Luche,<sup>£</sup> Grant J. Carr,<sup>£</sup> Yuri L. Khmel'nitsky,<sup>¶</sup> Jiffry Ismail,<sup>¶</sup> Mark Chung,<sup>§</sup> Mei Bai,<sup>§</sup> Wei Yee Leong,<sup>§</sup> Nidhi Sachdev,<sup>§</sup> Srividya Swaminathan,<sup>§</sup> and Andrew J. Mhyre<sup>£,¶</sup>

<sup>†</sup>AMRI, Department of Medicinal Chemistry, East Campus, 3 University Place, Rensselaer, NY 12144, USA

<sup>§</sup>AMRI, Discovery Research and Development Chemistry Singapore Research Center, 61 Science Park Road, Science Park III, 117525, Singapore

<sup>¶</sup>AMRI, Drug Metabolism and Pharmacokinetics, East Campus, 17 University Place, Rensselaer, NY 12144, USA

<sup>£</sup>AMRI, Bothell Research Center, 22215 26th Ave SE, Bothell, WA 98021-4425, USA

**Abstract:** We previously disclosed the discovery of rationally designed *N*-((1-(4-(propylsulfonyl)piperazin-1-yl)cycloalkyl)methyl)benzamide inhibitors of glycine

1  
2  
3 transporter-1 (GlyT-1), represented by analogues **10** and **11**. We describe herein further  
4  
5 structure-activity relationship (SAR) exploration of this series via an optimization  
6  
7 strategy that primarily focused on the sulfonamide and benzamide appendages of the  
8  
9 scaffold. These efforts led to the identification of advanced leads possessing a desirable  
10  
11 balance of excellent *in vitro* GlyT-1 potency and selectivity, favorable ADME and *in vitro*  
12  
13 pharmacological profiles, and suitable pharmacokinetic (PK) and safety characteristics.  
14  
15 Representative analogue (+)-**67** exhibited robust *in vivo* activity in the cerebral spinal  
16  
17 fluid (CSF) glycine biomarker model in both rodents and non-human primates.  
18  
19 Furthermore, rodent microdialysis experiments also demonstrated that oral  
20  
21 administration of (+)-**67** significantly elevated extracellular glycine levels within the  
22  
23 medial prefrontal cortex (mPFC).  
24  
25  
26  
27  
28  
29  
30  
31  
32

### 33 ■ INTRODUCTION

34  
35  
36 The neurotransmitter glycine (**1**) (Figure 1) plays a key role in both inhibitory and  
37  
38 excitatory neurotransmission within the central nervous system (CNS). Glycine acts as  
39  
40 an endogenous agonist at the strychnine-sensitive glycine-A binding site of ionotropic  
41  
42 glycine receptors (GlyRs), which induce inhibitory post synaptic potentials (IPSPs) via Cl<sup>-</sup>  
43  
44 influx and membrane hyperpolarization.<sup>1, 2</sup> GlyRs are largely expressed within the  
45  
46 hindbrain and spinal cord where their respective interneurons facilitate sensory motor  
47  
48 learning, process sensory stimuli such as pain, relay reflex responses, and modulate  
49  
50 respiratory rates and rhythm patterns.<sup>3</sup>  
51  
52  
53  
54  
55  
56  
57  
58  
59  
60

1  
2  
3 Glycine, along with D-serine, also serves as an obligatory co-agonist that binds to the  
4 strychnine-insensitive glycine-B site located on the GluN1 sub-unit of *N*-methyl-D-  
5 aspartate (NMDA) receptors.<sup>4</sup> NMDA receptors are ligand and voltage-gated calcium  
6 permeable ionotropic glutamate receptors (iGluRs) involved in excitatory  
7 neurotransmission and CNS processes that underlie executive function, including long-  
8 term potentiation (LTP), long-term depression (LTD), and synaptic plasticity.<sup>5</sup> Activation  
9 of NMDA receptors relies on simultaneous binding of L-glutamate at the GluN2 sub-unit  
10 and obligatory co-agonist glycine or D-serine at the GluN1 sub-unit followed by  
11 expulsion of a magnesium block from the channel pore via membrane depolarization.<sup>4</sup>  
12  
13  
14  
15  
16  
17  
18  
19  
20  
21  
22  
23  
24

25  
26 Homeostatic glycine levels within the CNS are maintained via two high affinity  
27 transporters; GlyT-1 and glycine transporter-2 (GlyT-2).<sup>6</sup> Both transporters are of the  
28 Na<sup>+</sup>/Cl<sup>-</sup> solute carrier family 6 (SLC6), share an approximate 50% sequence homology,  
29 and present overlapping expression patterns within caudal areas of the CNS (e.g.,  
30 cerebellum, brainstem, and spinal cord). In addition, GlyT-1 is also expressed within the  
31 forebrain (e.g., hippocampus, striatum, and pre-frontal cortex (PFC))<sup>7</sup> and on amacrine,  
32 ganglion, and Muller cells within mammalian and non-mammalian retinae.<sup>8</sup>  
33  
34  
35  
36  
37  
38  
39  
40  
41  
42

43  
44 Within the GlyR-rich hindbrain, GlyT-1 is primarily expressed on glial astrocytes and is  
45 co-localized with GlyT-2, where it serves to modulate inhibitory neurotransmission by  
46 clearing glycine from the synaptic space surrounding the GlyRs. Thus, inhibition of GlyT-  
47 1 may lead to increased extracellular glycine levels with concomitant enhanced GlyR  
48 activity and inhibitory neurotransmission.<sup>9</sup> At excitatory glutamatergic synapses, GlyT-1  
49 is highly co-localized with NMDA receptors on both glial and neuronal cells where it  
50  
51  
52  
53  
54  
55  
56  
57  
58  
59  
60

1  
2  
3 tightly maintains synaptic glycine concentrations at sub-saturation levels.<sup>10</sup> Inhibition of  
4  
5  
6 GlyT-1 in these areas may lead to increased synaptic glycine levels and glycine-B site  
7  
8  
9 occupancy resulting in a potentiation of NMDA receptor function.<sup>11</sup> Thus, GlyT-1  
10  
11 inhibition can potentially lead to enhanced GlyR and/or NMDA receptor activity and the  
12  
13 approach has been under investigation to treat various CNS disorders that may be  
14  
15 ameliorated by modulation of either inhibitory glycinergic or excitatory glutamatergic  
16  
17 neurotransmission.  
18  
19

20  
21 Numerous structurally diverse GlyT-1 inhibitors have been disclosed, and  
22  
23 representatives of this class (e.g., **2**,<sup>12</sup> **3**,<sup>13</sup> **4**,<sup>14</sup> **5**,<sup>15</sup> **6**,<sup>16</sup> **7**,<sup>17</sup> **8**,<sup>18</sup> **9**<sup>19</sup>) are highlighted in  
24  
25 Figure 1. Due to the emergence of the NMDA receptor hypofunction hypothesis for  
26  
27 schizophrenia (i.e., the glutamate hypothesis),<sup>20</sup> selective inhibition of GlyT-1 became an  
28  
29 attractive approach to enhance NMDA receptor activity by increasing local synaptic  
30  
31 concentrations of glycine. Indeed, many of these agents were reported to be efficacious  
32  
33 in several *in vivo* models predictive of antipsychotic and pro-cognitive activity.<sup>21</sup> Several  
34  
35 GlyT-1 inhibitors entered clinical trials for the treatment of schizophrenia and the  
36  
37 approach enjoyed proof-of-concept in a series of Phase II trials<sup>22</sup>; however, a GlyT-1  
38  
39 inhibitor has yet to emerge as a novel antipsychotic available to treat patients.<sup>21, 23</sup>  
40  
41  
42  
43  
44  
45

46 GlyT-1 inhibition has also been studied in proof-of-concept clinical trials for other CNS  
47  
48 disorders including depression,<sup>24</sup> obsessive compulsive disorder (OCD),<sup>25</sup> and  
49  
50 addiction.<sup>26, 27</sup> Furthermore, GlyT-1 inhibitors have also demonstrated efficacy in animal  
51  
52 models of neuropathic pain,<sup>26, 28</sup> anxiety,<sup>29</sup> and epilepsy.<sup>30</sup> In addition, pre-clinical  
53  
54 studies have shown that the approach may also promote neuroprotection,<sup>31</sup> provide a  
55  
56  
57  
58  
59  
60

therapeutic strategy for autism spectrum disorders (ASDs),<sup>32</sup> and potentially present utility as an adjuvant treatment for symptomology associated Parkinson's disease.<sup>33</sup> Lastly, recent pre-clinical studies suggest that GlyT-1 inhibition may also prevent hypoxia-induced neuronal degeneration of the retina<sup>34</sup> as well as provide a novel approach for the treatment of hematological disorders such as sickle cell anemia.<sup>35</sup>

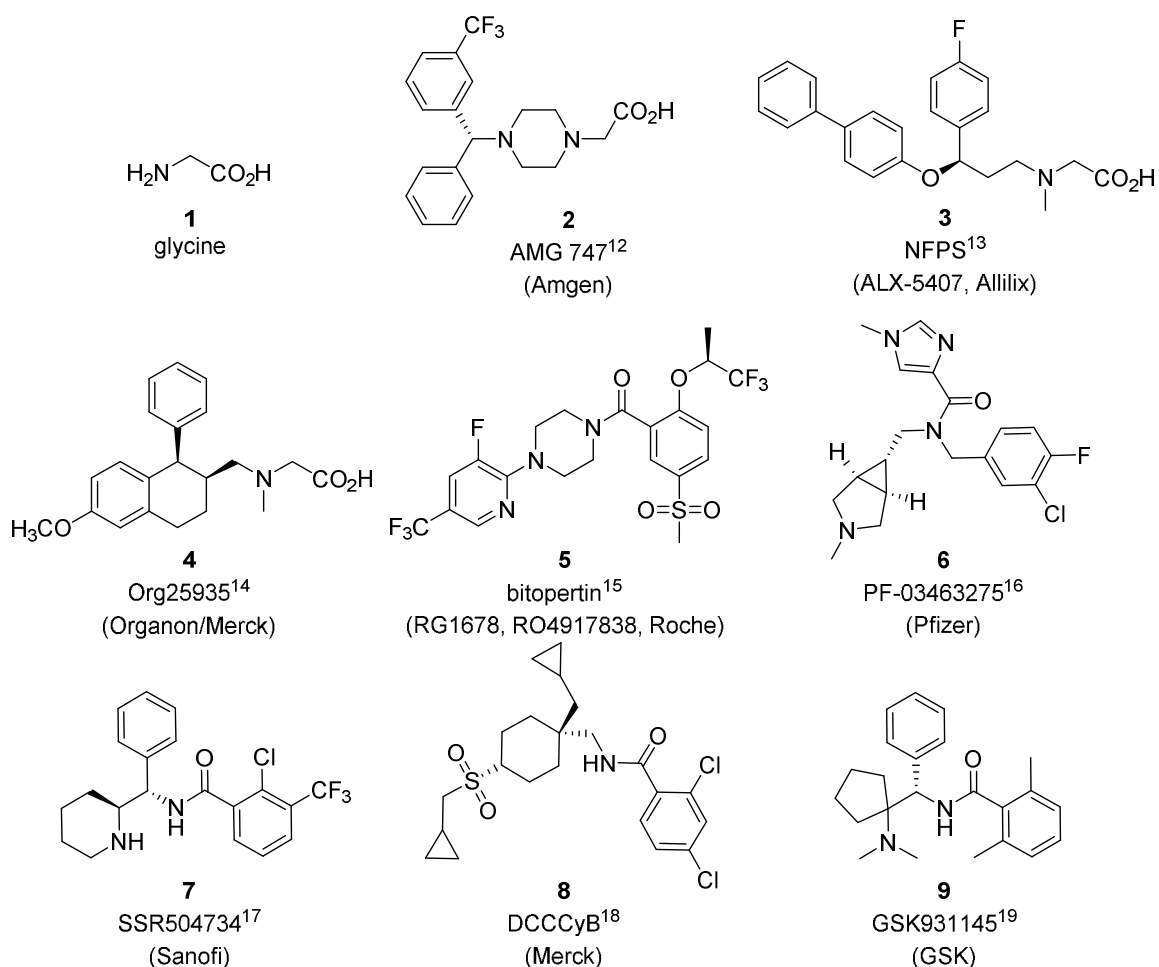


**Figure 1.** Representative GlyT-1 inhibitors.

1  
2  
3 We previously disclosed a novel series of *N*-((1-(4-(propylsulfonyl)piperazin-1-  
4 yl)cycloalkyl)methyl)benzamide GlyT-1 inhibitors derived from rationally designed hit **10**  
5 (Figure 2).<sup>36</sup> Subsequent SAR campaigns led to the identification of compound **11**, which  
6 possesses a favorable balance of *in vitro* GlyT-1 potency and selectivity, ADME and *in*  
7 *vitro* pharmacological properties, and pharmacokinetic (PK) characteristics in rat.  
8 Inhibitor **11** also provided *in vivo* proof-of-concept for the series by producing a dose-  
9 dependent increase in rat cerebral spinal fluid (CSF) glycine levels upon oral  
10 administration.<sup>36</sup> We report herein further refinement to our series whereby  
11 optimization efforts focused on the sulfonamide and benzamide regions of the scaffold.  
12 This strategy led to the identification of advanced lead compounds that exhibited  
13 exquisite *in vitro* GlyT-1 potency, favorable ADME profiles, desirable binding  
14 characteristics, and robust *in vivo* glycine elevation activity within the CNS of both  
15 rodents and non-human primates.  
16  
17  
18  
19  
20  
21  
22  
23  
24  
25  
26  
27  
28  
29  
30  
31  
32  
33  
34  
35  
36  
37  
38  
39  
40  
41  
42  
43  
44  
45  
46  
47  
48  
49  
50  
51  
52  
53  
54  
55  
56  
57  
58  
59  
60

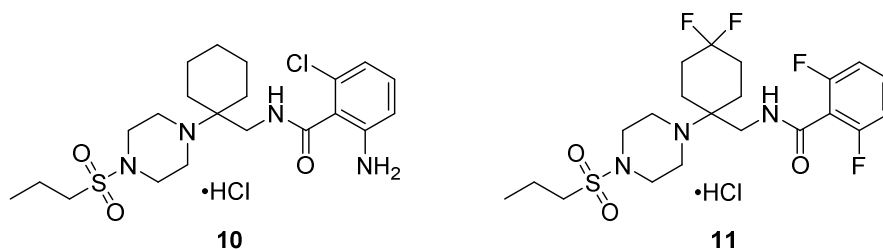
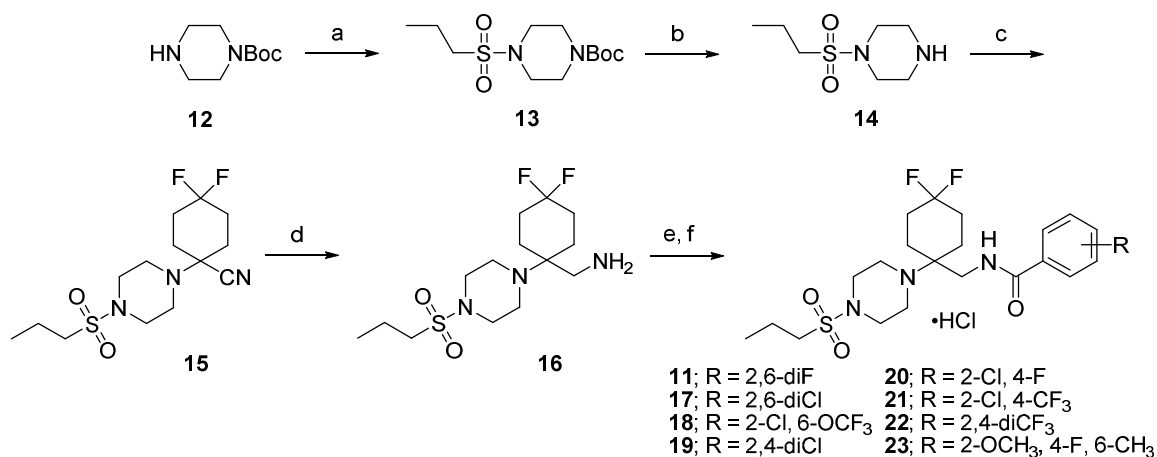


**Figure 2.** Previously reported *N*-((1-(4-(propylsulfonyl)piperazin-1-yl)cycloalkyl)methyl)benzamide GlyT-1 inhibitors **10** and **11**.

## ■ CHEMISTRY

The synthesis of *n*-propyl sulfonamide analogues **11** and **17–23** presented in Scheme 1 began with the sulfonylation of *tert*-butyl piperazine-1-carboxylate (**12**) followed by Boc-deprotection to afford *n*-propyl sulfonamide **14** in good yield.<sup>36, 37</sup> Strecker condensation between piperazine **14** and 4,4-difluorocyclohexanone in the presence of Et<sub>2</sub>AlCN and Ti(*i*-PrO)<sub>4</sub> furnished quaternary amino nitrile **15**, which was subsequently reduced with LiAlH<sub>4</sub> to provide aminomethyl intermediate **16**. The desired final compounds were readily manufactured via acylation of **16** with either the corresponding benzoyl chloride or benzoic acid, followed by treatment with aqueous HCl to give the corresponding hydrochloride salts.<sup>37</sup> The synthesis of 4-fluoro-2-methoxy-6-methylbenzoic acid, which was used to manufacture analogue **23**, was achieved following the route reported by Coulton and co-workers.<sup>38</sup>

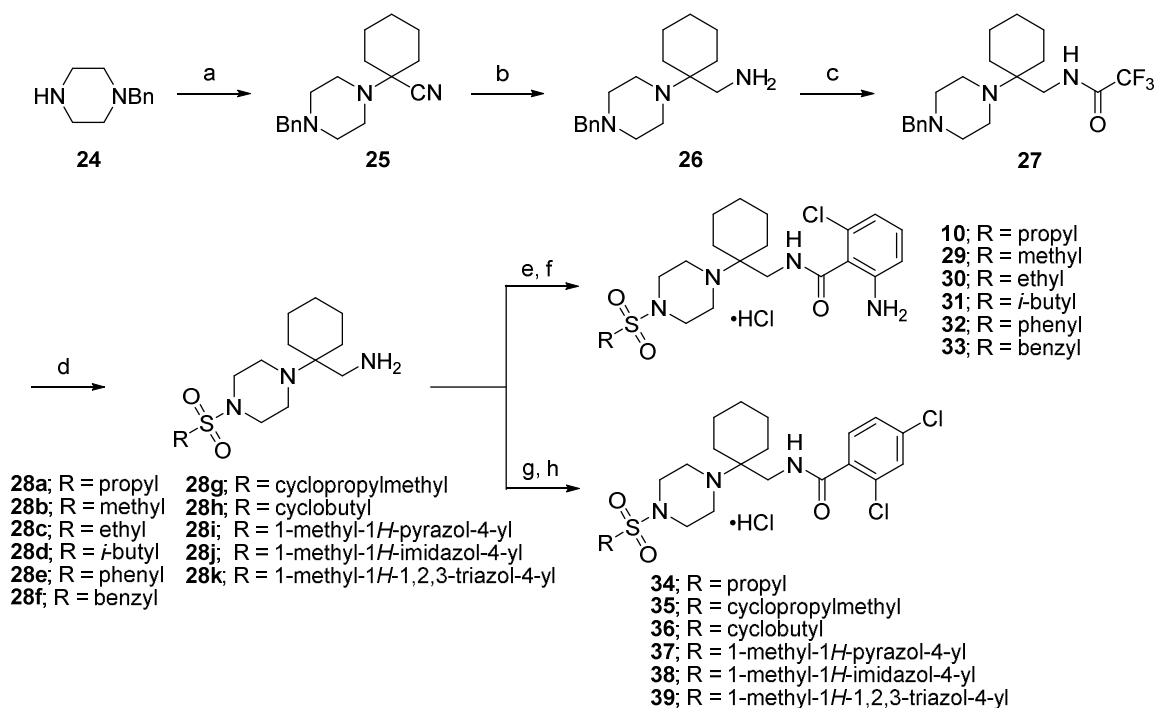
Scheme 1<sup>a</sup>



1  
2  
3 <sup>a</sup>Reagents and conditions: (a) 1-propanesulfonyl chloride, Et<sub>3</sub>N, CH<sub>2</sub>Cl<sub>2</sub>, 0 °C to rt, 3 h; (b), TFA,  
4 CH<sub>2</sub>Cl<sub>2</sub>, 0 °C to rt, 16 h; (c) 4,4-difluorocyclohexanone, Et<sub>2</sub>AlCN, Ti(*i*-PrO)<sub>4</sub>, toluene, 0 °C to rt for  
5 16 h; (d) LiAlH<sub>4</sub>, Et<sub>2</sub>O, 0 °C to rt, 12 h; (e) substituted benzoyl chloride, Et<sub>3</sub>N, CH<sub>2</sub>Cl<sub>2</sub>, 0 °C to rt, 4  
6 16 h; (f) LiAlH<sub>4</sub>, Et<sub>2</sub>O, 0 °C to rt, 12 h; (g) substituted benzoyl chloride, Et<sub>3</sub>N, CH<sub>2</sub>Cl<sub>2</sub>, 0 °C to rt, 4  
7 h; or substituted benzoic acid, EDCI•HCl, HOBT, Et<sub>3</sub>N, DMF, rt, 16 h; (h) 1.0 M HCl in H<sub>2</sub>O, CH<sub>3</sub>CN,  
8 0 °C to rt, 30 min.  
9  
10  
11  
12  
13  
14  
15  
16

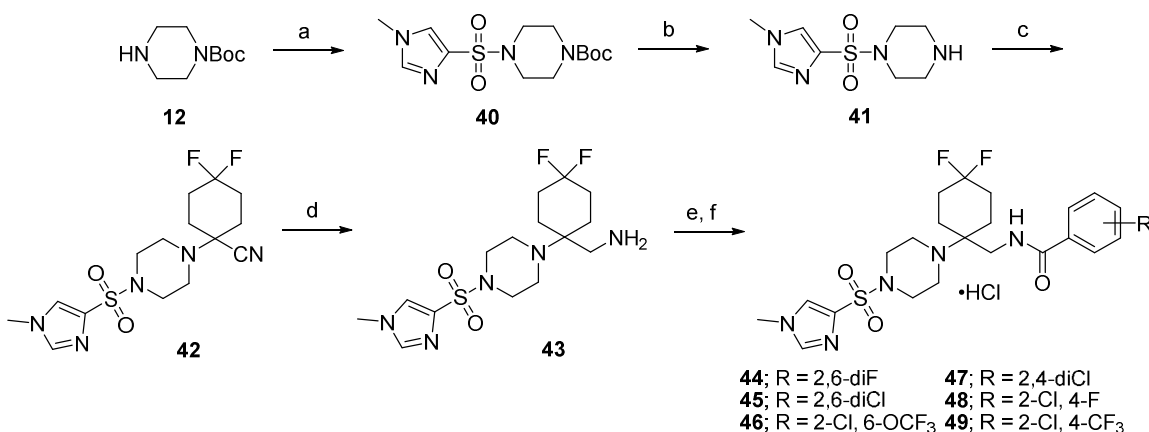
17 Scheme 2 highlights the synthetic routes used to access analogues **10** and **29–39**. A  
18 PTSA-mediated Strecker reaction between 1-benzylpiperazine (**24**) and cyclohexanone  
19 in the presence of KCN afforded amino nitrile **25** in good yield, which underwent  
20 smooth reduction with LiAlH<sub>4</sub> to provide aminomethyl intermediate **26**. Treatment of  
21 **26** with trifluoroacetic anhydride gave the trifluoroacetamide **27**. Advanced  
22 aminomethyl intermediates **28a–28k** were obtained via a three-step process that  
23 involved initial hydrogenolysis of **27** followed by sulfonylation of the resulting de-  
24 benzylated piperazine with the corresponding sulfonyl chlorides and subsequent  
25 hydrolysis of the trifluoroacetamide with K<sub>2</sub>CO<sub>3</sub> and H<sub>2</sub>O in refluxing CH<sub>3</sub>OH. Analogues  
26 **10** and **29–33** were then synthesized via an HBTU-mediated peptide coupling between  
27 precursor intermediates **28a–28f** and 2-amino-6-chlorobenzoic acid, followed by  
28 conversion to the hydrochloride salts in the presence of HCl. Compounds **34–39** were  
29 prepared via acylation of **28g–28k** with 2,4-dichlorobenzoyl chloride, followed by  
30 treatment with HCl to give the corresponding hydrochloride salts.<sup>37</sup>  
31  
32  
33  
34  
35  
36  
37  
38  
39  
40  
41  
42  
43  
44  
45  
46  
47  
48  
49  
50  
51  
52  
53  
54  
55  
56  
57  
58  
59  
60



Scheme 2<sup>a</sup>

<sup>a</sup>Reagents and conditions: (a) cyclohexanone, PTSA, KCN, H<sub>2</sub>O, rt, 16 h; (b) LiAlH<sub>4</sub>, Et<sub>2</sub>O, 0 °C to rt, 12 h; (c) trifluoroacetic anhydride, Et<sub>3</sub>N, CH<sub>2</sub>Cl<sub>2</sub>, 0 °C to rt, 16 h; (d) (i) 10% Pd/C, NH<sub>4</sub>HCO<sub>2</sub>, CH<sub>3</sub>OH, 65 °C, 3 h; (ii) substituted sulfonyl chloride, Et<sub>3</sub>N, CH<sub>2</sub>Cl<sub>2</sub>, 0 °C to rt, 1 h; (iii) K<sub>2</sub>CO<sub>3</sub>, H<sub>2</sub>O, CH<sub>3</sub>OH, reflux, 16 h; (e) 2-amino-6-chlorobenzoic acid, HBTU, Et<sub>3</sub>N, DMF, rt, 16 h; (f) 1.0 M HCl in Et<sub>2</sub>O, CH<sub>2</sub>Cl<sub>2</sub>, 0 °C to rt, 30 min; (g) 2,4-dichlorobenzoyl chloride, Et<sub>3</sub>N, CH<sub>2</sub>Cl<sub>2</sub>, 0 °C to rt, 16 h; (h) 10% HCl in H<sub>2</sub>O, CH<sub>3</sub>CN, 0 °C to rt, 30 min; or 1.0 M HCl in Et<sub>2</sub>O, Et<sub>2</sub>O, 0 °C to rt, 30 min.

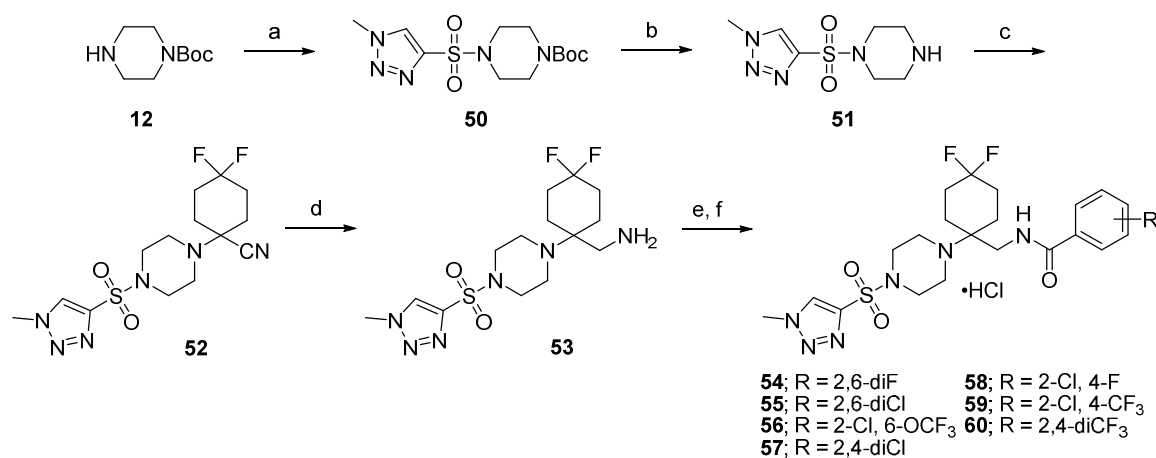
The synthesis of *N*-((4,4-difluoro-1-(4-((1-methyl-1H-imidazol-4-yl)sulfonyl)piperazin-1-yl)cyclohexyl)methyl)benzamide analogues **44–49** is depicted in Scheme 3. Sulfonylation of **12** with 1-methyl-1H-imidazole-4-sulfonyl chloride followed by Boc-deprotection afforded sulfonamide **41**, which provided amino nitrile **42** using the aforementioned Strecker conditions. LiAlH<sub>4</sub> reduction of **42** afforded aminomethyl intermediate **43**, which was used to manufacture **44–49** via acylation with the corresponding benzoyl chloride or benzoic acid using standard peptide coupling conditions followed by treatment with HCl to give the corresponding hydrochloride salts.<sup>37</sup>

Scheme 3<sup>a</sup>

<sup>a</sup>Reagents and conditions: (a) 1-methyl-1H-imidazole-4-sulfonyl chloride, Et<sub>3</sub>N, CH<sub>2</sub>Cl<sub>2</sub>, 0 °C to rt, 5 h; (b), 12 N HCl, 1,4-dioxane, 0 °C to rt, 2 h; (c) 4,4-difluorocyclohexanone, TMSCN, ZnI<sub>2</sub>, toluene, CH<sub>3</sub>OH, 0 °C then reflux for 4 h followed by rt for 16 h; (d) LiAlH<sub>4</sub>, THF, 0 °C to rt, 5 h; (e) substituted benzoyl chloride, Et<sub>3</sub>N, CH<sub>2</sub>Cl<sub>2</sub>, 0 °C to rt, 4 h; or substituted benzoic acid, EDCI•HCl, HOBT, Et<sub>3</sub>N, DMF, rt, 16 h; (f) 1.0 M HCl in H<sub>2</sub>O, CH<sub>3</sub>CN, 0 °C to rt, 30 min.

Construction of *N*-((4,4-difluoro-1-(4-((1-methyl-1*H*-1,2,3-triazol-4-yl)sulfonyl)piperazin-1-yl)cyclohexyl)methyl)benzamide analogues **54–60** was readily achieved following the route presented in Scheme 4. Sulfonylation of **12** with 1-methyl-1*H*-1,2,3-triazole-4-sulfonyl chloride<sup>37</sup> followed by subsequent Boc-deprotection and Strecker condensation with 4,4-difluorocyclohexanone in the presence of TMSCN and ZnI<sub>2</sub> provided amino nitrile **52**. Reduction of **52** with LiAlH<sub>4</sub> provided aminomethyl intermediate **53**, which was used to manufacture **54–60** via acylation with the corresponding benzoyl chloride or benzoic acid followed by treatment with HCl to give the corresponding hydrochloride salts.<sup>37</sup>

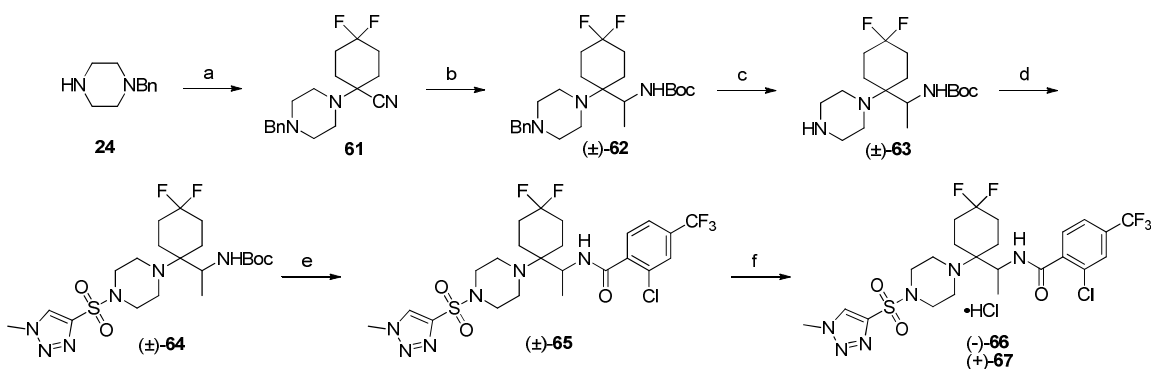
#### Scheme 4<sup>a</sup>



<sup>a</sup>Reagents and conditions: (a) 1-methyl-1*H*-1,2,3-triazole-4-sulfonyl chloride, Et<sub>3</sub>N, CH<sub>2</sub>Cl<sub>2</sub>, 0 °C to rt, 5 h; (b), TFA, CH<sub>2</sub>Cl<sub>2</sub>, 0 °C to rt, 16 h; (c) 4,4-difluorocyclohexanone, TMSCN, ZnI<sub>2</sub>, toluene, CH<sub>3</sub>OH, 0 °C then reflux for 4 h followed by rt for 16 h; (d) LiAlH<sub>4</sub>, THF, 0 °C to rt, 5 h; (e) substituted benzoyl chloride, Et<sub>3</sub>N, CH<sub>2</sub>Cl<sub>2</sub>, 0 °C to rt, 4 h; or substituted benzoic acid, EDCl•HCl, HOBt, Et<sub>3</sub>N, DMF, rt, 16 h; (f) 1.0 M HCl in H<sub>2</sub>O, CH<sub>3</sub>CN, 0 °C to rt, 30 min.

We also explored the potential impact that substitution at the methylene alpha to the benzamide NH would have on GlyT-1 potency and ADME properties for the series. The preparation of the methyl-substituted enantiomers (-)-**66** and (+)-**67** is shown in Scheme 5. Strecker condensation between **24** and 4,4-difluorocyclohexanone in the presence of  $\text{Et}_2\text{AlCN}$  and  $\text{Ti}(i\text{-PrO})_4$  afforded amino nitrile **61** in good yield. Nitrile **61** was subsequently treated with  $\text{CH}_3\text{Li}$  followed by  $\text{NaBH}_4$  reduction, and the resulting racemic amine was Boc-protected to give carbamate ( $\pm$ )-**62**.<sup>37</sup> Hydrogenolysis of ( $\pm$ )-**62** provided de-benzylated piperazine ( $\pm$ )-**63**, which was sulfonylated with 1-methyl-1H-1,2,3-triazole-4-sulfonyl chloride to afford sulfonamide ( $\pm$ )-**64** in good yield. HCl-promoted Boc-deprotection of ( $\pm$ )-**64** followed by HOBt-mediated peptide coupling of the resulting amine with 2-chloro-4-(trifluoromethyl)benzoic acid afforded racemic benzamide ( $\pm$ )-**65**. Racemic ( $\pm$ )-**65** was resolved via chiral preparatory HPLC to give the corresponding enantiomers (-)-**66** and (+)-**67**.<sup>37</sup>

### Scheme 5<sup>a</sup>



1  
2  
3  
4  
5  
6  
7  
8  
9  
10  
11  
12  
13  
14  
15  
16  
17  
18  
19  
20  
21  
22  
23  
24  
25  
26  
27  
28  
29  
30  
31  
32  
33  
34  
35  
36  
37  
38  
39  
40  
41  
42  
43  
44  
45  
46  
47  
48  
49  
50  
51  
52  
53  
54  
55  
56  
57  
58  
59  
60

<sup>a</sup>Reagents and conditions: (a) 4,4-difluorocyclohexanone, TMSCN, ZnI<sub>2</sub>, Et<sub>2</sub>O, CH<sub>3</sub>OH, toluene, rt for 4 h then reflux for 12 h; (b) (i) CH<sub>3</sub>Li (3.0 M in DME), reflux, 6 h; (ii) NaBH<sub>4</sub>, CH<sub>3</sub>OH, rt, 2 h; (iii) Boc<sub>2</sub>O, Et<sub>3</sub>N, CH<sub>2</sub>Cl<sub>2</sub>, rt, 5 h; (c) 10% Pd/C, NH<sub>4</sub>HCO<sub>2</sub>, CH<sub>3</sub>OH, reflux, 4 h; (d) 1-methyl-1H-1,2,3-triazole-4-sulfonyl chloride, Et<sub>3</sub>N, CH<sub>2</sub>Cl<sub>2</sub>, 0 °C to rt, 2 h; (e) (i) 12 N HCl, CH<sub>3</sub>OH, 0 °C to rt, 5 h; (ii) 2-chloro-4-(trifluoromethyl)benzoic acid, HOBt, EDCI·HCl, Et<sub>3</sub>N, DMF, rt, 16 h; (f) (i) resolution of the enantiomers via preparative chiral HPLC (Daicel 5 cm I.D. × 50 cm L, eluting with an isocratic mobile phase of 70% heptanes and 30% *i*-PrOH); (ii) 1.0 M HCl in H<sub>2</sub>O, CH<sub>3</sub>CN, 0 °C to rt, 30 min.

## ■ RESULTS AND DISCUSSION

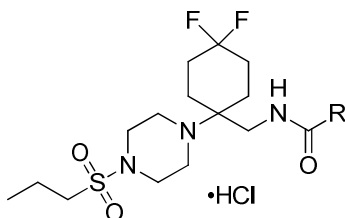
We previously conducted a rational design effort with the objective of identifying novel chemical matter that incorporated benzamide and sulfonamide functionality positioned within a pharmacophoric proximity relative to several reported GlyT-1 inhibitors. These efforts led to the discovery of 2-amino-6-chloro-*N*-((1-(4-(propylsulfonyl)piperazin-1-yl)cyclohexyl)methyl)benzamide **10**, which exhibited good *in vitro* potency (GlyT-1 IC<sub>50</sub> = 15.1 nM) and excellent selectivity versus GlyT-2 (GlyT-2 IC<sub>50</sub> > 75 μM).<sup>36</sup> Initial exploration of the benzamide SAR from hit **10** revealed that: 1) the benzamide NH was critical for potency (methylation of the benzamide nitrogen significantly diminished potency), 2) at least two substituents were required on the benzamide phenyl ring for appreciable potency, 3) optimal GlyT-1 potency required at least one substituent to be positioned *ortho* to the benzamide carbonyl, and 3) mono-substitution at the *meta* position was highly disfavored. These efforts led to the

1  
2  
3 discovery of highly potent GlyT-1 inhibitors, yet this initial series containing diverse  
4  
5 benzamide analogues suffered from poor metabolic stability in the presence of human  
6  
7 liver microsomes (HLM). Subsequent modifications to the central cyclohexyl ring  
8  
9 suggested that this region of the scaffold provided potential metabolic soft-spots for  
10  
11 CYP-mediated oxidation. Thus, installation of a 4,4-*gem*-difluoro moiety onto the central  
12  
13 cyclohexyl ring led to the discovery *N*-((4,4-difluoro-1-(4-(propylsulfonyl)piperazin-1-  
14  
15 yl)cyclohexyl)methyl)-2,6-difluorobenzamide **11**, which exhibited a favorable balance of  
16  
17 potency (GlyT-1 IC<sub>50</sub> = 67.5 nM), selectivity (GlyT-2 IC<sub>50</sub> > 75 μM), and significantly  
18  
19 improved HLM stability.<sup>36</sup> Compound **11** also provided *in vivo* proof-of-concept for the  
20  
21 series by inducing a dose-dependent increase in rat CSF glycine levels upon acute oral  
22  
23 administration of 20.8, 62.5, and 156.4 μmol/kg (10, 30, and 75 mg/kg).<sup>36</sup> The work  
24  
25 reported herein describes follow-up optimization efforts on the sulfonamide and  
26  
27 benzamide regions of analogues **10** and **11**, respectively. Key findings from both SAR  
28  
29 campaigns converged to provide optimized lead compounds, which were further  
30  
31 assessed for *in vivo* activity in rodents and non-human primates.  
32  
33  
34  
35  
36  
37  
38  
39  
40

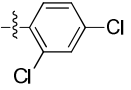
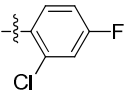
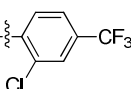
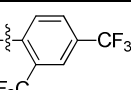
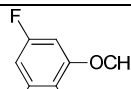
41 **Structure-Activity Relationships.** Guided by our previously reported SAR trends for  
42  
43 the original *N*-((1-(4-(propylsulfonyl)piperazin-1-yl)cycloalkyl)methyl)benzamide series,<sup>36</sup>  
44  
45 we sought to enhance the potency of analogue **11** while maintaining or improving its  
46  
47 favorable HLM metabolic stability by initially varying the benzamide component of the  
48  
49 scaffold while keeping the propyl sulfonamide in place. GlyT-1 potency and *in vitro*  
50  
51 human and rat microsomal intrinsic clearance data (CL<sub>int</sub>) for representatives of this  
52  
53 series are shown in Table 1. The SAR for this series revealed that potency trends  
54  
55  
56  
57  
58  
59  
60

mirrored that of the previously reported *N*-((1-(4-(propylsulfonyl)piperazin-1-yl)cycloalkyl)methyl)benzamide series; the most potent analogues featured two substituents on the benzamide phenyl ring with at least one substituent positioned *ortho* to the benzamide carbonyl and there was no potency differentiation between substituents possessing electron-donating (**23**) or electron-withdrawing (**11**, **17-22**) character. Furthermore, this sample set (and the series as a whole) continued to demonstrate excellent selectivity for GlyT-1 versus GlyT-2 (GlyT-2 IC<sub>50</sub> >75 μM). This campaign led to the discovery of key analogues **21** and **22**, which exhibited significantly improved GlyT-1 potency with comparable CL<sub>int</sub> values relative to **11**.

**Table 1. SAR of Representative *N*-((4,4-Difluoro-1-(4-(propylsulfonyl)piperazin-1-yl)cyclohexyl)methyl)benzamide Analogues**



Compound	R	GlyT-1 IC <sub>50</sub> (nM) <sup>a</sup>	Human CL <sub>int</sub> <sup>b</sup> (μL/min/mg)	Rat CL <sub>int</sub> <sup>b</sup> (μL/min/mg)
<b>11</b>		67.5 ± 5.4	13	5.5
<b>17</b>		42.4 ± 4.1	3.8	4.3
<b>18</b>		29.0	ND <sup>c</sup>	ND

19		36.4	37	27
20		38.4	ND	ND
21		12.6 ± 5.3	16	11
22		8.4 ± 1.5	19	4.9
23		28.5	ND	ND

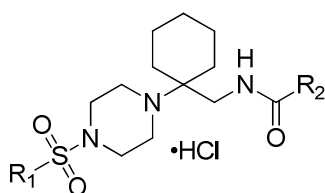
*In vitro* inhibitory GlyT-1 activity was determined using a whole-cell scintillation proximity assay (SPA).<sup>37</sup> The potency of each compound was assessed in inhibiting the uptake of radiolabeled glycine ([<sup>14</sup>C]glycine) using the human choriocarcinoma cell line, JAR cells (ATCC#HTB-144), which endogenously express human GlyT-1 (*hGlyT-1b*).<sup>a</sup>For those compounds that were only tested twice (*n* = 2), the IC<sub>50</sub> data is shown as the mean of two independent experiments. For compounds tested more than two times (*n* >2), the IC<sub>50</sub> data is represented as the mean ± standard deviation (SD).<sup>b</sup>Microsomes were incubated at 37 °C with the necessary cofactor regeneration system and individual test compounds at 3 μM. Reactions were terminated at 0, 5, 15, 30, 45, and 60 min time intervals in duplicate, and the amount of test compound remaining in the system was determined using LCMS quantitation. The residual compound remaining (%R) was determined by comparison to a zero time-point and the ln(%R) plotted vs. time. The slope was normalized to the protein content in the incubation reaction to determine the intrinsic clearance (CL<sub>int</sub>) value. Testosterone incubated at 10 μM was used as a standard. <sup>c</sup>ND = not determined.



1  
2  
3 Concurrent with our benzamide SAR efforts, we explored alternative sulfonamide  
4  
5  
6 appendages starting from benchmark analogues 2-amino-6-chloro-*N*-((1-(4-  
7  
8 (propylsulfonyl)piperazin-1-yl)cyclohexyl)methyl)benzamide (**10**, GlyT-1 IC<sub>50</sub> = 15.1 nM)  
9  
10 and 2,4-dichloro-*N*-((1-(4-(propylsulfonyl)piperazin-1-yl)cyclohexyl)methyl)benzamide  
11  
12 (**34**, GlyT-1 IC<sub>50</sub> = 22.7 nM). The results from this campaign revealed very narrow SAR for  
13  
14 this region of the scaffold, which is highlighted in Table 2. Truncating the sulfonamide *n*-  
15  
16 propyl chain to ethyl (**30**) led to a 5-fold decrease in potency relative to **10**, whereas  
17  
18 further truncation to methyl (**29**) led to a more significant diminishment in potency.  
19  
20 Introduction of bulkier *iso*-butyl (**31**), phenyl (**32**), or benzyl (**33**) sulfonamides was not  
21  
22 well tolerated and also led to significant losses of potency relative to parent **10**.  
23  
24 Interestingly, incorporation of a cyclopropylmethyl sulfonamide (**35**) resulted in a  
25  
26 modest 2-fold loss in potency relative to *n*-propyl comparator **34**, whereas cyclobutyl  
27  
28 (**36**) induced a >10-fold loss in potency. Acknowledging previously disclosed GlyT-1  
29  
30 inhibitors,<sup>39</sup> we also explored five-membered heteroaromatic systems as potential  
31  
32 sulfonamide appendages within our series. Installation of 1-methyl-1*H*-pyrazole  
33  
34 sulfonamide (**37**) led to ~6-fold loss in potency relative to **34**, however incorporation of  
35  
36 1-methyl-1*H*-imidazole (**38**) or 1-methyl-1*H*-1,2,3-triazole (**39**) led to an approximate 10  
37  
38 to 20-fold improvement in GlyT-1 potency values, respectively. Interestingly, 2,6-  
39  
40 difluorobenzamide analogues containing a regioisomeric 2-methyl-2*H*-1,2,3-triazole- or  
41  
42 a des-methyl 1*H*-1,2,3-triazole-4-sulfonamide appendage exhibited a significant loss of  
43  
44 potency relative to 1-methyl-1*H*-1,2,3-triazole **39** (GlyT-1 IC<sub>50</sub> = 906.9 nM and 21.96 μM,  
45  
46 respectively; structures not shown). The encouraging GlyT-1 potency results obtained  
47  
48  
49  
50  
51  
52  
53  
54  
55  
56  
57  
58  
59  
60

for **38** and **39** were tempered by very poor *in vitro* HLM stability (5% remaining at 60 min and 0% remaining at 15 minutes, respectively). Thus, we explored a series of 1-methyl-1*H*-imidazole and 1-methyl-1*H*-1,2,3-triazole sulfonamide analogues that incorporated a central 4,4-*gem*-difluoro cyclohexyl ring while varying the benzamide region of the scaffold.

**Table 2. Sulfonamide SAR for Representative *N*-((1-(4-(Sulfonyl)piperazin-1-yl)cyclohexyl)methyl)benzamide Analogues**



Compound	R <sub>1</sub>	R <sub>2</sub>	GlyT-1 IC <sub>50</sub> (nM) <sup>a</sup>
<b>10</b>			15.1 ± 5.1
<b>29</b>	CH <sub>3</sub>		339 ± 171
<b>30</b>	CH <sub>2</sub> CH <sub>3</sub>		73.8 ± 1.9
<b>31</b>			952
<b>32</b>			2294
<b>33</b>			9363
<b>34</b>			22.7 ± 9.1

35			56.6 ± 15.6
36			319 ± 114
37			146
38			2.14
39			1.54

*In vitro* inhibitory GlyT-1 activity was determined using a whole-cell scintillation proximity assay (SPA).<sup>37</sup> The potency of each compound was assessed in inhibiting the uptake of radiolabeled glycine (<sup>14</sup>C]glycine) using the human choriocarcinoma cell line, JAR cells (ATCC#HTB-144), which endogenously express human GlyT-1 (*hGlyT-1b*). <sup>a</sup>For those compounds that were only tested twice (n = 2), the IC<sub>50</sub> data is shown as the mean of two independent experiments. For compounds tested more than two times (n >2), the IC<sub>50</sub> data is represented as the mean ± standard deviation (SD).

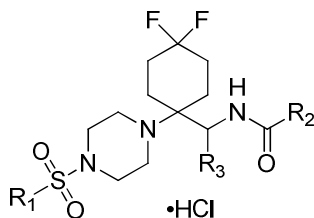
Table 3 captures GlyT-1 potency, HLM, and rat liver microsomal (RLM) metabolic stability data for a series of 1-methyl-1*H*-imidazole and 1-methyl-1*H*-1,2,3-triazole sulfonamide analogues that feature a central 4,4-*gem*-difluoro cyclohexyl ring and varying benzamides. Strategic benzamide SAR for these series incorporated substituents and substitution patterns that provided the most potent analogues within the aforementioned *N*-((4,4-difluoro-1-(4-(propylsulfonyl)piperazin-1-yl)cyclohexyl)methyl)benzamide series. Nearly all of these analogues displayed excellent

1  
2  
3 GlyT-1 potency, selectivity over GlyT-2 ( $IC_{50} > 75 \mu M$ ), and improved HLM metabolic  
4 stability relative to parent compounds **38** and **39**. Analogues **45–60** exhibited low single  
5 digit nanomolar to sub-nanomolar potency, with the 1-methyl-1*H*-1,2,3-triazole  
6 sulfonamides **54–59** exhibiting an approximate 2-fold improvement in potency values  
7 relative to their 1-methyl-1*H*-imidazole sulfonamide congeners **44–49**. In addition,  
8 introduction of a methyl group alpha to the benzamide nitrogen was well tolerated,  
9 with racemic ( $\pm$ )-**65** exhibiting a GlyT-1  $IC_{50}$  value = 1.03 nM. Interestingly, an  
10 enantiopreference was observed as chiral analogue (+)-**67** (GlyT-1  $IC_{50}$  = 1.06 nM) was  
11 approximately 30-fold more potent than its corresponding enantiomer (-)-**66** (GlyT-1  
12  $IC_{50}$  = 33.1 nM).

13  
14  
15  
16  
17  
18  
19  
20  
21  
22  
23  
24  
25  
26  
27  
28  
29  
30  
31  
32  
33  
34  
35  
36  
37  
38  
39  
40  
41  
42  
43  
44  
45  
46  
47  
48  
49  
50  
51  
52  
53  
54  
55  
56  
57  
58  
59  
60  
Due to its exquisite potency and favorable microsomal stability, emerging analogue  
(+)-**67** was chosen for further evaluation and the respective ADME and *in vitro*  
pharmacological profile is captured in Table 4. Compound (+)-**67** exhibited moderate  
thermodynamic (shake flask) solubility, favorable  $CL_{int}$  values (human, rat, and  
cynomolgus monkey), and no significant off-target activity at the hERG channel, CYPs, or  
within a standard panel of 69 GPCRs, ion channels, enzymes, and transporters (data not  
shown). Lastly, (+)-**67** exhibited favorable lipophilicity ( $cLogP = 3.40$ ) and the compound  
was classified as highly permeable in a standard Caco-2 permeability assay (efflux ratio =  
2).

Table 3. SAR of Representative 1-Methyl-1H-imidazole and 1-Methyl-1H-1,2,3-triazole

## Sulfonamide GlyT-1 Inhibitors



Compound	R <sub>1</sub>	R <sub>2</sub>	R <sub>3</sub>	GlyT-1 <sup>a</sup> IC <sub>50</sub> (nM)	% Remaining <sup>b</sup> HLM <sup>c</sup> , RLM <sup>d</sup>
44			H	18.3 ± 5.7	72, 92
45			H	5.56	22, 94
46			H	1.49	9.2, 91
47			H	5.29	30, 88
48			H	5.09 ± 0.94	85, 100
49			H	2.35	60, 90
54			H	5.10 ± 1.0	64, 95

55			H	1.27 ± 0.05	33, 91
56			H	0.726	24, 87
57			H	1.24	46, 80
58			H	1.14 ± 0.19	69, 100
59			H	0.671 ± 0.19	60, 85
60			H	0.733 ± 0.16	64, 95
(±)-65			CH <sub>3</sub>	1.03	54, 66
(-)-66			CH <sub>3</sub>	33.1	51 (HLM)
(+)-67			CH <sub>3</sub>	1.06 ± 0.38	74, 76

*In vitro* inhibitory GlyT-1 activity was determined using a whole-cell scintillation proximity assay (SPA).<sup>37</sup> The potency of each compound was assessed in inhibiting the uptake of radiolabeled glycine ([<sup>14</sup>C]glycine) using the human choriocarcinoma cell line, JAR cells (ATCC#HTB-144), which endogenously express human GlyT-1 (*hGlyT-1b*).<sup>a</sup>For those compounds that were only tested twice (*n* = 2), the IC<sub>50</sub> data is shown as the mean of two independent experiments. For compounds tested more than two times (*n* >2), the IC<sub>50</sub> data is represented as the mean ± standard deviation (SD).<sup>b</sup>Compound concentration was 3 μM and incubation time with the liver microsomes was 15 min. <sup>c</sup>HLM = human liver microsomes. <sup>d</sup>RLM = rat liver microsomes.

**Table 4. *In Vitro* ADMET Profile for GlyT-1 Inhibitor (+)-67**

Solubility <sup>a</sup>	CL <sub>int</sub> (μL/mL/min) <sup>b</sup>			CYP Inhibition (IC <sub>50</sub> ) 3A4, 2C9, 2D6, 2C19	hERG <sup>c</sup> (IC <sub>50</sub> )	%PPB <sup>d</sup>			Caco-2 Permeability (P <sub>app</sub> (x10 <sup>-6</sup> cm/sec))		tPSA <sup>e</sup>	cLogP <sup>e</sup>
	H	R	cyno			H	R	monkey	A-B	B-A		
22.2 μM	4	6	12	All > 7.2 μM	20.2 μM	88	87	81	23.9	47.4	94.03	3.40

<sup>a</sup>Thermodynamic (shake flask) solubility measured in PBS (pH= 7.4). <sup>b</sup>Intrinsic clearance. <sup>c</sup>Patch-Xpress' patch-clamp assay; compounds were tested (n = 3) in a five-point concentration-response on HE293 cells stably expressing the hERG channel. <sup>d</sup>%PPB = plasma protein binding; <sup>e</sup>t-PSA and cLogP values were determined by ChemDraw Ultra 12; H = human, R = rat, cyno = cynomolgus monkey.

**In Vivo Properties: PK Characteristics in Rat and Cynomolgus Monkeys.** The overall favorable *in vitro* attributes of (+)-**67** prompted us to further investigate its PK profile in rat and cynomolgus monkey (*Macaca fascicularis*) (Table 5). Single dose PK studies were conducted with Sprague Dawley rats at 3.1 μmol/kg (2 mg/kg) IV and 15.7 μmol/kg (10 mg/kg) PO and with cynomolgus monkeys at 1.5 μmol/kg (1 mg/kg) IV and 7.8 μmol/kg (5 mg/kg) PO. Compound (+)-**67** exhibited moderate CL and V<sub>ss</sub> values with good half-lives (t<sub>1/2</sub>) for both species. Maximal plasma concentrations (C<sub>max</sub>) of 352 ng/mL for rat and 105 ng/mL for cynomolgus monkey were achieved at 2.67 and 1.67 h post oral dose, respectively. The observed plasma exposures (AUC<sub>last</sub>) were good for both species, ranging between 1955 hr·ng/mL for rat and 690 hr·ng/mL for cynomolgus monkey, with resulting oral bioavailabilities (%F) of 27.2 and 31.0%, respectively.

**Table 5. Rat and Cynomolgus Monkey PK Parameters of (+)-67**

Species	Dose	CL <sup>a</sup>	C <sub>max</sub> <sup>b</sup> (ng/mL)	T <sub>max</sub> <sup>c</sup> (h)	T <sub>1/2</sub> <sup>d</sup> (h)	V <sub>ss</sub> <sup>e</sup>	AUC <sub>last</sub> <sup>f</sup> (hr•ng/mL)	%F <sup>g</sup>
Rat <sup>h</sup>	3.1 μmol/kg (IV) 15.7 μmol/kg (PO)	23.3 ± 2.83 (mL/min/kg)	352 ± 113	2.67 ± 2.89	4.33	1.75 ± 0.08 (L/Kg)	1955 ± 611	27.2 ± 8.5
Cyno <sup>j</sup>	1.5 μmol/kg (IV) 7.8 μmol/kg (PO)	1494 ± 219 (mL/h/kg)	105.0 ± 43.9	1.67 ± 0.58	6.27 ± 4.19	1929 ± 592 (mL/Kg)	690.0 ± 395.1	31.0 ± 21.1

Dosing groups consisted of three drug naïve adult male Sprague-Dawley rats or three female cynomolgus monkeys. Data represented as mean ± SD. <sup>a</sup>Total body clearance. <sup>b</sup>Maximum observed concentration of compound in plasma. <sup>c</sup>Time of maximum observed concentration of compound in plasma. <sup>d</sup>Apparent half-life of the terminal phase of elimination of compound from plasma. <sup>e</sup>Volume of distribution at steady state. <sup>f</sup>Area under the plasma concentration versus time curve from 0 to the last time point compound was quantifiable in plasma. <sup>g</sup>Bioavailability;  $F = (AUC_{INFPO} \times Dose_{IV}) \div AUC_{INFIV} \times Dose_{PO}$ . <sup>h</sup>IV formulation = 5% DMSO and 10% Solutol in saline; IV dosing volume = 5 mL/kg; PO formulation = 5% Solutol and 10% Captisol in 25 mM phosphate buffered saline (PBS; composition = 137 mM NaCl, 2.7 mM KCl, 4.3 mM Na<sub>2</sub>HPO<sub>4</sub>, 1.47 mM KH<sub>2</sub>PO<sub>4</sub>), pH adjusted to 2 with HCl. <sup>i</sup>IV formulation = 5% DMSO and 10% Solutol in saline, pH=6.5; IV dosing volume = 2 mL/kg. <sup>j</sup>PO formulation = 5% Solutol in 20% Captisol, 25 mM PBS, pH=2; PO dosing volume = 5 mL/kg.

***In Vivo* Activity: Rat CSF Glycine Biomarker Model.** Inhibition of GlyT-1 leads to elevated levels of extracellular glycine throughout the CNS, which spills over and pools within the CSF where it can be readily measured. The rat CSF glycine biomarker model allows for facile assessment of both *in vivo* GlyT-1 engagement and potential exposure-response relationships by providing both CSF glycine concentrations as well as drug exposure levels in plasma, brain, and CSF from a single study.<sup>40</sup> Encouraged by the



1  
2  
3 suitable PK characteristics observed for (+)-**67**, we initially studied the compound's  
4 effect on CSF glycine levels in an acute dose-response study with rats. Drug naïve  
5 Sprague Dawley rats were orally administered vehicle or (+)-**67** at four different doses  
6 (0.4, 1.5, 4.7, and 15.7  $\mu\text{mol/kg}$ ; 0.3, 1, 3, and 10  $\text{mg/kg}$ ) and CSF glycine levels were  
7 subsequently measured 2 h post. The rats were euthanized by  $\text{CO}_2$  asphyxiation and a  
8 hypodermic needle was inserted into the cisterna magna to withdraw 50–100  $\mu\text{l}$  of CSF.  
9 The CSF was diluted with deuterated-glycine as an internal standard and glycine levels  
10 were quantified by LC/MS/MS. As shown in Table 6, oral administration of (+)-**67**  
11 produced increases in rat CSF glycine levels relative to vehicle that were statistically  
12 significant at the 4.7 and 15.7  $\mu\text{mol/kg}$  doses, suggesting that the compound is engaging  
13 GlyT-1 *in vivo*. In addition, concentrations of (+)-**67** in plasma, brain, and CSF increased  
14 in a dose-dependent manner. Noteworthy, compound (+)-**67** exhibited statistically  
15 significant pharmacodynamic (PD) activity in this assay by inducing CSF glycine increases  
16 at the 4.7 and 15.7  $\mu\text{mol/kg}$  dose levels despite relatively low total brain-to-plasma (B/P)  
17 (0.2–0.1) and CSF-to-unbound plasma concentration ( $C_{\text{CSF}}/C_{\text{u,p}}$ ) ( $>0.1$ ) ratios. The  
18 observed low CNS exposure of (+)-**67** may be attributed to a combination of relatively  
19 high topological polar surface area (tPSA = 94.03) and molecular weight (MW = 599.01  
20 g/mol), which could be hindering passive permeability ( $P_{\text{app}}$ ) across the blood brain  
21 barrier (BBB). However, due to the high potency of the compound, the projected free  
22 drug concentrations in the CNS ( $C_{\text{u,b}}$  and  $C_{\text{CSF}}$ ) at the 4.7 and 15.7  $\mu\text{mol/kg}$  doses appear  
23 to equal or slightly exceed that required to significantly inhibit GlyT-1 as measured by  
24 the whole cell SPA assay (GlyT-1  $\text{IC}_{50}$  = 1.06 nM), leading to the observed CSF glycine  
25  
26  
27  
28  
29  
30  
31  
32  
33  
34  
35  
36  
37  
38  
39  
40  
41  
42  
43  
44  
45  
46  
47  
48  
49  
50  
51  
52  
53  
54  
55  
56  
57  
58  
59  
60

level elevation trend.<sup>41</sup> Furthermore, the dissociative half-life (residence time) of (+)-67 at GlyT-1 has not been established, thus it is unclear to what extent this factor may also be contributing to the observed CSF glycine elevation trends.<sup>42</sup> Transporter occupancy data has also not yet been determined.

**Table 6. Glycine Elevation in CSF and (+)-67 Concentrations in CSF, Brain, and Plasma 2 Hours Post Oral Dosing in Rat**

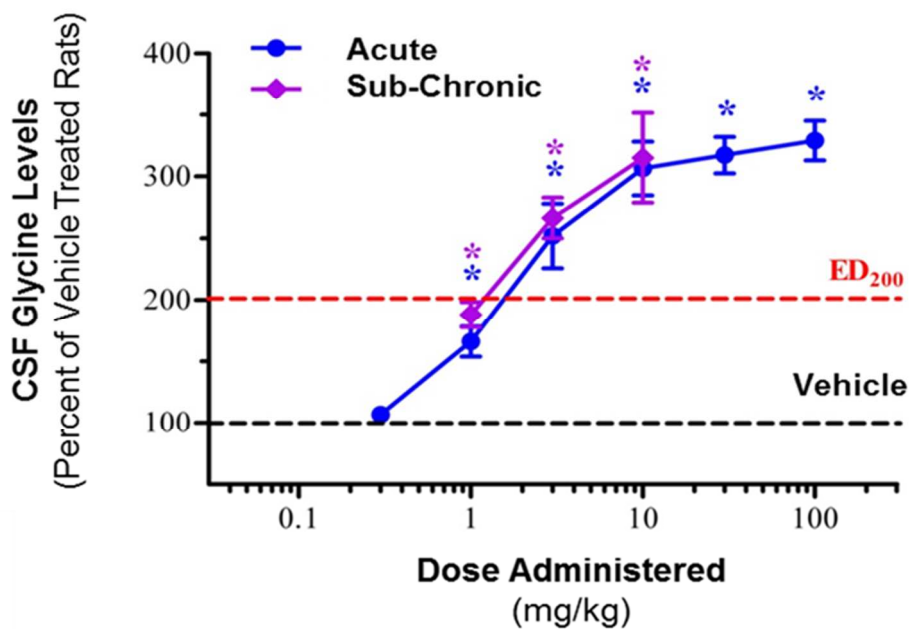
Dose (μmol/kg)	CSF Glycine (ng/mL)	% Vehicle Control CSF Glycine <sup>a</sup>	Concentration of (+)-67 (nM)		
			CSF	Brain	Plasma
0.4	470 ± 38.9	100.4 ± 8.3	bql <sup>b</sup>	3.2 ± 0.8	3.2 ± 0.5
1.5	558 ± 33.7	119.3 ± 7.2	0.1 ± 0.002	3.6 ± 0.4	11.4 ± 2.2
4.7	751 ± 44.0	160.5 ± 9.4*	0.5 ± 0.1	12.5 ± 4	52.2 ± 7.4
15.7	1528 ± 168.9	326.4 ± 36.1*	1.7 ± 0.3	32.2 ± 1.9	317.9 ± 49

Dosing groups consisting of drug naïve adult male Sprague-Dawley rats (n = 4–5/group). <sup>a</sup>CSF glycine is summarized by treatment group mean % vehicle control CSF glycine ± standard error of the mean (SEM); p < 0.05 vs. vehicle control. The CSF glycine level taken as 100% = 468.2 ± 27.3 ng/mL, which was obtained 30 min post vehicle dosing. Data were analyzed by 2-way ANOVA followed by Tukey's post-hoc test using JMP v.6.0 statistical software. \*Statistical significance; p < 0.05 versus vehicle control. Test article vehicle = 5% Solutol and 10% Captisol in 25 mM phosphate buffered saline (PBS; composition = 137 mM NaCl, 2.7 mM KCl, 4.3 mM

1  
2  
3 Na<sub>2</sub>HPO<sub>4</sub>, 1.47 mM KH<sub>2</sub>PO<sub>4</sub>), pH adjusted to 2 with HCl. <sup>b</sup>bql = below quantitation limit (1.0  
4 ng/mL).  
5  
6  
7  
8  
9

10 Analogous inhibitor **59**, which possesses an *in vitro* pharmacological and rodent *in vivo*  
11 CNS exposure profile similar to that of (+)-**67** (data not shown), was concurrently  
12 analyzed in the rat CSF glycine model in both an acute dose-response and subsequent 5-  
13 day sub-chronic oral dosing study in an effort to understand the potential effects of  
14 chronic exposure on PD. Figure 3 presents CSF glycine elevation (as % versus vehicle)  
15 and drug exposure levels of **59** (CSF, brain, and plasma) obtained from both studies. In  
16 the acute dose-response study, drug naïve Sprague Dawley rats were administered oral  
17 dose of vehicle or **59** (0.4, 1.6, 4.8, 16.1, 48.2, and 160.9 μmol/kg; 0.3, 1, 3, 10, 30, and  
18 100 mg/kg) and then sacrificed 2 h post dose. As shown in Figure 3A, **59** produced  
19 increases in CSF glycine levels that were statistically significant from vehicle control in  
20 the 1.6 to 160.9 μmol/kg dose range. The study demonstrated that similar to (+)-**67**,  
21 analogue **59** also possesses excellent *in vivo* potency, as the effective oral dose required  
22 to double CSF glycine levels relative to vehicle (ED<sub>200</sub>) lies between 1.6 and 4.8 μmol/kg.  
23 The CSF, brain, and plasma exposure levels of **59** also increased in the 0.4 to 16.1  
24 μmol/kg dose group (Figure 3B). Drug exposure levels did not increase in a dose-  
25 dependent fashion from the 48.2 to 160.9 μmol/kg doses, which may be attributed to  
26 oral absorption limitations due to the moderate solubility of the compound (shake flask  
27 solubility = 9.9 μM). In a subsequent sub-chronic dosing study, drug naïve Sprague  
28 Dawley rats were administered vehicle or an oral dose of **59** (1.6, 4.8, or 16.1 μmol/kg)  
29  
30  
31  
32  
33  
34  
35  
36  
37  
38  
39  
40  
41  
42  
43  
44  
45  
46  
47  
48  
49  
50  
51  
52  
53  
54  
55  
56  
57  
58  
59  
60

once daily (QD) over a 5-day period. The animals were then sacrificed 2 or 48 h post last-dose. The observed CSF glycine elevations for the cohorts sacrificed 2 h post last-dose were comparable to those observed for the same dose levels in the acute dose-response study (1.6, 4.8, and 16.1  $\mu\text{mol}/\text{kg}$ ), indicating that no tolerance for **59** had occurred. In addition, drug exposure levels for the animals sacrificed 2 h post last dose were within a 2-fold range of those observed for the same dose levels in the acute study, suggesting that there was no significant accumulation of **59** over the 5-day QD dosing period. CSF glycine levels returned to baseline 48 h post last-dose for all three dose groups, demonstrating that the effect of **59** was reversible (data not shown). Lastly, no gross behavioral abnormalities with the animals were noted for either the acute dose-response study or throughout the duration of the sub-chronic dosing study.

**A****B**

CSF Glycine Study	Dose ( $\mu\text{mol/kg}$ )	CSF Glycine (ng/mL)	% Vehicle Control CSF Glycine	Concentration of 59 (nM)		
				CSF	Brain	Plasma
Acute	0.4	432.8 $\pm$ 18.3	106.6 $\pm$ 4.0	2.7 $\pm$ 0.2	7.5 $\pm$ 2.3	18 $\pm$ 4.0
	1.6	673.8 $\pm$ 55.7	166.0 $\pm$ 12.3*	3.7 $\pm$ 0.3	13.1 $\pm$ 0.9	76.9 $\pm$ 17.7
	4.8	1022.4 $\pm$ 117.9	251.8 $\pm$ 26.0*	4.0 $\pm$ 0.4	39.2 $\pm$ 7.9	203.8 $\pm$ 55.6
	16.1	1244.0 $\pm$ 99.0	306.4 $\pm$ 21.8*	7.5 $\pm$ 0.8	64.9 $\pm$ 2.0	432.2 $\pm$ 60.4
	48.2	1288.0 $\pm$ 59.8	317.2 $\pm$ 14.7*	8.3 $\pm$ 1.1	66.8 $\pm$ 12.9	490 $\pm$ 103.3
	160.9	1336.0 $\pm$ 64.9	329.1 $\pm$ 16.0*	7.6 $\pm$ 0.6	46.3 $\pm$ 8.1	333.9 $\pm$ 71.9
Sub-Chronic (2 h post last dose)	1.6	980.0 $\pm$ 54.1	188.0 $\pm$ 10.4*	1.0 $\pm$ 0.1	21.0 $\pm$ 7.2	38.2 $\pm$ 4.7
	4.8	1388.0 $\pm$ 86.0	266.3 $\pm$ 16.5*	1.1 $\pm$ 0.1	44.8 $\pm$ 12.2	122.0 $\pm$ 21.2
	16.1	1642.0 $\pm$ 189.6	315.0 $\pm$ 36.4*	1.9 $\pm$ 0.3	69.4 $\pm$ 7.3	237.0 $\pm$ 28.2

**Figure 3.** (A) The effects of compound **59** on the % increase of CSF glycine from vehicle control for both acute (0.4, 1.6, 4.8, 16.1, 48.2, and 160.9  $\mu\text{mol/kg}$ , PO; represented as blue) and sub-chronic dosing (1.6, 4.8, and 16.1  $\mu\text{mol/kg}$ , PO, QD, 5 days; represented as magenta). CSF glycine is summarized by treatment group mean % vehicle control CSF glycine  $\pm$  SEM;  $p < 0.05$  vs. vehicle control. The CSF glycine level taken as 100% for the acute study = 406.0  $\pm$  17.6 ng/mL, which was obtained 30 min post vehicle dosing. The CSF glycine level taken as 100% for the sub-chronic study = 521.2  $\pm$  21.5 ng/mL, which was obtained 2 h post last-dose after QD dosing of vehicle over 5 days. All dose-response curves were plotted using the software program SigmaPlot, version 11.0. Data were analyzed by 2-way ANOVA followed by Tukey's post-hoc test using JMP v.6.0 statistical software. Data are expressed as mean  $\pm$  SEM;  $n = 5$ /group for each study. (B) Exposure levels of **59** in CSF, brain, and plasma for both acute and sub-chronic dosing (data acquired at the 2 h time-point post last-dose). Data are expressed as

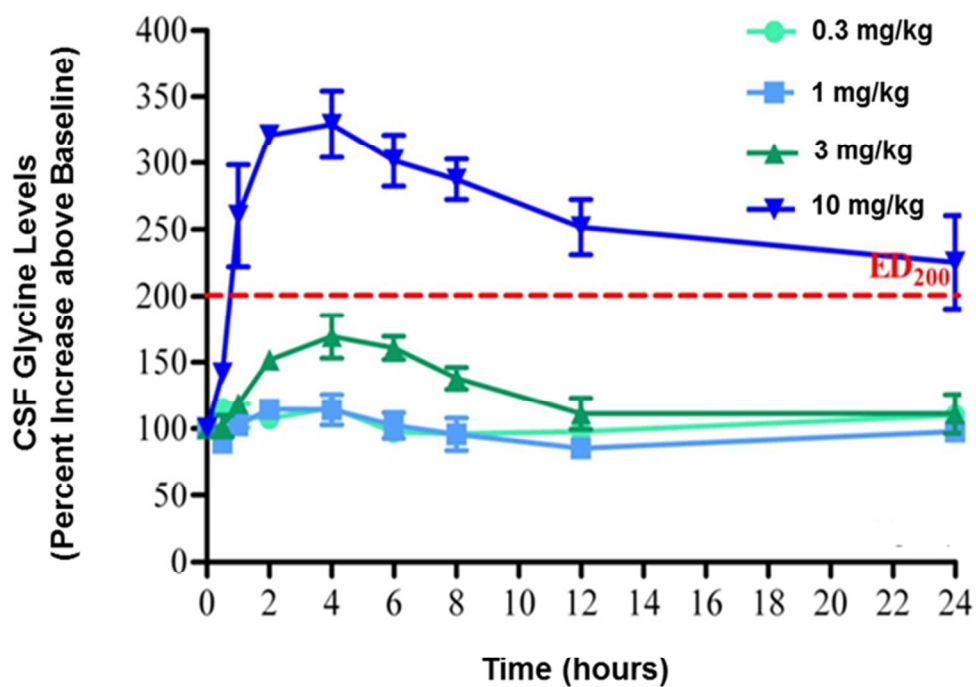
1  
2  
3 mean  $\pm$  SEM; n = 5/group. \*Statistical significance; p < 0.05 vs. vehicle control. Vehicle  
4  
5 preparation; 20 g of Captisol<sup>®</sup> was added to 100 mL of 25 mM PBS. The pH was lowered to 2 via  
6  
7 addition of HCl. The mixture was stirred for 30 minutes, or until dissolved and stored at 4°C  
8  
9 after use. Test article preparation; test compound was weighed and dissolved in Solutol (5% of  
10  
11 total volume). Once dissolved, the solution is quickly stirred with 20% Captisol in 25 mM PBS,  
12  
13 pH=2 as stipulated above to the final compound concentration. The solution is then sonicated  
14  
15 at room temperature for 20 min prior to dosing.  
16  
17  
18  
19  
20  
21  
22  
23

24 ***In Vivo* Activity: Cynomolgus Monkey CSF Glycine Biomarker Model.** Analogue (+)-  
25  
26 **67** was subsequently studied in an acute dose-response CFS glycine study in cynomolgus  
27  
28 monkeys. All of the animals used in the study were surgically prepared with indwelling  
29  
30 cannulae inserted into the cisterna magna and connected to a subcutaneous port to  
31  
32 permit cerebrospinal fluid sampling. CSF samples (approximately 0.30 mL) were  
33  
34 obtained using a sterile Huber needle inserted into the subcutaneous ports at the  
35  
36 following time-points in relation to dosing: pre-dose (0), 0.5, 1, 2, 3, 4, 8, 12 and 24 h  
37  
38 post dosing. Blood samples were also taken at these time points to assess drug exposure  
39  
40 levels in the plasma.  
41  
42  
43  
44  
45

46 (+)-**67** was orally administered over a dose range of 0.4, 1.5, 4.7, and 15.7  $\mu\text{mol}/\text{kg}$   
47  
48 and statistically significant increases in CSF glycine levels were observed for the 4.7 and  
49  
50 15.7  $\mu\text{mol}/\text{kg}$  doses (Figure 4A). Notably, the 15.7  $\mu\text{mol}/\text{kg}$  dose produced a robust  
51  
52 increase in glycine levels that exceeded 300% relative to vehicle control. Similar to rat,  
53  
54 (+)-**67** exhibited highly potent PD activity in the cynomolgus monkey with a CSF glycine  
55  
56  
57  
58  
59  
60

1  
2  
3 ED<sub>200</sub> residing between 4.7 and 15.7 μmol/kg. The highest CSF glycine elevation levels  
4  
5  
6 occurred between the 2 and 4 h time-points, which were trending back to baseline over  
7  
8  
9 the remainder of the 24 h time-course. In addition, the time-points correlating with  
10  
11 observed peak CSF glycine elevation track well with the (+)-**67** T<sub>max</sub> obtained from the  
12  
13 cynomolgus monkey PK study (1.67 h). Drug plasma exposure levels obtained in the CSF  
14  
15 glycine study for the 4.7 and 15.7 μmol/kg doses also increased in a dose-dependent  
16  
17 manner (Figure 4B), whereas drug levels for the 0.4 and 1.5 μmol/kg doses were below  
18  
19 detection limits (< 1.0 ng/mL). CSF drug exposure levels for the 15.7 μmol/kg dose group  
20  
21 were also measurable; however, exposure levels for the 0.4, 1.5, and 4.7 μmol/kg dose  
22  
23 groups were below detection limits. Similar to rat, a good correlation between (+)-**67**  
24  
25 exposure levels (plasma and CSF) and CSF glycine elevation was observed for the 15.7  
26  
27 μmol/kg dose throughout the study time-course. Lastly, no gross behavioral  
28  
29 abnormalities with the animals were observed throughout the duration of the study.  
30  
31  
32  
33  
34  
35

36 **A**  
37  
38  
39  
40  
41  
42  
43  
44  
45  
46  
47  
48  
49  
50  
51  
52  
53  
54  
55  
56  
57  
58  
59  
60



## B

Time-point (h)	Plasma Exposure of (+)-67 (ng/mL)				CSF Exposure of (+)-67 (ng/mL)	
	4.7 $\mu$ mol/kg dose	%CV	15.7 $\mu$ mol/kg dose	%CV	15.7 $\mu$ mol/kg dose	%CV
0.5	1.6 $\pm$ 0.6	34	67.9 $\pm$ 55.4	82	1.8	nc
1	3.6 $\pm$ 2.0	54	202.6 $\pm$ 170.5	84	5.9 $\pm$ 4.0	69
2	3.6 $\pm$ 2.3	63	221.7 $\pm$ 91.0	41	11.3 $\pm$ 6.0	53
3	5.7 $\pm$ 4.7	83	205.0 $\pm$ 117.0	57	11.3 $\pm$ 4.5	39
4	3.7 $\pm$ 2.4	66	224.3 $\pm$ 23.7	55	8.4 $\pm$ 2.3	43
8	2.0	nc <sup>a</sup>	156.3 $\pm$ 84.0	54	7.6 $\pm$ 1.6	30
12	bql <sup>b</sup>	nc	135.1 $\pm$ 53.4	40	5.0	32
24	bql	nc	10.3 $\pm$ 8.7	85	1.2	nc



1  
2  
3 **Figure 4.** (A) The effects of compound (+)-**67** at 0.4, 1.5, 4.7, and 15.7  $\mu\text{mol/kg}$  on CSF glycine  
4 levels in cynomolgus monkeys. Data are expressed as mean  $\pm$  SD; n = 3/group. (B)  
5  
6 Corresponding plasma exposure levels of (+)-**67** for the 4.7 and 15.7  $\mu\text{mol/kg}$  dosing groups  
7  
8 and CSF exposure levels for the 15.7  $\mu\text{mol/kg}$  dosing group. Plasma concentration data were  
9  
10 analyzed with WinNonlin 5.2 software. <sup>a</sup>nc = non-calculable. <sup>b</sup>bql = below quantitation limit (1.0  
11  
12 ng/mL). %CV = Coefficient of Variation. Vehicle preparation; 20 g of Captisol<sup>®</sup> was added to 100  
13  
14 mL of 25 mM PBS. The pH was lowered to 2 via addition of HCl. The mixture was stirred for 30  
15  
16 minutes, or until dissolved and stored at 4°C after use. Test article preparation; test compound  
17  
18 was weighed and dissolved in Solutol (5% of total volume). Once dissolved, the solution is  
19  
20 quickly stirred with 20% Captisol in 25mM PBS, pH=2 as stipulated above to the final compound  
21  
22 concentration. The solution is then sonicated at room temperature for 20 min prior to dosing.  
23  
24  
25  
26  
27  
28  
29  
30

31 ***In Vivo* Activity: Rat Medial Pre-Frontal Cortex Microdialysis Experiments.** We next  
32  
33 examined if (+)-**67** could also elevate extracellular glycine levels within the rat medial  
34  
35 prefrontal cortex (mPFC). Freely moving Sprague Dawley rats were given an oral gavage  
36  
37 of 1.5, 4.7, and 15.7  $\mu\text{mol/kg}$  of (+)-**67** and dialysate samples were taken from the mPFC  
38  
39 over a 5 h time-course, which were analyzed by HPLC and tandem mass spectrometry.  
40  
41 As shown in Figure 5, the mean normalized glycine levels within the rat mPFC were  
42  
43 significantly increased compared to basal levels (t = -80 to 0 min) from time-points t = 80  
44  
45 to 300 min for the 4.7 and 15.7  $\mu\text{mol/kg}$  dose groups ( $p < 0.001$ ). Notably, the 4.7 and  
46  
47 15.7  $\mu\text{mol/kg}$  doses increased the mean normalized glycine levels in a robust manner  
48  
49 (>150% of vehicle control basal levels) and glycine elevation was sustained out to 5 h.  
50  
51  
52  
53  
54  
55  
56  
57  
58  
59  
60

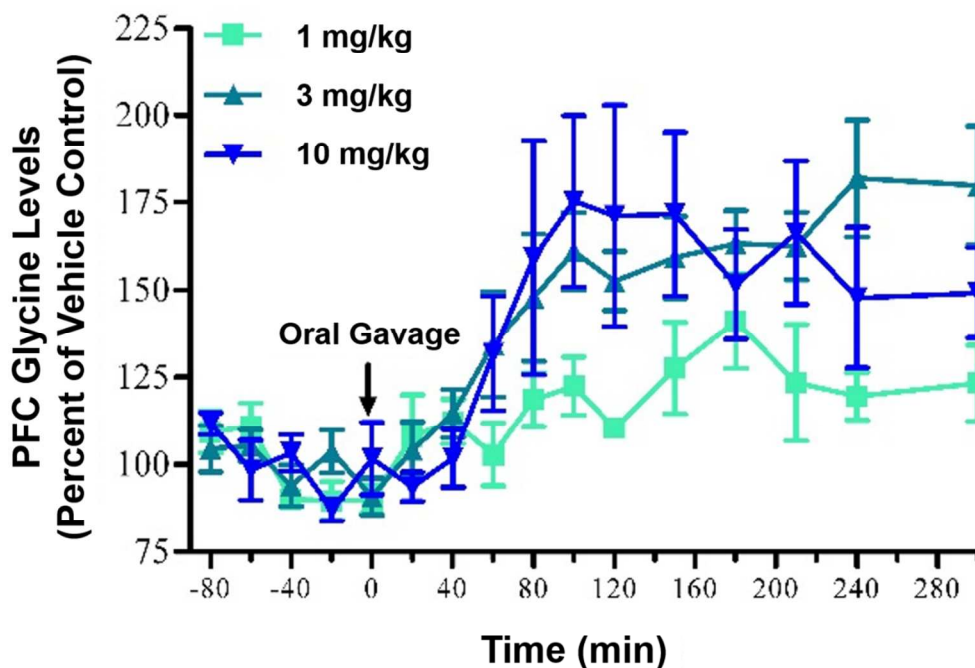


**Figure 5.** The effects of compound (+)-67 on the extracellular levels of glycine in the mPFC of freely moving drug naïve adult male Sprague-Dawley rats ( $n = 5$ ) administered by oral gavage of 1.5, 4.7, and 15.7  $\mu\text{mol/kg}$  (1, 3, and 10 mg/kg) at time = 0. Data are expressed as mean  $\pm$  SE;  $n = 5$  or 6/group. The mean normalized glycine levels were significantly increased compared to basal levels ( $t = -80$  to 0 min) from time points  $t = 80$  to 300 min ( $p < 0.001$ ) and glycine elevation was sustained over the 5 h time-course. Statistical analysis was performed using Sigmaxstat 3.2 for Windows (SPSS Corporation). Compound effects were compared, using two-way (time  $\times$  dose) ANOVA for repeated measurements followed by Student Newman Keuls post-hoc test. Vehicle preparation; 20 g of Captisol<sup>®</sup> was added to 100 mL of 25 mM PBS. The pH was lowered to 2 via addition of HCl. The mixture was stirred for 30 minutes, or until dissolved and stored at 4°C after use. Test article preparation; test compound was weighed and dissolved in Solutol (5% of total volume). Once dissolved, the solution is quickly stirred with 20% Captisol in 25 mM PBS, pH=2 as stipulated above to the final compound concentration. The solution is then sonicated at room temperature for 20 min prior to dosing.

1  
2  
3  
4  
5  
6       **Mechanism of Binding.** It has been suggested that competitive GlyT-1 inhibitors  
7  
8 might offer potential therapeutic advantages over non-competitive inhibitors as the  
9  
10 degree of competitive inhibition could potentially depend on physiological glycine  
11  
12 concentrations, whereas non-competitive inhibition would not.<sup>43</sup> Thus, competitive  
13  
14 inhibitors may provide more impactful inhibition in areas of the CNS where physiological  
15  
16 glycine concentrations are lower (i.e., forebrain). In addition, competitive inhibition is  
17  
18 potentially surmountable, which may circumvent potential mechanism-based adverse  
19  
20 events due to excessive and prolonged glycine elevation.<sup>43</sup> Employing similar Michaelis-  
21  
22 Menten saturation binding experiments reported by Mezler and co-workers,<sup>43</sup> we  
23  
24 assessed the mechanism of binding for (+)-**67** at GlyT-1. A series of glycine transport  
25  
26 experiments using a whole cell SPA assay with transfected HEK-293 cells expressing  
27  
28 GlyT-1 were conducted whereby changes in  $B_{max}$  and  $K_d$  values were measured by  
29  
30 increasing [<sup>3</sup>H]-glycine concentrations in the presence of varying concentrations of (+)-  
31  
32 **67** (Figure 6). Increasing concentrations of inhibitor (+)-**67** exhibited no effect on the  
33  
34  $B_{max}$  values for glycine whereas its  $K_d$  values increased, indicating that the compound  
35  
36 was competing with glycine for the same binding site at GlyT-1. Several additional  
37  
38 analogues within our series were also studied in these experiments and all of them were  
39  
40 confirmed to be competitive inhibitors of GlyT-1 (data not shown). In contrast,  
41  
42 increasing concentrations of the known non-competitive GlyT-1 inhibitor NFPS (ALX-  
43  
44 5407) (**3**), which has been reported to induce mechanism-based toxicity,<sup>44</sup> led to  
45  
46 changes in  $B_{max}$  values but did not alter the  $K_d$  values for glycine. These results confirm  
47  
48  
49  
50  
51  
52  
53  
54  
55  
56  
57  
58  
59  
60

that **3** is not competing with glycine for binding at GlyT-1, and these findings were consistent with previously reported data.<sup>44</sup>

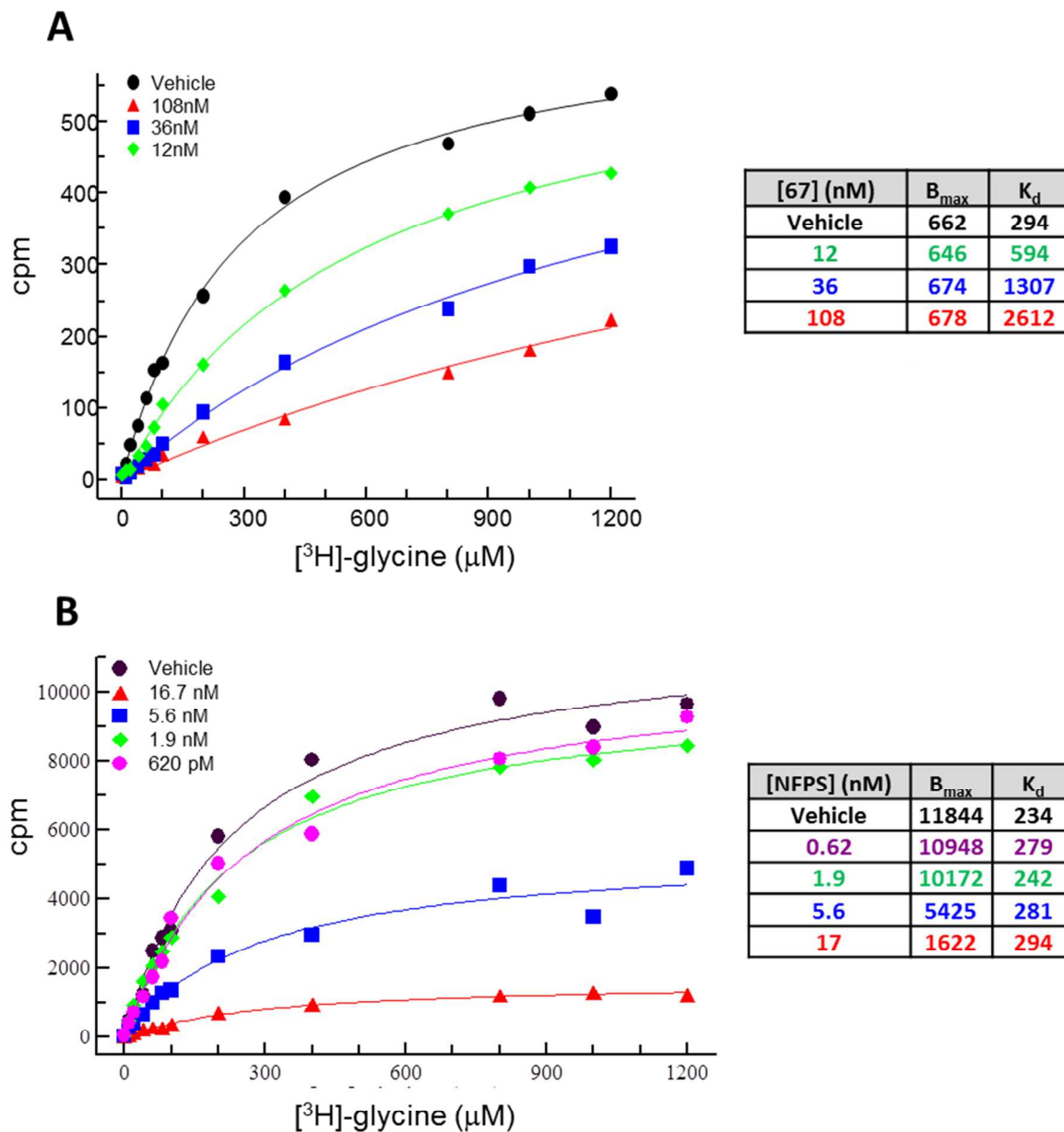


**Figure 6.** Determination of the mechanism of binding for compound (+)-**67**. A) Glycine transport experiments conducted whereby B<sub>max</sub> and K<sub>d</sub> values were obtained by increasing concentration of [<sup>3</sup>H]-glycine in the presence of varying concentrations of (+)-**67**. B) Glycine transport

1  
2  
3 experiments conducted whereby  $B_{\max}$  and  $K_d$  values were obtained by increasing concentration  
4 of [ $^3\text{H}$ ]-glycine in the presence of varying concentrations of **3**.  
5  
6  
7  
8  
9

## 10 ■ CONCLUSIONS

11  
12 Lead optimization efforts for our GlyT-1 inhibitor series began with benzamide SAR  
13 exploration starting from previously reported *N*-((4,4-difluoro-1-(4-  
14 (propylsulfonyl)piperazin-1-yl)cyclohexyl)methyl)benzamide **11**. These efforts led to the  
15 discovery of key inhibitors **21** and **22**, which were found to possess superior GlyT-1  
16 potency and comparable *in vitro* microsomal metabolic stability relative to parent **11**.  
17  
18 Concurrent with this campaign, sulfonamide SAR exploration of benchmark *N*-((1-(4-  
19 (propylsulfonyl)piperazin-1-yl)cyclohexyl)methyl)benzamide inhibitors **10** and **34** was  
20 conducted, which lead to the discovery of key *N*-methyl imidazole and triazole  
21 sulfonamide analogues **38** and **39**. Our sulfonamide SAR findings were converged with  
22 the benzamide SAR campaign to provide standout analogues **59** and (+)-**67**.  
23  
24  
25  
26  
27  
28  
29  
30  
31  
32  
33  
34  
35  
36  
37

38 Advanced lead (+)-**67** possesses a favorable balance of potency, ADME, and *in vitro*  
39 pharmacological profiles. The compound exhibited suitable rat and non-human primate  
40 PK characteristics and produced statistically significant elevations of CSF glycine levels  
41 for both species. In an acute dose-response rat CSF glycine study, analogues **59** and (+)-  
42 **67** induced dose-dependent and robust increases in glycine levels that correlated well  
43 with increasing plasma, brain, and CSF drug exposure levels. A subsequent 5-day sub-  
44 chronic dosing study with **59** revealed that CSF glycine elevation levels mirrored those  
45 observed in the acute dosing study at the same doses, suggesting that tolerance to the  
46  
47  
48  
49  
50  
51  
52  
53  
54  
55  
56  
57  
58  
59  
60

1  
2  
3 inhibitor had not occurred. In addition, exposures of **59** in the sub-chronic dosing study  
4  
5 were also similar to those observed in the acute study for the same doses, providing  
6  
7 evidence that there was no accumulation of the compound over the 5-day, QD dosing  
8  
9 period. Furthermore, CSF glycine levels returned to baseline after a 48 h washout period  
10  
11 for all dose groups, demonstrating that the effect of **59** was reversible.  
12  
13  
14

15  
16 The results obtained for the CSF glycine experiments prompted us to examine  
17  
18 whether analogues from our series were also capable of elevating glycine levels in the  
19  
20 mPFC, which is regarded as the putative site of action for neuropsychiatric disorders  
21  
22 such as schizophrenia. Indeed, microdialysis experiments showed that inhibitor (+)-**67**  
23  
24 produced robust increases in extracellular glycine levels within the mPFC of freely  
25  
26 moving Sprague Dawley rats, verifying that the compound is capable of engaging GlyT-1  
27  
28 in the forebrain.  
29  
30  
31

32  
33 Saturation binding experiments confirmed that compound (+)-**67** (in addition to  
34  
35 several other analogues within our series) is competitive with glycine for binding at  
36  
37 GlyT-1, demonstrating that the series possesses a differentiating and potentially  
38  
39 preferable mechanism of binding relative to non-competitive inhibitors such as NFPS  
40  
41 (ALX-5407) (**3**). In conclusion, we believe that analogues from our series of *N*-((4,4-  
42  
43 difluoro-1-(4-(sulfonyl)piperazin-1-yl)cyclohexyl)methyl)benzamide GlyT-1 inhibitors  
44  
45 possess favorable *in vitro* and *in vivo* profiles that may prove beneficial for the  
46  
47 treatment of the various neurological and neuropsychiatric disorders for which the field  
48  
49 has been reported to show promise.  
50  
51  
52  
53  
54

## 55 56 **EXPERIMENTAL SECTION**

57  
58  
59  
60

1  
2  
3  
4  
5       **General Chemistry.** All reactions were performed under a dry atmosphere of  
6  
7 nitrogen unless otherwise specified. Indicated reaction temperatures refer to the  
8  
9 reaction bath, while room temperature (rt) is noted as 25 °C. Commercial grade  
10  
11 reagents and anhydrous solvents were used as received from vendors and no attempts  
12  
13 were made to purify or dry these components further. Removal of solvents under  
14  
15 reduced pressure was accomplished with a Buchi rotary evaporator at approximately 28  
16  
17 mm Hg pressure using a Teflon-linked KNF vacuum pump. Thin layer chromatography  
18  
19 was performed using 1" x 3" AnalTech No. 02521 silica gel plates with fluorescent  
20  
21 indicator. Visualization of TLC plates was made by observation with either short wave  
22  
23 UV light (254 nm lamp), 10% phosphomolybdic acid in ethanol or in iodine vapors.  
24  
25 Preparative thin layer chromatography was performed using Analtech, 20 x 20 cm, 1000  
26  
27 micron preparative TLC plates. Flash column chromatography was carried out using a  
28  
29 Teledyne Isco CombiFlash Companion Unit with RediSep® Rf silica gel columns. If  
30  
31 needed, products were purified by reverse phase chromatography, using a Teledyne  
32  
33 Isco CombiFlash Companion Unit with RediSep® Gold C18 reverse phase column. Proton  
34  
35 NMR spectra were obtained either on a 300 MHz, 400 MHz, or a 500 MHz Bruker  
36  
37 Nuclear Magnetic Resonance Spectrometer and chemical shifts ( $\delta$ ) are reported in parts  
38  
39 per million (ppm), coupling constant ( $J$ ) values given in Hz, and with the following  
40  
41 spectral pattern designations: s, singlet; d, doublet; t, triplet, q, quartet; dd, doublet of  
42  
43 doublets; m, multiplet; br, broad. Tetramethylsilane (TMS) was used as an internal  
44  
45 reference. Melting points are uncorrected and were obtained using a MEL-TEMP  
46  
47 Electrothermal melting point apparatus. Mass spectroscopic analyses were performed  
48  
49  
50  
51  
52  
53  
54  
55  
56  
57  
58  
59  
60

1  
2  
3 using the following: 1) ESI ionization on a Varian ProStar LCMS with a 1200L quadrapole  
4 mass spectrometer; 2) ESI, APCI, or DUIS ionization on a Shimadzu LCMS-2020 single  
5 quadrapole mass spectrometer. High pressure liquid chromatography (HPLC) purity  
6 analysis was performed using the following: 1) Varian Pro Star HPLC system with a  
7 binary solvent system A and B using a gradient elusion [A, H<sub>2</sub>O with either 0.05% or 0.1%  
8 trifluoroacetic acid (TFA); B, CH<sub>3</sub>CN with either 0.05% or 0.1% TFA] and flow rate = 1  
9 mL/min, with UV detection at either 223 or 254 nm; 2) Shimadzu LC-20A HPLC system  
10 with a binary solvent system A and B using a gradient elusion [A, H<sub>2</sub>O with either 0.05%  
11 TFA; B, CH<sub>3</sub>CN with either 0.05% or 0.1% TFA] and flow rate = 1 mL/min, with UV  
12 detection at either 223 or 254 nm. All final compounds were purified to ≥95% purity and  
13 these purity levels were measured by using the following HPLC methods:  
14  
15  
16  
17  
18  
19  
20  
21  
22  
23  
24  
25  
26  
27  
28  
29  
30  
31  
32

- 33 A) Varian Pro Star HPLC system; Phenomenex Luna C18(2) 5 μm column (4.6 ×  
34 150 mm), mobile phase, A = H<sub>2</sub>O with 0.05% TFA and B = CH<sub>3</sub>CN with 0.05%  
35 TFA; gradient: 10–90% B (0.0–15.0 min), UV detection at 223 nm.  
36  
37  
38  
39  
40  
41 B) Shimadzu LC-20A HPLC system; Phenomenex Luna C18(2) 5 μm column (4.6 ×  
42 250 mm), mobile phase, A = H<sub>2</sub>O with 0.05% TFA and B = CH<sub>3</sub>CN with 0.05%  
43 TFA; gradient: 10–90% B (0.0–15.0 min), UV detection at 223 nm or 254 nm.  
44  
45  
46  
47  
48  
49 C) Shimadzu LC-20A HPLC system; Xterra MS C18 5 μm column (4.6 × 150 mm);  
50 mobile phase, A = H<sub>2</sub>O with 0.05% TFA and B = CH<sub>3</sub>CN with 0.05% TFA;  
51 gradient: 10–90% B (0.0–15.0 min), UV detection at 223 nm or 254 nm.  
52  
53  
54  
55  
56  
57  
58  
59  
60



1  
2  
3 D) Varian Pro Star HPLC system; Inertsil ODS C18 5  $\mu\text{m}$  column (4.6  $\times$  250 mm),  
4  
5  
6 mobile phase, A =  $\text{H}_2\text{O}$  with 0.1% TFA and B =  $\text{CH}_3\text{CN}$  with 0.1% TFA; gradient:  
7  
8  
9 10–90% B (0.0–15.0 min), UV detection at 254 nm.

10  
11  
12  
13 Racemic ( $\pm$ )-**65** was resolved by preparative chiral HPLC using a Daicel 5 cm I.D.  $\times$  50 cm  
14  
15  
16 L chiral preparative column, eluting with an isocratic mobile phase of 70% heptanes and  
17  
18 30% *i*-PrOH, flow rate = 1 mL/min, to give enantiopure (-)-**66** and (+)-**67**.

19  
20  
21  
22  
23 Enantiopurity analysis for chiral compounds (-)-**66** and (+)-**67** was performed using a  
24  
25  
26 Shimadzu LC-20A HPLC system with a binary solvent system A and B using an isocratic  
27  
28 elution [30% A, *i*-PrOH; 70% B, heptanes] and flow rate = 1 mL/min, with UV detection  
29  
30 at 254 nm (Method E). Optical rotation for (-)-**66** and (+)-**67** was measured using a  
31  
32  
33 Perkin Elmer polarimeter model 341. Measurements were performed at 20  $^\circ\text{C}$  using a  
34  
35  
36 Na source lamp (589 nm) and  $\text{CH}_3\text{OH}$  as the solvent.

37  
38  
39  
40  
41 ***In Vitro* GlyT-1 Inhibition Assessment.** *In vitro* inhibitory GlyT-1 activity was  
42  
43 determined using a whole-cell scintillation proximity assay (SPA).<sup>37</sup> The potency of each  
44  
45 compound was assessed in inhibiting the uptake of radiolabeled glycine ( $[\text{}^{14}\text{C}]$ glycine)  
46  
47 using the human choriocarcinoma cell line, JAR cells (ATCC#HTB-144), which  
48  
49 endogenously express human GlyT-1 (*hGlyT-1b*). In brief, 50,000 JARS cells were plated  
50  
51 per well of tissue culture treated 96-well Cytostar-T plate (PerkinElmer) in RPMI media  
52  
53 supplemented with 10% heat inactivated FBS and allowed to attach overnight at 37  $^\circ\text{C}$   
54  
55  
56  
57  
58  
59  
60

1  
2  
3 and 5% CO<sub>2</sub>. The compounds were then diluted into Uptake Buffer (10 mM Hepes, 120  
4  
5 mM NaCl, 2 mM KCl, 1 mM CaCl<sub>2</sub>, 1 mM MgCl<sub>2</sub>, and 5 mM alanine, pH 7.4) with a final  
6  
7 DMSO concentration of 0.75% (v/v). Following the overnight incubation, the media was  
8  
9 replaced with Uptake Buffer in the presence or absence of diluted compound and pre-  
10  
11 incubated at room temperature for 10 min prior to the addition of [<sup>14</sup>C]glycine at a final  
12  
13 concentration of 5 mM. Following a 3 h incubation period at 37 °C and 5% CO<sub>2</sub>, the  
14  
15 plates were sealed and placed at room temperature in the dark for 15 min prior to  
16  
17 quantification of incorporated radioactivity using a MicroBeta Trilux scintillation plate  
18  
19 reader (PerkinElmer). Compounds were serially diluted 3-fold in DMSO generating a  
20  
21 nine data point response curve for each compound. A minimum of two replicates were  
22  
23 performed per determination. Data were plotted using XLfit software (IDBS) and fit into  
24  
25 a four-parameter logistic model to determine the inhibitor concentration at half-  
26  
27 maximal response (IC<sub>50</sub>). Plate statistics tracked included average, standard deviation  
28  
29 (SD) and CV of the positive (max) and negative control wells (min); signal ratio; z' of the  
30  
31 plate; IC<sub>50</sub> value of the positive control, its r<sup>2</sup> and hill slope. The following was tracked  
32  
33 for each compound: IC<sub>50</sub> values (in nM); % inhibition at maximum concentration; r<sup>2</sup> and  
34  
35 hill slopes of the fitted response curves. Calculations were based on the following  
36  
37 formulas: signal ratio = (positive control) / (negative control) z' = 1-(((3\*SD negative  
38  
39 control) + (3\*SD positive control)) / (average of positive control – average of negative  
40  
41 control)) % inhibition of sample = (100-((sample – average of negative control) /  
42  
43 (average of positive control – average of negative control)) x 100. The assay window was  
44  
45 established by control wells incubated with [<sup>14</sup>C]glycine in the presence or absence of 10  
46  
47  
48  
49  
50  
51  
52  
53  
54  
55  
56  
57  
58  
59  
60

1  
2  
3 mM non-labeled glycine. A dose response curve for a synthesized reference standard  
4  
5  
6 was generated on every plate as a positive control.<sup>29</sup> Plate performances were assessed  
7  
8  
9 using a combination of assay window,  $z'$  and  $IC_{50}$  of positive control.

10  
11 ***In Vitro* GlyT-2 Inhibition Assessment.** Selectivity for GlyT-1 versus GlyT-2 was  
12  
13 established using a GlyT-2 transfected cell model.<sup>37</sup> The cDNA for the human gene of  
14  
15 GlyT-2 (SLC6A5 – solute carrier family 6, member 5; Accession #NM\_004211) was  
16  
17 synthesized (Enzymax LLC) and sub-cloned into mammalian expression vector,  
18  
19 pcDNA3.1 (Invitrogen Corp.) using standard molecular biology techniques. HEK293 cells  
20  
21 (ATCC #CRL-1573) transfected with GlyT-2 modified pcDNA3.1 (Invitrogen Corp.) were  
22  
23 selected for stable incorporation of the construct by resistance to the selective pressure  
24  
25 of Geneticin (450 mg/mL; Invitrogen Corp.). A polyclonal HEK-GlyT2 cell population was  
26  
27 used in the [<sup>14</sup>C]glycine uptake assay previously described to evaluate the activity of the  
28  
29 compounds of the invention with the following protocol modifications. The HEK-GlyT-2  
30  
31 cells were plated on Poly-L-lysine coated Cytostar-T plates in DMEM media  
32  
33 supplemented with 10% heat inactivated FBS. After an overnight incubation at 37 °C and  
34  
35 5% CO<sub>2</sub>, the media was removed and the assay was conducted as described above.  
36  
37  
38  
39  
40  
41  
42  
43  
44  
45  
46  
47  
48  
49  
50  
51  
52  
53  
54  
55  
56  
57  
58  
59  
60  
Compounds of the invention were diluted in Uptake Buffer and tested against JAR or  
HEK-GlyT-2 cells in parallel to evaluate relative potency and selectivity for GlyT-1 versus  
GlyT-2.<sup>29</sup>

1  
2  
3  
4  
5  
6  
7  
8  
9  
10  
11  
12  
13  
14  
15  
16  
17  
18  
19  
20  
21  
22  
23  
24  
25  
26  
27  
28  
29  
30  
31  
32  
33  
34  
35  
36  
37  
38  
39  
40  
41  
42  
43  
44  
45  
46  
47  
48  
49  
50  
51  
52  
53  
54  
55  
56  
57  
58  
59  
60

*2-Amino-6-chloro-N-((1-(4-(propylsulfonyl)piperazin-1-yl)cyclohexyl)methyl)benzamide Hydrochloride (10)*. Step A: Cyclohexanone (5.0 g, 50.9 mmol) was added to a solution of 1-benzylpiperazine (**24**, 6.30 g, 34.0 mmol) and PTSA (7.76 g, 40.8 mmol) in H<sub>2</sub>O (40 mL). The mixture stirred at rt for 30 min followed by addition of a solution of KCN (2.88 g, 44.2 mmol) in H<sub>2</sub>O (20 mL). The mixture stirred at rt for 16 h and was filtered to afford 1-(4-benzylpiperazin-1-yl)cyclohexanecarbonitrile (**25**) as an off-white solid (9.05 g, 94%) <sup>1</sup>H NMR (300 MHz, CDCl<sub>3</sub>) δ 7.32–7.24 (m, 5H), 3.50 (s, 2H), 2.79–2.60 (m, 4H), 2.60–2.38 (m, 4H), 2.14–2.09 (m, 2H), 1.79–1.72 (m, 2H), 1.59–1.51 (m, 5H), 1.31–1.24 (m, 1H).

Step B: A solution of 1-(4-benzylpiperazin-1-yl) cyclohexanecarbonitrile (**25**, 5.0 g, 17.6 mmol) in Et<sub>2</sub>O (90 mL) was added dropwise over 30 min to a 0 °C cooled suspension of LiAlH<sub>4</sub> (1.40 g, 35.2 mmol) in Et<sub>2</sub>O (100 mL) and the resulting mixture stirred at rt for 12 h. The reaction was quenched by careful addition of H<sub>2</sub>O (5 mL) and 1 N aq NaOH (2 mL). The mixture was filtered through a pad of Celite and the filtrate was extracted with Et<sub>2</sub>O (100 mL). The combined organic extracts were washed with H<sub>2</sub>O (50 mL), brine (50 mL). The organic layer was dried over Na<sub>2</sub>SO<sub>4</sub>, filtered, and concentrated under reduced pressure to afford the (1-(4-benzylpiperazin-1-yl)cyclohexyl)methanamine (**26**) as a colorless oil (5.0 g, quantitative): <sup>1</sup>H NMR (300 MHz, CDCl<sub>3</sub>) δ 7.30–7.23 (m, 5H), 3.47 (s, 2H), 2.68 (s, 2H), 2.65–2.56 (m, 4H), 2.52–2.35 (m, 4H), 1.68 (s, 2H), 1.59–1.29 (m, 10H).

Step C: To a 0 °C solution of (1-(4-benzylpiperazin-1-yl)cyclohexyl)methanamine (**26**, 5.0 g, 17.4 mmol) and Et<sub>3</sub>N (7.3 mL, 52.3 mmol) in CH<sub>2</sub>Cl<sub>2</sub> (80 mL) was added trifluoroacetic anhydride (3.0 mL, 21.2 mmol). The resulting mixture stirred at rt for 16 h

1  
2  
3 and was then washed with saturated aqueous NaHCO<sub>3</sub> solution (50 mL), H<sub>2</sub>O (50 mL),  
4  
5 and brine (50 mL). The organic layer was dried over Na<sub>2</sub>SO<sub>4</sub>, filtered, and concentrated  
6  
7 under reduced pressure and the resulting residue was chromatographed over silica gel  
8  
9 (0–50% EtOAc in hexanes) to give to afford *N*-((1-(4-benzylpiperazin-1-  
10  
11 yl)cyclohexyl)methyl)-2,2,2-trifluoroacetamide (**27**) as a colorless oil (4.74 g, 71%) <sup>1</sup>H  
12  
13 NMR (300 MHz, CDCl<sub>3</sub>) δ 7.34–7.21 (m, 5H), 3.48 (s, 2H), 2.40 (bs, 2H), 2.67–2.54 (m,  
14  
15 4H), 2.52–2.33 (m, 4H), 1.71–1.30 (m, 9H), 1.20–1.05 (m, 1H).

20  
21 Step D: A mixture of *N*-((1-(4-benzylpiperazin-1-yl)cyclohexyl)methyl)-2,2,2-  
22  
23 trifluoroacetamide (**27**, 10.0 g, 26.1 mmol), Pd/C (10% w/w, 1.50 g), and NH<sub>4</sub>HCO<sub>2</sub> (4.93  
24  
25 g, 78.3 mmol) in CH<sub>3</sub>OH (200 mL) was heated at 65 °C for 3 h. The reaction was allowed  
26  
27 to cool to rt and was filtered through a pad of Celite, which was rinsed with CH<sub>3</sub>OH (100  
28  
29 mL). The filtrate was concentrated under reduced pressure and the resulting residue  
30  
31 was dissolved in CH<sub>2</sub>Cl<sub>2</sub> (100 mL), washed with saturated aqueous NaHCO<sub>3</sub> (3 × 100 mL),  
32  
33 and brine (100 mL). The organic layer was dried over Na<sub>2</sub>SO<sub>4</sub>, filtered, and concentrated  
34  
35 under reduced pressure to afford 2,2,2-trifluoro-*N*-((1-(piperazin-1-  
36  
37 yl)cyclohexyl)methyl)acetamide as a clear oil (5.50 g, 72%). To a 0 °C solution of 2,2,2-  
38  
39 trifluoro-*N*-((1-(piperazin-1-yl)cyclohexyl)methyl)acetamide (5.50 g, 18.8 mmol) and  
40  
41 Et<sub>3</sub>N (8.7 mL, 56.3 mmol) in CH<sub>2</sub>Cl<sub>2</sub> (80 mL) was added a solution of propane-1-sulfonyl  
42  
43 chloride (2.94 g, 20.6 mmol) in CH<sub>2</sub>Cl<sub>2</sub> (30 mL) dropwise. The reaction mixture stirred at  
44  
45 rt for 1 h and was then washed with H<sub>2</sub>O (100 mL). The organic layer was dried over  
46  
47 Na<sub>2</sub>SO<sub>4</sub>, filtered, and concentrated under reduced pressure. The resulting residue was  
48  
49 dissolved in CH<sub>3</sub>OH (5 mL) and H<sub>2</sub>O (0.5 mL) to which K<sub>2</sub>CO<sub>3</sub> (3.71 g, 26.8 mmol) was  
50  
51  
52  
53  
54  
55  
56  
57  
58  
59  
60

1  
2  
3 added. The reaction mixture stirred at reflux for 16 h, and was then allowed to cool to rt  
4  
5  
6 and diluted with H<sub>2</sub>O (30 mL). The aqueous mixture was extracted with CH<sub>2</sub>Cl<sub>2</sub> (3 × 30  
7  
8 mL) and the organic extracts were dried over Na<sub>2</sub>SO<sub>4</sub>, filtered, and concentrated under  
9  
10 reduced pressure to afford the (1-(4-(propylsulfonyl)piperazin-1-  
11 yl)cyclohexyl)methanamine (**28a**) as a clear oil (0.39 g, 68%) <sup>1</sup>H NMR (500 MHz, DMSO-  
12 d<sub>6</sub>) δ 10.03 (bs, 1H), 7.56 (d, *J* = 8.1 Hz, 1H), 7.38 (d, *J* = 7.1 Hz, 1H), 7.22 (m, 2H), 5.13  
13  
14 (dd, *J* = 14.3 Hz, 1.0 Hz, 2H), 4.71 (m, 1H), 3.83 (s, 3H), 3.73 (m, 1H), 3.48 (m, 1H), 3.31–  
15  
16 3.19 (m, 3H), 2.42 (m, 1H), 2.18 (m 1H), 1.99–1.97 (m, 3H); ESI MS *m/z* 296 [M+H]<sup>+</sup>.

17  
18  
19  
20  
21  
22  
23 Step E: A mixture of (1-(4-(propylsulfonyl)piperazin-1-yl)cyclohexyl)methanamine  
24  
25 (**28a**, 0.630 g, 2.07 mmol), 2-amino-6-chlorobenzoic acid (0.374 g, 2.17 mmol), Et<sub>3</sub>N  
26  
27 (0.86 mL, 6.21 mmol), and HBTU (1.17 g, 3.10 mmol) in DMF (20 mL) stirred at rt for 16  
28  
29 h. The mixture was diluted with H<sub>2</sub>O (100 mL) and extracted with EtOAc (3 × 80 mL).  
30  
31 The combined organic extracts were washed with H<sub>2</sub>O (3 × 80 mL), brine (80 mL), dried  
32  
33 over Na<sub>2</sub>SO<sub>4</sub>, filtered, and concentrated under reduced pressure. The resulting residue  
34  
35 was chromatographed over silica gel (0–50% EtOAc in hexanes) to give 2-amino-6-  
36  
37 chloro-*N*-((1-(4-(propylsulfonyl)piperazin-1-yl)cyclohexyl)methyl)benzamide as a white  
38  
39 foam (0.756 g, 80%) <sup>1</sup>H NMR (500 MHz, DMSO-*d*<sub>6</sub>) δ 10.03 (bs, 1H), 7.56 (d, *J* = 8.1 Hz,  
40  
41 1H), 7.38 (d, *J* = 7.1 Hz, 1H), 7.22 (m, 2H), 5.13 (dd, *J* = 14.3 Hz, 1.0 Hz, 2H), 4.71 (m, 1H),  
42  
43 3.83 (s, 3H), 3.73 (m, 1H), 3.48 (m, 1H), 3.31–3.19 (m, 3H), 2.42 (m, 1H), 2.18 (m 1H),  
44  
45 1.99–1.97 (m, 3H); ESI MS *m/z* 296 [M+H]<sup>+</sup>.

46  
47  
48  
49  
50  
51  
52  
53 Step F: To a 0 °C solution of 2-amino-6-chloro-*N*-((1-(4-(propylsulfonyl)piperazin-1-  
54  
55 yl)cyclohexyl)methyl)benzamide (0.750 g, 1.64 mmol) in CH<sub>2</sub>Cl<sub>2</sub> (5 mL) was added a 1.0  
56  
57  
58  
59  
60

1  
2  
3 M solution of HCl in Et<sub>2</sub>O (4.92 mL, 4.92 mmol). The mixture was concentrated under  
4  
5 reduced pressure to give 2-amino-6-chloro-*N*-((1-(4-(propylsulfonyl)piperazin-1-  
6  
7 yl)cyclohexyl)methyl)benzamide hydrochloride (**10**), which was lyophilized from CH<sub>3</sub>CN  
8  
9 and H<sub>2</sub>O (0.790 g, quantitative): <sup>1</sup>H NMR (500 MHz, DMSO-*d*<sub>6</sub>) δ 10.03 (bs, 1H), 7.15 (d, *J*  
10  
11 = 8.1 Hz, 1H), 6.81–6.68 (m, 3H), 3.74 (m, 8H), 3.34 (m, 2H), 3.08 (m, 2H), 2.11–1.98 (m,  
12  
13 4H), 1.74–1.57 (m, 8H), 1.17 (m, 2H), 1.01 (t, *J* = 7.5 Hz, 3H); ESI MS *m/z* 296 [M+H]<sup>+</sup>;  
14  
15 HPLC >99% (AUC), (Method A), *t*<sub>R</sub> = 12.5 min.  
16  
17  
18  
19

20  
21 *N*-((4,4-Difluoro-1-(4-(propylsulfonyl)piperazin-1-yl)cyclohexyl)methyl)-2,6-  
22  
23 difluorobenzamide Hydrochloride (**11**). Step A: To a 0 °C solution of *tert*-butyl piperazine-  
24  
25 1-carboxylate (**12**, 10.0 g, 53.69 mmol) and Et<sub>3</sub>N (22.4 mL, 161 mmol) in CH<sub>2</sub>Cl<sub>2</sub> (200 mL)  
26  
27 was slowly added 1-propanesulfonyl chloride (7.65 g, 53.6 mmol). The mixture stirred  
28  
29 at rt for 3 h, then washed with 2 N aq NaOH (50 mL), 2 N aq HCl (50 mL), H<sub>2</sub>O (50 mL),  
30  
31 and brine (50 mL). The organic extracts were dried over Na<sub>2</sub>SO<sub>4</sub>, filtered, and  
32  
33 concentrated under reduced pressure to afford *tert*-butyl 4-(propylsulfonyl)piperazine-  
34  
35 1-carboxylate (**13**) as an off-white solid (15.7 g, quantitative): <sup>1</sup>H NMR (500 MHz, CDCl<sub>3</sub>)  
36  
37 δ 7.91 (d, *J* = 1.7 Hz, 1H), 7.48 (d, *J* = 1.6 Hz, 1H), 7.21 (m, 1H), 7.14 (s, 1H), 7.09 (s, 1H),  
38  
39 3.96 (s, 3H), 3.75 (s, 3H); ESI MS *m/z* 293 [M + H]<sup>+</sup>.  
40  
41  
42  
43  
44  
45

46  
47 Step B: To a 0 °C solution of *tert*-butyl 4-(propylsulfonyl)piperazine-1-carboxylate  
48  
49 (**13**, 15.7 g, 53.6 mmol) in CH<sub>2</sub>Cl<sub>2</sub> (200 mL) was slowly added TFA (21.4 mL, 268 mmol).  
50  
51 The mixture stirred at rt for 16 h and was washed with 2 N aq NaOH (3 × 50 mL), H<sub>2</sub>O (50  
52  
53 mL), and brine (50 mL). The organic layer was dried over Na<sub>2</sub>SO<sub>4</sub>, filtered, and  
54  
55 concentrated under reduced pressure to afford 1-(propylsulfonyl)piperazine (**14**) as a  
56  
57  
58  
59  
60

1  
2  
3 crystalline solid (10.3 g, quantitative):  $^1\text{H}$  NMR (500 MHz,  $\text{CDCl}_3$ )  $\delta$  7.91 (d,  $J = 1.7$  Hz,  
4 1H), 7.48 (d,  $J = 1.6$  Hz, 1H), 7.21 (m, 1H), 7.14 (s, 1H), 7.09 (s, 1H), 3.96 (s, 3H), 3.75 (s,  
5 3H).  
6  
7  
8  
9

10  
11 Step C: To a 0 °C solution of 4,4-difluorocyclohexanone (0.200 g, 1.49 mmol) in  
12 toluene (2 mL) was added a solution of piperazine-4-propyl sulfonamide (**14**, 0.287 g,  
13 1.49 mmol) in toluene (2 mL), followed by dropwise addition of  $\text{Ti}(i\text{-PrO})_4$  (0.87 mL, 2.98  
14 mmol). The reaction mixture stirred at rt for 2 h, then cooled back down to 0 °C. To this  
15 was added a 1.0 M solution of  $\text{Et}_2\text{AlCN}$  in toluene (2.98 mL, 2.98 mmol) dropwise. The  
16 mixture then stirred at rt for 16 h.  $\text{H}_2\text{O}$  (10 mL) was then carefully added and the  
17 resulting precipitate was filtered. To the filtrate was added  $\text{CH}_2\text{Cl}_2$  (20 mL) and  $\text{H}_2\text{O}$  (20  
18 mL), and the aqueous layer was separated and extracted with  $\text{CH}_2\text{Cl}_2$  (3  $\times$  20 mL). The  
19 combined organic extracts were dried over  $\text{Na}_2\text{SO}_4$ , filtered, and concentrated under  
20 reduced pressure. The resulting residue was chromatographed over silica gel (0–30%  
21 EtOAc in hexanes) to give 4,4-difluoro-1-(4-(propylsulfonyl)piperazin-1-yl)  
22 cyclohexanecarbonitrile (**15**) as a white foam (0.233 g, 50%):  $^1\text{H}$  NMR (300 MHz,  $\text{CDCl}_3$ )  
23  $\delta$  3.38–3.34 (m, 4H), 2.93–2.90 (m, 2H), 2.75–2.72 (m, 4H), 2.18–2.02 (m, 8H), 1.90–1.83  
24 (m, 2H), 1.07 (t,  $J = 4.9$  Hz, 3H).  
25  
26  
27  
28  
29  
30  
31  
32  
33  
34  
35  
36  
37  
38  
39  
40  
41  
42  
43  
44  
45

46 Step D: To a 0 °C solution of 4,4-difluoro-1-(4-(propylsulfonyl)piperazin-1-yl)  
47 cyclohexanecarbonitrile (**15**, 2.95 g, 8.79 mmol) in  $\text{Et}_2\text{O}$  (60 mL) was added  $\text{LiAlH}_4$  (0.67  
48 g, 18 mmol). The mixture stirred at rt for 12 h, cooled back to 0 °C, then quenched by  
49 the sequential addition of  $\text{H}_2\text{O}$  (0.87 mL), 4 N aq NaOH (0.87 mL), and  $\text{H}_2\text{O}$  (4 mL). The  
50 resulting mixture was stirred at rt for 30 min, then filtered. The filtrate was  
51  
52  
53  
54  
55  
56  
57  
58  
59  
60



1  
2  
3 concentrated under reduced pressure and the resulting residue was chromatographed  
4  
5  
6 over silica gel (0–10% CH<sub>3</sub>OH in CH<sub>2</sub>Cl<sub>2</sub>) to give (4,4-difluoro-1-(4-  
7  
8 (propylsulfonyl)piperazin-1-yl)cyclohexyl)methanamine (**16**) as a colorless oil (2.2 g,  
9  
10 74%): <sup>1</sup>H NMR (300 MHz, CDCl<sub>3</sub>) δ 3.23 (t, *J* = 4.8 Hz, 4H), 2.94–2.85 (m, 2H), 2.76 (t, *J* =  
11  
12 4.8 Hz, 4H), 2.72 (s, 2H), 2.15–1.75 (m, 10H), 1.70–1.45 (m, 2H), 1.07 (t, *J* = 7.5 Hz, 3H);  
13  
14 ESI MS *m/z* 340 [M+H]<sup>+</sup>.  
15

16  
17  
18 Step E: To a 0 °C solution of (4,4-difluoro-1-(4-(propylsulfonyl)piperazin-1-  
19  
20 yl)cyclohexyl)methanamine (**16**, 0.15 g, 0.44 mmol) in CH<sub>2</sub>Cl<sub>2</sub> (5 mL) was added Et<sub>3</sub>N  
21  
22 (0.12 mL, 0.88 mmol) and 2,6-difluorobenzoyl chloride (0.05 mL, 0.44 mmol). The  
23  
24 resulting mixture stirred at rt for 4 h, was diluted with CH<sub>2</sub>Cl<sub>2</sub>, then washed with  
25  
26 saturated aqueous NaHCO<sub>3</sub> (10 mL). The organic layer was dried over Na<sub>2</sub>SO<sub>4</sub>, filtered,  
27  
28 and concentrated under reduced pressure. The resulting residue was chromatographed  
29  
30 over silica gel (0–50% EtOAc in hexanes) to give *N*-((4,4-difluoro-1-(4-  
31  
32 (propylsulfinyl)piperazin-1-yl)cyclohexyl)methyl)-2,6-difluorobenzamide as a white solid  
33  
34 (0.072 g, 46%): <sup>1</sup>H NMR (300 MHz, CDCl<sub>3</sub>): δ 7.42–7.36 (m, 1H), 6.96 (t, *J* = 8.1 Hz, 2H),  
35  
36 6.13 (bs, 1H), 3.55 (d, *J* = 3.15 Hz, 2H), 3.34–3.27 (m, 4H), 2.91–2.85 (m, 2 H), 2.79–2.72  
37  
38 (m, 4 H), 2.02–1.82 (m, 8H), 1.71–1.56 (m, 2H), 1.06 (t, *J* = 4.9 Hz, 3H); ESI MS *m/z* 480  
39  
40 [M+H]<sup>+</sup>.  
41  
42  
43  
44  
45  
46  
47

48  
49 Step F: To a 0 °C solution of *N*-((4,4-difluoro-1-(4-(propylsulfonyl)piperazin-1-  
50  
51 yl)cyclohexyl)methyl)-2,6-difluorobenzamide (0.065 g, 0.135 mmol) in CH<sub>3</sub>CN (1 mL) was  
52  
53 added a 1.0 M solution of HCl in H<sub>2</sub>O (1.5 mL). The mixture stirred at rt for 30 min and  
54  
55 was lyophilized to give *N*-((4,4-difluoro-1-(4-(propylsulfonyl)piperazin-1-  
56  
57  
58  
59  
60

1  
2  
3 yl)cyclohexyl)methyl)-2,6-difluorobenzamide hydrochloride (**11**) as an amorphous white  
4  
5 solid (0.068 g, quantitative): mp 165–169 °C; <sup>1</sup>H NMR (300 MHz, DMSO-*d*<sub>6</sub>) δ 10.68 (bs,  
6  
7 1H), 9.32 (m, 0.4H), 8.78 (m, 0.6H), 7.62–7.42 (m, 1H), 7.30–7.13 (m, 2H), 4.00–3.68 (m,  
8  
9 7H), 3.56–2.94 (m, 6H), 2.79 (m, 2H), 2.30–1.54 (m, 7H), 0.99 (t, *J* = 4.8 Hz, 3H); APCI MS  
10  
11 *m/z* 480 [M+H]<sup>+</sup>; HPLC >99% (AUC), (Method B), *t*<sub>R</sub> = 22.3 min.  
12  
13  
14

15  
16 *2,6-Dichloro-N-((4,4-difluoro-1-(4-(propylsulfonyl)piperazin-1-*  
17  
18 *yl)cyclohexyl)methyl)benzamide Hydrochloride (17)*. Compound **17** was prepared  
19  
20 according to a similar procedure described for the synthesis of **11**. mp 220–223 °C; <sup>1</sup>H  
21  
22 NMR (300 MHz, DMSO-*d*<sub>6</sub>) δ 10.48 (bs, 1H), 9.12 (bs, 0.3H), 8.63 (bs, 0.7H), 7.68–7.38  
23  
24 (m, 3H), 3.92–2.99 (m, 9H), 2.80–2.68 (m, 3H), 2.30–1.58 (m, 10H), 0.99 (t, *J* = 7.5 Hz,  
25  
26 3H); APCI MS *m/z* 512 [M + H]<sup>+</sup>; HPLC 95.7% (AUC), (Method B), *t*<sub>R</sub> = 23.1 min.  
27  
28  
29  
30

31  
32 *2-Chloro-N-((4,4-difluoro-1-(4-(propylsulfonyl)piperazin-1-yl)cyclohexyl)methyl)-6-*  
33  
34 *(trifluoromethoxy)benzamide Hydrochloride (18)*. Step A: (4,4-difluoro-1-(4-  
35  
36 (propylsulfonyl)piperazin-1-yl)cyclohexyl)methanamine (**16**, 0.15 g, 0.44 mmol), 2-  
37  
38 chloro-6-(trifluoromethoxy)benzoic acid (0.105 g, 0.44 mmol), EDCI•HCl (0.09 g, 0.44  
39  
40 mmol), HOBt (0.07 g, 0.44 mmol), and Et<sub>3</sub>N (0.3 mL, 1.91 mmol) in DMF (10 mL) stirred  
41  
42 at rt for 16 h. The mixture was diluted with H<sub>2</sub>O (20) mL and extracted with EtOAc (3 ×  
43  
44 20 mL). The combined organic extracts were washed with H<sub>2</sub>O (3 × 20 mL), and brine (20  
45  
46 mL). The organic layers were then dried over Na<sub>2</sub>SO<sub>4</sub>, filtered, and concentrated under  
47  
48 reduced pressure. The resulting residue was chromatographed over silica gel (0–50%  
49  
50 EtOAc in hexanes) to give 2-chloro-N-((4,4-difluoro-1-(4-(propylsulfonyl)piperazin-1-  
51  
52  
53  
54  
55  
56  
57  
58  
59  
60

1  
2  
3  
4  
5  
6  
7  
8  
9  
10  
11  
12  
13  
14  
15  
16  
17  
18  
19  
20  
21  
22  
23  
24  
25  
26  
27  
28  
29  
30  
31  
32  
33  
34  
35  
36  
37  
38  
39  
40  
41  
42  
43  
44  
45  
46  
47  
48  
49  
50  
51  
52  
53  
54  
55  
56  
57  
58  
59  
60

yl)cyclohexyl)methyl)-6-(trifluoromethoxy)benzamide as a white solid (0.155 g, 63%): ESI MS  $m/z$  562 [M+H]<sup>+</sup>.

Step B: To a 0 °C solution of 2-chloro-N-((4,4-difluoro-1-(4-(propylsulfonyl)piperazin-1-yl)cyclohexyl)methyl)-6-(trifluoromethoxy)benzamide (0.050 g, 0.08 mmol) in CH<sub>3</sub>CN (5 mL) was added a 1.0 M solution of HCl in H<sub>2</sub>O (1.0 mL, 1.0 mmol). The mixture stirred at rt for 30 min and was lyophilized to give 2-chloro-N-((4,4-difluoro-1-(4-(propylsulfonyl)piperazin-1-yl)cyclohexyl)methyl)-6-(trifluoromethoxy)benzamide hydrochloride (**18**) as a white solid (0.058 g, quantitative): mp 200–205 °C; <sup>1</sup>H NMR (300 MHz, DMSO-*d*<sub>6</sub>) δ 10.55 (bs, 1H), 9.15 (m, 0.3H), 8.77 (m, 0.7H), 7.62–7.31 (m, 3H), 4.00–3.00 (m, 9H), 2.80–2.68 (m, 3H), 2.29–1.60 (m, 10H), 1.00 (t, *J* = 7.5 Hz, 3H); ESI MS  $m/z$  562 [M + H]<sup>+</sup>; HPLC >99% (AUC), (Method C), *t*<sub>R</sub> = 20.4 min.

*2,4-Dichloro-N-((4,4-difluoro-1-(4-(propylsulfonyl)piperazin-1-yl)cyclohexyl)methyl)benzamide Hydrochloride (19)*. Compound **19** was prepared according to a similar procedure described for the synthesis of **11**. mp 124–126 °C; <sup>1</sup>H NMR (300 MHz, DMSO-*d*<sub>6</sub>) δ 10.66 (bs, 1H), 8.96 (bs, 0.5H), 8.47 (bs, 0.5H), 7.80–7.35 (m, 3H), 3.95–3.00 (m, 9H), 2.82 (m, 3H), 2.30–1.50 (m, 10H), 0.99 (t, *J* = 7.5 Hz, 3H); ESI MS  $m/z$  512 [M + H]<sup>+</sup>; HPLC 98.2% (AUC), (Method B), *t*<sub>R</sub> = 23.5 min.

*2-Chloro-N-((4,4-difluoro-1-(4-(propylsulfonyl)piperazin-1-yl)cyclohexyl)methyl)-4-fluorobenzamide Hydrochloride (20)*. Compound **20** was prepared according to a similar procedure described for the synthesis of **18**. mp 220–225 °C; <sup>1</sup>H NMR (300 MHz, DMSO-*d*<sub>6</sub>) δ 10.91 (s, 1H), 9.00 (m, 0.7H), 8.66 (m, 0.3H), 7.61–7.43 (m, 2H), 7.42–7.31 (m, 1H), 4.00 (m, 4H), 3.82–3.59 (m, 4H), 3.31–3.22 (m, 2H), 3.26–3.01 (m, 3H), 2.75 (bs, 1H),

1  
2  
3 2.30–1.99 (m, 6H), 1.75 (m, 2H), 0.98 (t,  $J = 7.5$  Hz, 3H); ESI MS  $m/z$  496  $[M + H]^+$ ; HPLC  
4  
5 98.2% (AUC), (Method C),  $t_R = 18.8$  min.

6  
7  
8 *2-Chloro-N-((4,4-difluoro-1-(4-(propylsulfonyl)piperazin-1-yl)cyclohexyl)methyl)-4-*  
9  
10 *(trifluoromethyl)benzamide Hydrochloride (21)*. Compound **21** was prepared according  
11  
12 to a similar procedure described for the synthesis of **18**. mp 115–120 °C;  $^1H$  NMR (400  
13  
14 MHz, DMSO- $d_6$ )  $\delta$  11.20 (bs, 1H), 9.12 (bs, 1H), 8.00 (m, 1H), 7.62–7.59 (m, 2H), 3.90–  
15  
16 3.61 (m, 6H), 3.30 (m, 2H), 3.21–3.00 (m, 3H), 2.76 (m, 1H), 2.31–1.72 (m, 10H), 1.05 (t,  $J$   
17  
18 = 7.3 Hz, 3H); ESI MS  $m/z$  546  $[M + H]^+$ ; HPLC >99% (AUC), (Method B),  $t_R = 29.6$  min.

19  
20  
21 *N-((4,4-Difluoro-1-(4-(propylsulfonyl)piperazin-1-yl)cyclohexyl)methyl)-2,4-*  
22  
23 *bis(trifluoromethyl)benzamide Hydrochloride (22)*. Compound **22** was prepared  
24  
25 according to a similar procedure described for the synthesis of **18**. mp 124–131 °C;  $^1H$   
26  
27 NMR (300 MHz, DMSO- $d_6$ )  $\delta$  11.20 (bs, 1H), 9.14 (bs, 1H), 8.20–8.17 (m, 2H), 7.98–7.73  
28  
29 (m, 1H), 4.24–4.13 (m, 3H), 3.94–3.67 (m, 4H), 3.30–3.02 (m, 4H), 2.73–2.50 (m, 1H),  
30  
31 2.20–1.53 (m, 10H), 0.97 (t,  $J = 7.3$  Hz, 3H). ESI MS  $m/z$  580  $[M + H]^+$ ; HPLC >99% (AUC),  
32  
33 (Method C),  $t_R = 21.6$  min.

34  
35  
36 *N-((4,4-Difluoro-1-(4-(propylsulfonyl)piperazin-1-yl)cyclohexyl)methyl)-4-fluoro-2-*  
37  
38 *methoxy-6-methylbenzamide (23)*.<sup>38</sup> To a stirring suspension of 4-fluoro-2-  
39  
40 hydroxybenzoic acid (10.0 g, 64.0 mmol) and  $K_2CO_3$  (22.0 g, 160 mmol) in DMF (200 mL)  
41  
42 was slowly added  $CH_3I$  (20.0 g, 140 mmol) at rt. The mixture was then heated at 90 °C  
43  
44 for 16 h. After allowing to cool to rt, the mixture was concentrated under reduced  
45  
46 pressure, and the resulting white solid rinsed over a plug of silica gel ( $CH_2Cl_2$  eluent) to  
47  
48  
49  
50  
51  
52  
53  
54  
55  
56  
57  
58  
59  
60

1  
2  
3 afford methyl 4-fluoro-2-methoxybenzoate as clear oil (10.0 g, 92%). The intermediate  
4  
5  
6 was taken into the next step without any further analysis.

7  
8 To a solution of 4-fluoro-2-methoxybenzoate (10.0 g, 58.8 mmol) in CH<sub>3</sub>OH (50 mL)  
9  
10 was slowly added 6 N aq NaOH (30 mL) over a period of 15 min. The mixture stirred for  
11  
12 at rt for 1 h and was acidified to pH = 2 with 6 N aq HCl. The resulting precipitate was  
13  
14 collected via vacuum filtration to afford 4-fluoro-2-methyl benzoic acid (9.2 g, 85 %) <sup>1</sup>H  
15  
16 NMR (300 MHz, CDCl<sub>3</sub>) δ 8.21 (dd, *J* = 9.0 Hz, 6.9 Hz, 1H), 6.82–6.88 (m, 1H), 6.79 (dd, *J* =  
17  
18 7.8 Hz, 2.1 Hz, 1H), 4.07 (s, 1H).  
19  
20  
21  
22

23 To a -78 °C cooled solution of TMEDA (1.95 mL, 19.2 mmol) in THF (8 mL) was slowly  
24  
25 added *sec*-BuLi (1.4 M solution in cyclohexane, 18.5 mL, 25.8 mmol), followed by a  
26  
27 solution of 4-fluoro-2-methyl-benzoic acid (1.0 g, 5.88 mmol) in THF (2 mL). The mixture  
28  
29 stirred at -78 °C for 2 h before addition of a solution of CH<sub>3</sub>I (1.46 mL, 23.5 mmol) in THF  
30  
31 (2 mL). The mixture stirred at -78 °C for 1 h, and was then allowed to warm to rt and  
32  
33 quenched with H<sub>2</sub>O (10 mL). The crude mixture was diluted with H<sub>2</sub>O (10 mL) and  
34  
35 extracted with EtOAc (50 mL). The aqueous layer was collected and acidified to pH = 2  
36  
37 with 2 N aq HCl then extracted with EtOAc (2 × 20 mL). The combined organic extracts  
38  
39 were dried over Na<sub>2</sub>SO<sub>4</sub>, filtered, and concentrated under reduced pressure. The  
40  
41 resulting residue was chromatographed over silica gel (0–50% EtOAc in hexanes) to give  
42  
43 4-fluoro-2-methoxy-6-methyl benzoic acid as a white solid (0.18 g, 16%) <sup>1</sup>H NMR (300  
44  
45 MHz, CDCl<sub>3</sub>) δ 6.53–6.62 (m, 2H), 3.90 (s, 1H), 2.48 (s, 1H); MS (ESI+) *m/z* 185 (M+H).  
46  
47  
48  
49  
50  
51  
52

53 Step E: To a 0 °C solution of 2-methoxy-6-methyl-4-fluorobenzoic acid (0.08 g, 0.44  
54  
55 mmol) in CH<sub>2</sub>Cl<sub>2</sub> (4 mL) was added oxalyl chloride (0.08 mL, 0.88 mmol) followed by 2  
56  
57  
58  
59  
60

1  
2  
3 drops of DMF, and the mixture was stirred at rt for 1.5 h to generate 2-methoxy-6-  
4 methyl-4-fluorobenzoyl chloride. This mixture was concentrated under reduced  
5 pressure and dissolved in CH<sub>2</sub>Cl<sub>2</sub> (1 mL), which was then added to a 0 °C solution of (4,4-  
6 difluoro-1-(4-(propylsulfonyl)piperazin-1-yl)cyclohexyl)methanamine (**16**, 0.15 g, 0.44  
7 mmol) and Et<sub>3</sub>N (0.18 mL, 1.31 mmol) in CH<sub>2</sub>Cl<sub>2</sub> (4 mL). The resulting mixture stirred at rt  
8 for 4 h, and was then diluted with CH<sub>2</sub>Cl<sub>2</sub> and washed with saturated aqueous NaHCO<sub>3</sub>  
9 solution (5 mL). The organic layer was dried over Na<sub>2</sub>SO<sub>4</sub>, filtered, and concentrated  
10 under reduced pressure and the resulting residue was chromatographed over silica gel  
11 (0–50% EtOAc in hexanes) to give *N*-((4,4-difluoro-1-(4-(propylsulfonyl)piperazin-1-  
12 yl)cyclohexyl)methyl)-4-fluoro-2-methoxy-6-methylbenzamide (**23**) as a white solid (0.13  
13 g, 58%): mp 160–163 °C; <sup>1</sup>H NMR (300 MHz, DMSO-*d*<sub>6</sub>) δ 10.65 (bs, 1H), 8.71 (bs, 0.6H),  
14 8.15 (bs, 0.4H), 6.90–6.58 (m, 2H), 3.76 (s, 3H), 3.74–3.35 (m, 5H), 3.25–2.60 (m, 7H),  
15 2.19 (s, 3H), 2.05–1.52 (m, 10H), 0.98 (t, *J* = 7.5 Hz, 3H); APCI MS *m/z* 506 [M + H]<sup>+</sup>; HPLC  
16 >99% (AUC), (Method B), *t*<sub>R</sub> = 22.3 min.

17  
18  
19  
20  
21  
22  
23  
24  
25  
26  
27  
28  
29  
30  
31  
32  
33  
34  
35  
36  
37  
38  
39  
40  
41  
42  
43  
44  
45  
46  
47  
48  
49  
50  
51  
52  
53  
54  
55  
56  
57  
58  
59  
60

*2-Amino-6-chloro-N-((1-(4-(methylsulfonyl)piperazin-1-yl)cyclohexyl)methyl)benzamide Hydrochloride (29)*. Compound **29** was prepared according to a similar procedure described for the synthesis of **10** using methylsulfonyl chloride. mp 178–181 °C; <sup>1</sup>H NMR (300 MHz, DMSO-*d*<sub>6</sub>) δ 8.80 (bs, 1H), 7.08 (t, *J* = 8.1 Hz, 1H), 6.72–6.64 (m, 2H), 6.23 (bs, 2H), 3.84–3.27 (m, 10H), 2.91 (s, 3H), 2.17–2.01 (m, 2H), 1.80–1.44 (m, 7H), 1.25–1.02 (m, 1H); ESI MS *m/z* 429 [M+H]<sup>+</sup>; HPLC 96.6% (AUC), (Method B), *t*<sub>R</sub> = 19.6 min.

1  
2  
3  
4  
5  
6  
7  
8  
9  
10  
11  
12  
13  
14  
15  
16  
17  
18  
19  
20  
21  
22  
23  
24  
25  
26  
27  
28  
29  
30  
31  
32  
33  
34  
35  
36  
37  
38  
39  
40  
41  
42  
43  
44  
45  
46  
47  
48  
49  
50  
51  
52  
53  
54  
55  
56  
57  
58  
59  
60

*2-Amino-6-chloro-N-((1-(4-(ethylsulfonyl)piperazin-1-yl)cyclohexyl)methyl)benzamide Hydrochloride (30)*. Compound **30** was prepared according to a similar procedure described for the synthesis of **10** using ethylsulfonyl chloride. mp 170–173 °C; <sup>1</sup>H NMR (300 MHz, CD<sub>3</sub>OD) δ 7.46 (d, *J* = 2.0 Hz, 1H), 7.18 (s, 1H), 7.09 (s, 1H), 4.04–3.82 (m, 6H), 3.55–3.33 (m, 4H), 3.15 (q, *J* = 7.4 Hz, 2H), 2.18 (d, *J* = 11.8 Hz, 2H), 1.93–1.72 (m, 5H), 1.70–1.54 (m, 2H), 1.34 (t, *J* = 7.6 Hz, 3H), 1.30–1.25 (m, 1H), 1.01 (t, *J* = 7.5 Hz, 3H); ESI MS *m/z* 443 [M+H]<sup>+</sup>; HPLC >99% (AUC), (Method B), *t<sub>R</sub>* = 19.8 min.

*2-Amino-6-chloro-N-((1-(4-(isobutylsulfonyl)piperazin-1-yl)cyclohexyl)methyl)benzamide Hydrochloride (31)*. Compound **31** was prepared according to a similar procedure described for the synthesis of **10** using isobutylsulfonyl chloride. mp 195–198 °C; <sup>1</sup>H NMR (300 MHz, DMSO-*d*<sub>6</sub>) δ 8.79 (s, 1H), 7.07 (t, *J* = 7.8 Hz, 1H), 6.66 (q, *J* = 8.1 Hz, 2H), 5.78 (bs, 2H), 3.88–3.18 (m, 10H), 2.98 (d, *J* = 6.6 Hz, 2H), 2.25–2.06 (m, 3H), 1.98–1.39 (m, 7H), 1.23–1.08 (m, 1H), 1.03 (d, *J* = 6.6 Hz, 6H); APCI MS *m/z* 471 [M+H]<sup>+</sup>; HPLC 95.1% (AUC), (Method B), *t<sub>R</sub>* = 21.1 min.

*2-Amino-6-chloro-N-((1-(4-(phenylsulfonyl)piperazin-1-yl)cyclohexyl)methyl)benzamide Hydrochloride (32)*. Compound **32** was prepared according to a similar procedure described for the synthesis of **10** using phenylsulfonyl chloride. mp 230–232 °C; <sup>1</sup>H NMR (300 MHz, DMSO-*d*<sub>6</sub>) δ 8.77 (bs, 1H), 7.80–7.66 (m, 5H), 7.12–7.06 (m, 1H), 6.73–6.65 (m, 2H), 3.88–3.28 (m, 9H), 3.30–2.76 (m, 3H), 2.16–1.91 (m, 3H), 1.86–1.37 (m, 7H), 1.15–1.00 (m, 1H); APCI MS *m/z* 491 [M+H]<sup>+</sup>; HPLC 96.8% (AUC), (Method B), *t<sub>R</sub>* = 14.4 min.

1  
2  
3  
4  
5  
6  
7  
8  
9  
10  
11  
12  
13  
14  
15  
16  
17  
18  
19  
20  
21  
22  
23  
24  
25  
26  
27  
28  
29  
30  
31  
32  
33  
34  
35  
36  
37  
38  
39  
40  
41  
42  
43  
44  
45  
46  
47  
48  
49  
50  
51  
52  
53  
54  
55  
56  
57  
58  
59  
60

*2-Amino-N-((1-(4-(benzylsulfonyl)piperazin-1-yl)cyclohexyl)methyl)-6-chlorobenzamide Hydrochloride (33)*. Compound **33** was prepared according to a similar procedure described for the synthesis of **10**. mp 215–217 °C; <sup>1</sup>H NMR (300 MHz, DMSO-*d*<sub>6</sub>) δ 8.81 (bs, 1H), 7.44–7.33 (m, 5H), 7.10 (t, *J* = 8.1 Hz, 1H), 6.77–6.68 (m, 2H), 4.50 (s, 2H), 3.72–3.51 (m, 8H), 3.35–3.16 (m, 2H), 2.14–1.85 (m, 5H), 1.78–1.43 (m, 6H), 1.24–1.01 (m, 1H); ESI MS *m/z* 505 [M+H]<sup>+</sup>; HPLC 96.3% (AUC), (Method B), *t*<sub>R</sub> = 21.4 min.

*2,4-Dichloro-N-((1-(4-(propylsulfonyl)piperazin-1-yl)cyclohexyl)methyl)benzamide Hydrochloride (34)*. Step G: To a 0 °C solution of (1-(4-(propylsulfonyl)piperazin-1-yl)cyclohexyl) methanamine (**28a**, 0.30 g, 0.99 mmol) and Et<sub>3</sub>N (0.41 mL, 2.96 mmol) in CH<sub>2</sub>Cl<sub>2</sub> (3 mL) was added 2,4-dichloro benzoyl chloride (0.30 g, 1.48 mmol). The mixture stirred at rt for 16 h. The mixture was diluted with CH<sub>2</sub>Cl<sub>2</sub> and washed with 1 N aq NaOH (10 mL), H<sub>2</sub>O (10 mL), and brine (10 mL). The organic layers were dried over Na<sub>2</sub>SO<sub>4</sub>, filtered, and concentrated under reduced pressure. The resulting residue was chromatographed over silica gel (0–50% EtOAc in hexanes) to give 2,4-dichloro-*N-((1-(4-(propylsulfonyl)piperazin-1-yl)cyclohexyl)methyl)benzamide (34)* as an off-white solid (0.27 g, 57 %); <sup>1</sup>H NMR (300 MHz, CDCl<sub>3</sub>) δ (d, *J* = 8.4 Hz, 1H), 7.41 (d, *J* = 2.0 Hz, 1H), 7.33 (dd, *J* = 2.0 Hz, 8.4 Hz, 1H), 6.89 (bs, 1H), 3.60–3.52 (d, *J* = 5.1 Hz, 2H), 3.28–3.20 (m, 4H), 2.90–2.80 (m, 2), 2.79–2.69 (m, 4H), 1.90–1.78 (m, 2H), 1.72–1.40 (m, 10H), 1.08–1.03 (t, *J* = 7.4 Hz, 3H); ESI MS *m/z* 476 [M+H]<sup>+</sup>.

Step H: To a 0 °C solution of 2,4-dichloro-*N-((1-(4-(propylsulfonyl)piperazin-1-yl)cyclohexyl)methyl)benzamide* (0.27 g, 0.56 mmol) in CH<sub>3</sub>CN (1 mL) added 10% HCl in H<sub>2</sub>O (0.5 mL). The mixture stirred at rt for 30 min and was then lyophilized to give 2,4-



1  
2  
3 dichloro-*N*-((1-(4-(propylsulfonyl)piperazin-1-yl)cyclohexyl) methyl)benzamide  
4  
5 hydrochloride (**34**) as a white solid (0.28 g, quantitative): mp 202–208 °C; <sup>1</sup>H NMR (500  
6 MHz, DMSO-*d*<sub>6</sub>) δ 10.83 (bs, 1H), 8.91 (bs, 1H), 7.72 (s, 1H), 7.53 (m, 2H), 3.75–3.59 (m,  
7 8H), 3.28 (m, 2H), 3.11 (m, 2H), 2.08 (m, 2H), 1.93 (m, 2H), 1.69–1.50 (m, 7H), 1.16 (m,  
8 1H), 1.02 (t, *J* = 7.4 Hz, 3H); ESI MS *m/z* 476 [M+H]<sup>+</sup>; HPLC 98.7% (AUC), (Method A), *t*<sub>R</sub> =  
9 22.3 min.  
10  
11  
12  
13  
14  
15  
16  
17

18 *2,4-Dichloro-N-((1-(4-((cyclopropylmethyl)sulfonyl)piperazin-1-*  
19 *yl)cyclohexyl)methyl)benzamide Hydrochloride (35)*. Compound **35** was prepared  
20 according to a similar procedure described for the synthesis of **34**. mp 217–219 °C; <sup>1</sup>H  
21 NMR (300 MHz, DMSO-*d*<sub>6</sub>) δ 11.01 (bs, 1H), 8.92 (t, *J* = 6.0 Hz, 1H), 7.72 (d, *J* = 1.2 Hz,  
22 1H), 7.57–7.50 (m, 2H), 3.83–3.40 (m, 10H), 3.11 (d, *J* = 6.9 Hz, 2H), 2.12–1.85 (m, 4H),  
23 1.77–1.46 (m, 5H), 1.22–0.95 (m, 2H), 0.62–0.55 (m, 2H), 0.42–0.35 (m, 2H); ESI MS *m/z*  
24 488 [M+H]<sup>+</sup>; HPLC >99% (AUC), (Method B), *t*<sub>R</sub> = 20.5 min.  
25  
26  
27  
28  
29  
30  
31  
32  
33  
34  
35

36 *Cyclobutanesulfonyl Chloride*. Step A: To a suspension of magnesium turnings (0.79  
37 g, 32.0 mmol) in Et<sub>2</sub>O (20 mL) was added a solution of cyclobutyl bromide (1.8 mL, 19.1  
38 mmol) in Et<sub>2</sub>O (20 mL) portion-wise. After the initial exothermic reaction had ceased,  
39 the mixture was heated at reflux for 1 h. The suspension was allowed to cool to rt, and  
40 the supernatant was collected and added portion-wise to a 0 °C solution of sulfuryl  
41 chloride (4.6 mL, 57.1 mmol) in CH<sub>2</sub>Cl<sub>2</sub> (30 mL). The mixture stirred at rt for 1 h and was  
42 concentrated under reduced pressure. The residue was taken up in hexanes (150 mL),  
43 and the resulting precipitate was filtered. The filtrate was concentrated under reduced  
44  
45  
46  
47  
48  
49  
50  
51  
52  
53  
54  
55  
56  
57  
58  
59  
60

1  
2  
3 pressure to give cyclobutylsulfonyl chloride **2** (3.1 g, crude, >99%) as a pale brown oil,  
4  
5  
6 which was carried into the next step without purification.  
7

8  
9 *2,4-Dichloro-N-((1-(4-(cyclobutylsulfonyl)piperazin-1-yl)cyclohexyl)methyl)benzamide*  
10  
11 *Hydrochloride (36)*. Compound **36** was prepared according to a similar procedure  
12  
13 described for the synthesis of **34** using cyclobutylsulfonyl chloride. mp 249–252 °C; <sup>1</sup>H  
14  
15 NMR (300 MHz, DMSO-*d*<sub>6</sub>) δ 10.57 (bs, 1H), 8.87 (t, *J* = 5.7 Hz, 1H), 7.73 (s, 1H), 7.53 (d, *J*  
16  
17 = 0.6 Hz, 2H), 4.10 (quintet, *J* = 8.4 Hz, 1H), 3.80–3.51 (m, 8H), 3.30–3.05 (m, 2H), 2.40–  
18  
19 2.18 (m, 4H), 2.12–1.45 (m, 12H); ESI MS *m/z* 488 [M+H]<sup>+</sup>; HPLC >99% (AUC), (Method  
20  
21 B), *t*<sub>R</sub> = 21.5 min.  
22  
23  
24  
25

26  
27 *2,4-Dichloro-N-((1-(4-((1-methyl-1H-pyrazol-4-yl)sulfonyl)piperazin-1-*  
28  
29 *yl)cyclohexyl)methyl)benzamide Hydrochloride (37)*. Compound **37** was prepared  
30  
31 according to a similar procedure described for the synthesis of **34** using 1-methyl-1H-  
32  
33 pyrazole-4-sulfonyl chloride. mp 164–165 °C; <sup>1</sup>H NMR (400 MHz, DMSO-*d*<sub>6</sub>) δ 9.40 (bs,  
34  
35 1H), 8.82 (bs, 1H), 8.44 (s, 1H), 7.86 (s, 1H), 7.74 (s, 1H), 7.53 (s, 2H), 3.92 (s, 3H), 3.79–  
36  
37 3.59 (m, 6H), 2.84–2.63 (m, 4H), 2.10–1.99 (m, 2H), 1.74–1.45 (m, 7H), 1.21–0.97 (m,  
38  
39 1H); APCI MS *m/z* 514 [M+H]<sup>+</sup>; HPLC 98.2% (AUC), (Method B), *t*<sub>R</sub> = 18.9 min.  
40  
41  
42  
43

44  
45 *2,4-Dichloro-N-((1-(4-((1-methyl-1H-imidazol-4-yl)sulfonyl)piperazin-1-*  
46  
47 *yl)cyclohexyl)methyl)benzamide Hydrochloride (38)*. Compound **38** was prepared  
48  
49 according to a similar procedure described for the synthesis of **34** using 1-methyl-1H-  
50  
51 imidazole-4-sulfonyl chloride. mp 172–173 °C; <sup>1</sup>H NMR (300 MHz, DMSO-*d*<sub>6</sub>): δ 10.14  
52  
53 (bs, 1H), 8.86 (s, 1H), 7.89 (d, *J* = 8.4 Hz, 2H), 7.73 (s, 1H), 7.52 (s, 2H), 3.79–3.58 (m, 9H),  
54  
55  
56  
57  
58  
59  
60

1  
2  
3 3.42–3.07 (m, 4H), 2.11–1.94 (m, 2H), 1.87–1.41 (m, 7H), 1.21–0.99 (m, 1H); ESI MS  $m/z$   
4  
5 514  $[M+H]^+$ ; HPLC 97.5% (AUC), (Method B),  $t_R = 20.5$  min.  
6  
7

8 *1-Methyl-1H-1,2,3-triazole-4-sulfonyl Chloride*. Step A: To a 10 °C solution of sodium  
9  
10 1H-1,2,3-triazole-4-thiolate (115 g, 0.93 mol) in EtOH (1.1 L) was added benzyl bromide  
11  
12 (111 mL, 0.93 mol) dropwise over a period of 20 min. The mixture stirred at rt for 20  
13  
14 min, and was then diluted with EtOAc (3 L). The organic layer was washed with H<sub>2</sub>O (2 ×  
15  
16 500 mL), brine (500 mL), dried over Na<sub>2</sub>SO<sub>4</sub>, filtered, and concentrated to afford crude 4-  
17  
18 (benzylthio)-1H-1,2,3-triazole as off white solid (165 g, 92%); <sup>1</sup>H NMR (300 MHz, CDCl<sub>3</sub>)  
19  
20  $\delta$  13.37 (bs, 1H), 7.48 (s, 1H), 7.21 (m, 5H), 4.09 (s, 2H); ESI MS  $m/z$  192  $[M+H]^+$ .  
21  
22  
23  
24  
25

26 Step B: To a solution of 4-(benzylthio)-1H-1,2,3-triazole (140 g, 0.73 mol) in DMF (1.4  
27  
28 L) was added K<sub>2</sub>CO<sub>3</sub> (202 g, 1.46 mol), and the resulting mixture stirred at rt for 30 min.  
29  
30 The reaction mixture was then cooled to 0 °C and dimethyl sulfate (104.5 mL, 1.09 mol)  
31  
32 was added dropwise over a period of 15 min. The mixture stirred at rt for 16 h, and was  
33  
34 then diluted with H<sub>2</sub>O (3 L). The aqueous mixture was extracted with EtOAc (5 × 500  
35  
36 mL), and the combined organic extracts were dried over Na<sub>2</sub>SO<sub>4</sub>, filtered, and  
37  
38 concentrated under reduced pressure. The resulting residue was chromatographed over  
39  
40 silica gel (0–50% EtOAc in hexanes) to give 4-(benzylthio)-1-methyl-1H-1,2,3-triazole as  
41  
42 off white solid (34.1 g, 23%); <sup>1</sup>H NMR (400 MHz, CD<sub>3</sub>OD)  $\delta$  7.65 (s, 1H), 7.24–7.16 (m,  
43  
44 5H), 4.04 (s, 2H), 4.0 (s, 3H); ESI MS  $m/z$  206  $[M+H]^+$ . The regioisomer was confirmed via  
45  
46 a <sup>1</sup>H NMR NOESY experiment, which exhibited a positive NOE enhancement between  
47  
48 the methyl group hydrogens and the triazole hydrogen. Furthermore, <sup>1</sup>H NMR NOESY  
49  
50 experiments for the corresponding regioisomers 4-(benzylsulfonyl)-2-methyl-2H-1,2,3-  
51  
52  
53  
54  
55  
56  
57  
58  
59  
60

1  
2  
3 triazole (34.1 g isolated, 23%) and 5-(benzylsulfonyl)-1-methyl-1H-1,2,3-triazole (34.1 g  
4  
5  
6 isolated, 23%) did not exhibit an NOE enhancement between the methyl group  
7  
8  
9 hydrogens and the triazole hydrogen.

10  
11 Step C: To a solution of 4-(benzylthio)-1-methyl-1H-1,2,3-triazole (12.0 g, 58.5 mmol)  
12  
13 in CH<sub>3</sub>CN (600 mL) was added HOAc (20 mL) and H<sub>2</sub>O (15 mL). The mixture was cooled to  
14  
15 5 °C and 1,3-dichloro-5,5-dimethylimidazolidine-2,4-dione (23.0 g, 117.0 mmol) was  
16  
17 added over a period of 20 min. The mixture continued to stir at 5 °C for an additional 2  
18  
19 h. The mixture was cooled to 0 °C and diluted with CH<sub>2</sub>Cl<sub>2</sub> (500 mL). To this was added a  
20  
21 solution of 5% aqueous NaHCO<sub>3</sub> (300 mL), and the mixture stirred for 10 min. The  
22  
23 separated organic layer was washed with brine (300 mL), dried over Na<sub>2</sub>SO<sub>4</sub>, filtered,  
24  
25 and concentrated to afford crude 1-methyl-1H-1,2,3-triazole-4-sulfonyl chloride (14.7 g),  
26  
27 which was used as is in the next step.  
28  
29  
30  
31  
32

33  
34 *2,4-Dichloro-N-((1-(4-((1-methyl-1H-1,2,3-triazol-4-yl)sulfonyl)piperazin-1-*  
35  
36 *yl)cyclohexyl)methyl)benzamide Hydrochloride (39)*. Compound **39** was prepared  
37  
38 according to a similar procedure described for the synthesis of **34** using 1-methyl-1H-  
39  
40 1,2,3-triazole-4-sulfonyl chloride. <sup>1</sup>H NMR (500 MHz, CDCl<sub>3</sub>) δ 7.95 (s, 1H), 7.71 (d, *J* = 8.5  
41  
42 Hz, 1H), 7.41 (d, *J* = 2.0 Hz, 1H), 7.33 (dd, *J* = 8.5, 2.0 Hz, 1H), 6.79 (bs, 1H), 4.19 (s, 3H),  
43  
44 3.57 (d, *J* = 5.0 Hz, 2H), 3.29–3.22 (m, 4H), 2.79–2.73 (m, 4H), 1.68–1.55 (m, 4H), 1.50–  
45  
46 1.40 (m, 5H), 1.28–1.21 (m, 1H); ESI MS *m/z* 515 [M+H]<sup>+</sup>; HPLC 96.6% (AUC), (Method  
47  
48 D), *t<sub>R</sub>* = 5.3 min.  
49  
50  
51  
52

53  
54 *N-((4,4-Difluoro-1-(4-((1-methyl-1H-imidazol-4-yl)sulfonyl)piperazin-1-*  
55  
56 *yl)cyclohexyl)methyl)-2,6-difluorobenzamide Hydrochloride (44)*. Step A: To a 0 °C  
57  
58  
59  
60

1  
2  
3 solution of *tert*-butyl piperazine-1-carboxylate (**12**, 10.0 g, 53.7 mmol) in CH<sub>2</sub>Cl<sub>2</sub> (50 mL)  
4  
5 was added Et<sub>3</sub>N (22.6 mL, 161 mmol) and a solution of 1-methyl-1*H*-imidazole-4-sulfonyl  
6  
7 chloride (11.6 g, 64.5 mmol) in CH<sub>2</sub>Cl<sub>2</sub> (50 mL) drop wise over 30 min while maintaining  
8  
9 the temperature of the reaction mixture below 5 °C. The reaction mixture stirred at rt  
10  
11 for an additional 5 h and was then quenched with a saturated aqueous solution of  
12  
13 NaHCO<sub>3</sub> (50 mL). The aqueous mixture was extracted with CH<sub>2</sub>Cl<sub>2</sub> (3 × 100 mL), and the  
14  
15 combined organic extracts were washed with brine (1 × 50mL), dried over Na<sub>2</sub>SO<sub>4</sub>,  
16  
17 filtered, and concentrated under reduced pressure to give a crude solid. The solids were  
18  
19 suspended in Et<sub>2</sub>O and stirred for 30 min at rt then filtered, washed with cold Et<sub>2</sub>O and  
20  
21 dried under vacuum to afford *tert*-butyl 4-(1-methyl-1*H*-imidazol-4-  
22  
23 ylsulfonyl)piperazine-1-carboxylate (**40**) as an off-white solid (16.8 g, 95 %): <sup>1</sup>H NMR  
24  
25 (300 MHz, CDCl<sub>3</sub>) δ (dd, *J* = 1.5 Hz, 14.5 Hz, 2H), 3.76 (s, 3H), 3.55–3.45 (m, 4H), 3.20–  
26  
27 3.10 (m, 4H), 1.43 (s, 9H); ESI MS *m/z* 331 [M+H]<sup>+</sup>.

28  
29  
30  
31  
32  
33  
34  
35  
36 Step B: To a 0 °C solution of *tert*-butyl 4-(1-methyl-1*H*-imidazol-4-  
37  
38 ylsulfonyl)piperazine-1-carboxylate (**40**, 6.0 g, 18.1 mmol) in 1,4-dioxane (30 mL) was  
39  
40 slowly added 12 N aq HCl (30 mL) dropwise over a period of 30 min. The reaction  
41  
42 mixture stirred at rt for 2 h and was concentrated under reduced pressure. The residue  
43  
44 was azeotroped with toluene (3 × 100 mL) and the resultant solids were dissolved in  
45  
46 H<sub>2</sub>O (100 mL). The aqueous mixture was washed with CH<sub>2</sub>Cl<sub>2</sub> (2 × 100 mL) then carefully  
47  
48 neutralized with solid K<sub>2</sub>CO<sub>3</sub> (15 g). The aqueous mixture was then extracted with CH<sub>2</sub>Cl<sub>2</sub>  
49  
50 (4 × 100 mL) and the combined organic extracts were washed with brine (50 mL), dried  
51  
52 over Na<sub>2</sub>SO<sub>4</sub>, filtered, and concentrated under reduced pressure to afford 1-(1-methyl-  
53  
54  
55  
56  
57  
58  
59  
60

1  
2  
3 1*H*-imidazol-4-ylsulfonyl)piperazine (**41**) as off-white foam (3.8 g, 90 %): <sup>1</sup>H NMR (400  
4 MHz, CDCl<sub>3</sub>) δ (dd, *J* = 1.1 Hz, 16.8 Hz, 2H), 3.80–3.75 (m, 5H), 3.74–3.65 (m, 2H), 3.37–  
5 3.1 (m, 2H), 3.0–3.25 (m, 2H); ESI MS *m/z* 231 [M+H]<sup>+</sup>.

6  
7  
8  
9  
10  
11 Step C: To a 0 °C solution of 4,4-difluorocyclohexanone (3.0 g, 22.3 mmol) in toluene  
12 (20 mL) was added TMSCN (3.3 mL, 24.8 mmol) dropwise, followed by ZnI<sub>2</sub> (0.360 g,  
13 1.13 mmol). The mixture stirred at rt for 15 min followed by addition of a solution of 1-  
14 (1-methyl-1*H*-imidazol-4-ylsulfonyl)piperazine (**41**, 5.12 g, 22.2 mmol) in CH<sub>3</sub>OH (90 mL).  
15  
16 The mixture was then heated at reflux for 4 h followed by stirring at rt for an additional  
17 16 h. The mixture was concentrated under reduced pressure and the resulting residue  
18 was dissolved in CH<sub>2</sub>Cl<sub>2</sub> (100 mL), washed with H<sub>2</sub>O (2 × 50 mL), dried over Na<sub>2</sub>SO<sub>4</sub>,  
19 filtered, and concentrated under reduced pressure to give 4,4- difluoro-1-(4-(1-methyl-  
20 1*H*-imidazol-4-ylsulfonyl)piperazin-1-yl)cyclohexanecarbonitrile (**42**) as an off-white solid  
21 (3.10 g, 37%): <sup>1</sup>H NMR (300 MHz, CDCl<sub>3</sub>) δ 7.52 (d, *J* = 1.2 Hz, 1H), 7.45 (d, *J* = 1.2 Hz, 1H),  
22 3.77 (s, 3H), 3.31 (m, 4H), 2.71 (m, 4H), 2.2–1.85 (m, 8H); APCI MS *m/z* 374 [M+H]<sup>+</sup>.

23  
24  
25  
26  
27  
28  
29  
30  
31  
32  
33  
34  
35  
36  
37  
38  
39 Step D: To a 0 °C solution of 4,4-difluoro-1-(4-(1-methyl-1*H*-imidazol-4-  
40 ylsulfonyl)piperazin-1-yl)cyclohexanecarbonitrile (**42**) (3.79 g, 10.2 mmol) in THF (80 mL)  
41 was added LiAlH<sub>4</sub> (1.32 g, 34.8 mmol) portion-wise over a period of 15 min. The mixture  
42 stirred at rt for 5 h and was then cooled to 0 °C and carefully quenched by with H<sub>2</sub>O (5  
43 mL) and 4 N aq NaOH (1.4 mL). The resulting mixture stirred at rt for 15 min followed by  
44 addition of Na<sub>2</sub>SO<sub>4</sub> (5 g). The mixture was filtered and the filtrate was concentrated  
45 under reduced pressure. The resulting residue was triturated with hexanes and the  
46 solids were filtered and dried under reduced pressure to give (4,4-difluoro-1-(4-((1-  
47  
48  
49  
50  
51  
52  
53  
54  
55  
56  
57  
58  
59  
60

1  
2  
3 methyl-1H-imidazol-4-yl)sulfonyl)piperazin-1-yl)cyclohexyl)methanamine (**43**) (3.36 g,  
4  
5 87%):  $^1\text{H NMR}$  (300 MHz,  $\text{CDCl}_3$ )  $\delta$  7.52 (d,  $J = 1.2$  Hz, 1H), 7.45 (d,  $J = 1.2$  Hz, 1H), 3.77 (s,  
6  
7 3H), 3.18 (m, 4H), 2.71 (m, 4H), 2.2–1.85 (m, 10H); APCI MS  $m/z$  378  $[\text{M}+\text{H}]^+$ .  
8  
9

10  
11 Step E: To a 0 °C solution of (4,4-difluoro-1-(4-((1-methyl-1H-imidazol-4-  
12  
13 yl)sulfonyl)piperazin-1-yl)cyclohexyl)methanamine (**43**, 0.50 g, 1.32 mmol) in  $\text{CH}_2\text{Cl}_2$  (10  
14  
15 mL) was added  $\text{Et}_3\text{N}$  (0.54 mL, 3.97 mmol) and 2,6-difluorobenzoyl chloride (0.233 g,  
16  
17 1.32 mmol). The resulting mixture stirred at rt for 4 h, was diluted with  $\text{CH}_2\text{Cl}_2$ , and then  
18  
19 washed with saturated aqueous  $\text{NaHCO}_3$  solution (10 mL). The organic layer was dried  
20  
21 over  $\text{Na}_2\text{SO}_4$ , filtered, and concentrated under reduced pressure. The resulting residue  
22  
23 was chromatographed over silica gel (0–50% EtOAc in hexanes) to give *N*-((4,4-difluoro-  
24  
25 1-(4-((1-methyl-1H-imidazol-4-yl)sulfonyl)piperazin-1-yl)cyclohexyl)methyl)-2,6-  
26  
27 difluorobenzamide as a white solid (0.409 g, 60%): ESI MS  $m/z$  518  $[\text{M}+\text{H}]^+$ .  
28  
29  
30  
31  
32

33  
34 Step F: To a 0 °C solution of *N*-((4,4-difluoro-1-(4-((1-methyl-1H-imidazol-4-  
35  
36 yl)sulfonyl)piperazin-1-yl)cyclohexyl)methyl)-2,6-difluorobenzamide (0.100 g, 0.19  
37  
38 mmol) in  $\text{CH}_3\text{CN}$  (1 mL) was slowly added a 1.0 M solution of HCl in  $\text{H}_2\text{O}$  (1.5 mL). The  
39  
40 mixture was lyophilized to give *N*-((4,4-difluoro-1-(4-((1-methyl-1H-imidazol-4-  
41  
42 yl)sulfonyl)piperazin-1-yl)cyclohexyl)methyl)-2,6-difluorobenzamide hydrochloride (**44**)  
43  
44 as an amorphous white solid (0.067 g, quantitative): mp 198–199 °C;  $^1\text{H NMR}$  (300 MHz,  
45  
46  $\text{DMSO}-d_6$ )  $\delta$  10.68 (bs, 1H), 9.25 (bs, 1H), 7.88 (m, 2H), 7.52 (m, 1H), 7.22 (m, 2H), 4.00–  
47  
48 3.12 (m, 11H), 2.35–2.03 (m, 10H); APCI MS  $m/z$  519  $[\text{M}+\text{H}]^+$ ; HPLC >99% (AUC),  
49  
50 (Method B),  $t_R = 20.6$  min.  
51  
52  
53  
54  
55  
56  
57  
58  
59  
60

1  
2  
3  
4  
5  
6  
7  
8  
9  
10  
11  
12  
13  
14  
15  
16  
17  
18  
19  
20  
21  
22  
23  
24  
25  
26  
27  
28  
29  
30  
31  
32  
33  
34  
35  
36  
37  
38  
39  
40  
41  
42  
43  
44  
45  
46  
47  
48  
49  
50  
51  
52  
53  
54  
55  
56  
57  
58  
59  
60

*2,6-Dichloro-N-((4,4-difluoro-1-(4-((1-methyl-1H-imidazol-4-yl)sulfonyl)piperazin-1-yl)cyclohexyl)methyl)benzamide Hydrochloride (45)*. Compound **45** was prepared according to a similar procedure described for the synthesis of **44** using 2,6-dichlorobenzoyl chloride. mp 174–175 °C; <sup>1</sup>H NMR (300 MHz, DMSO-*d*<sub>6</sub>) δ 10.56 (s, 1H), 9.16 (s, 1H), 7.89 (m, 2H), 7.58–7.46 (m, 3H), 3.73 (s, 3H), 3.62 (m, 2H), 3.41 (m, 4H), 3.25 (m, 4H), 2.40–2.00 (m, 8H); APCI MS *m/z* 551 [M+H]<sup>+</sup>; HPLC >99% (AUC), (Method B), *t*<sub>R</sub> = 19.0 min.

*2-Chloro-N-((4,4-difluoro-1-(4-((1-methyl-1H-imidazol-4-yl)sulfonyl)piperazin-1-yl)cyclohexyl)methyl)-6-(trifluoromethoxy)benzamide Hydrochloride (46)*. Step A: A mixture of (4,4-difluoro-1-(4-((1-methyl-1H-imidazol-4-yl)sulfonyl)piperazin-1-yl)cyclohexyl)methanamine (**43**, 0.150 g, 0.39 mmol), 2-chloro-6-(trifluoromethoxy)benzoic acid (0.09 g, 0.39 mmol), EDCl•HCl (0.07 g, 0.39 mmol), HOBT (0.05 g, 0.39 mmol), and Et<sub>3</sub>N (0.3 mL, 1.91 mmol) in DMF (10 mL) stirred at rt for 16 h. The mixture was diluted with H<sub>2</sub>O (20) mL and extracted with EtOAc (3 × 20 mL). The combined organic extracts were washed with H<sub>2</sub>O (3 × 20 mL), and brine (20 mL). The organic layers were then dried over Na<sub>2</sub>SO<sub>4</sub>, filtered, and concentrated under reduced pressure. The resulting residue was chromatographed over silica gel (0–50% EtOAc in hexanes) to give 2-chloro-*N-((4,4-difluoro-1-(4-((1-methyl-1H-imidazol-4-yl)sulfonyl)piperazin-1-yl)cyclohexyl)methyl)-6-(trifluoromethoxy)benzamide* as a white solid (0.057 g, 25%): ESI MS *m/z* 601 [M+H]<sup>+</sup>.

Step B: To a 0 °C solution of 2-chloro-*N-((4,4-difluoro-1-(4-((1-methyl-1H-imidazol-4-yl)sulfonyl)piperazin-1-yl)cyclohexyl)methyl)-6-(trifluoromethoxy)benzamide* (0.050 g,



0.08 mmol) in CH<sub>3</sub>CN (5 mL) was added a 1.0 M solution of HCl in H<sub>2</sub>O (1.0 mL, 1.0 mmol). The mixture stirred at rt for 30 min and was lyophilized to give 2-chloro-*N*-((4,4-difluoro-1-(4-((1-methyl-1*H*-imidazol-4-yl)sulfonyl)piperazin-1-yl)cyclohexyl)methyl)-6-(trifluoromethoxy)benzamide hydrochloride (**46**) as a white solid (0.021 g, 50%): mp 185–188 °C; <sup>1</sup>H NMR (300 MHz, DMSO-*d*<sub>6</sub>) δ 10.09 (s, 1H), 9.14 (s, 1H), 7.89 (m, 2H), 7.55 (m, 3H), 3.73 (s, 3H), 3.62 (m, 2H), 3.41 (m, 4H), 3.25 (m, 4H), 2.40–2.00 (m, 8H); ESI MS *m/z* 600 [M+H]<sup>+</sup>; HPLC >99% (AUC), (Method B), *t*<sub>R</sub> = 22.8 min.

*2,4-Dichloro-N*-((4,4-difluoro-1-(4-((1-methyl-1*H*-imidazol-4-yl)sulfonyl)piperazin-1-yl)cyclohexyl)methyl)benzamide Hydrochloride (**47**). Compound **47** was prepared according to a similar procedure described for the synthesis of **44** using 2,4-dichlorobenzoyl chloride. mp 235 °C; <sup>1</sup>H NMR (300 MHz, DMSO-*d*<sub>6</sub>) δ 10.27 (s, 1H), 8.97 (s, 1H), 7.89 (m, 2H), 7.74 (m, 1H), 7.55 (m, 2H), 7.58–7.46 (m, 3H), 3.73 (s, 3H), 3.62 (m, 3H), 3.41 (m, 2H), 3.25 (m, 2H), 2.40–2.00 (m, 8H); ESI MS *m/z* 550 [M+H]<sup>+</sup>; HPLC 97.8% (AUC), (Method B), *t*<sub>R</sub> = 19.5 min.

*2-Chloro-N*-((4,4-difluoro-1-(4-((1-methyl-1*H*-imidazol-4-yl)sulfonyl)piperazin-1-yl)cyclohexyl)methyl)-4-fluorobenzamide Hydrochloride (**48**). Compound **48** was prepared according to a similar procedure described for the synthesis of **46** using 2-chloro-4-fluorobenzoic acid. mp 232 °C; <sup>1</sup>H NMR (300 MHz, DMSO-*d*<sub>6</sub>) δ 10.15 (s, 1H), 8.91 (s, 1H), 7.86 (m, 2H), 7.80–7.34 (m, 3H), 3.73 (s, 3H), 3.62 (m, 2H), 3.41 (m, 4H), 3.25 (m, 4H), 2.40–2.00 (m, 8H); ESI MS *m/z* 534 [M+H]<sup>+</sup>; HPLC 97.1% (AUC), (Method B), *t*<sub>R</sub> = 19.6 min.

1  
2  
3  
4  
5  
6  
7  
8  
9  
10  
11  
12  
13  
14  
15  
16  
17  
18  
19  
20  
21  
22  
23  
24  
25  
26  
27  
28  
29  
30  
31  
32  
33  
34  
35  
36  
37  
38  
39  
40  
41  
42  
43  
44  
45  
46  
47  
48  
49  
50  
51  
52  
53  
54  
55  
56  
57  
58  
59  
60

*2-Chloro-N-((4,4-difluoro-1-(4-((1-methyl-1H-imidazol-4-yl)sulfonyl)piperazin-1-yl)cyclohexyl)methyl)-4-(trifluoromethyl)benzamide Hydrochloride (49)*. Compound **49** was prepared according to a similar procedure described for the synthesis of **46** using 2-chloro-4-(trifluoromethyl)benzoic acid. mp 181–183 °C; <sup>1</sup>H NMR (300 MHz, DMSO-*d*<sub>6</sub>) δ 10.78 (s, 1H), 9.07 (s, 1H), 7.89 (m, 4H), 7.71 (m, 1H), 3.73 (s, 3H), 3.62 (m, 2H), 3.41 (m, 4H), 3.25 (m, 4H), 2.40–2.00 (m, 8H); APCI MS *m/z* 585 [M+H]<sup>+</sup>; HPLC 98.8% (AUC), (Method B), *t*<sub>R</sub> = 20.3 min.

*N-((4,4-Difluoro-1-(4-((1-methyl-1H-1,2,3-triazol-4-yl)sulfonyl)piperazin-1-yl)cyclohexyl)methyl)-2,6-difluorobenzamide Hydrochloride (54)*. Step A: To a 0 °C solution of *tert*-butyl piperazine-1-carboxylate (**12**, 10.0 g, 53.7 mmol) and Et<sub>3</sub>N (22.6 mL, 161.2 mmol) in CH<sub>2</sub>Cl<sub>2</sub> (50 mL) was added and a solution of 1-methyl-1H-1,2,3-triazole-4-sulfonyl chloride (11.7 g, 64.5 mmol) in CH<sub>2</sub>Cl<sub>2</sub> (50 mL) dropwise over a period of 30 min. The reaction mixture stirred at rt for 5 h and was then washed with a saturated solution of NaHCO<sub>3</sub> (50 mL) and brine (50 mL). The organic layer was dried over Na<sub>2</sub>SO<sub>4</sub>, filtered, and concentrated under reduced pressure to give *tert*-butyl 4-((1-methyl-1H-1,2,3-triazol-4-yl)sulfonyl)piperazine-1-carboxylate (**50**) as a crude solid, which was used as is in the next step.

Step B: *Tert*-butyl 4-((1-methyl-1H-1,2,3-triazol-4-yl)sulfonyl)piperazine-1-carboxylate (**50**) was dissolved in CH<sub>2</sub>Cl<sub>2</sub> (50 mL). This solution was cooled to 0 °C and TFA (30.6 g, 268.5 mmol) was added. The mixture stirred at rt for 16 h and was then neutralized with a saturated aqueous solution of NaHCO<sub>3</sub>. The separated organic layer was washed with brine (50 mL), dried over Na<sub>2</sub>SO<sub>4</sub>, filtered, and concentrated under

1  
2  
3 reduced pressure to give 1-((1-methyl-1H-1,2,3-triazol-4-yl)sulfonyl)piperazine (**51**) as  
4  
5 crude solid, which was used as is in the next step (8.4 g, 68%): ESI MS  $m/z$  232 [M+H]<sup>+</sup>.  
6  
7

8 Step C: To a 0 °C solution of 4,4-difluorocyclohexanone (2.0 g, 14.9 mmol) in toluene  
9  
10 (20 mL) was added TMSCN (2.18 mL, 16.3 mmol) dropwise, followed by ZnI<sub>2</sub> (0.236 g,  
11  
12 0.74 mmol). The mixture stirred at rt for 15 min followed by addition of a solution of 1-  
13  
14 ((1-methyl-1H-1,2,3-triazol-4-yl)sulfonyl)piperazine (**51**, 3.43 g, 14.8 mmol) in CH<sub>3</sub>OH (90  
15  
16 mL). The mixture was heated at reflux for 4 h, then at rt for 16 h. The mixture was  
17  
18 concentrated under reduced pressure. The resulting residue was dissolved in CH<sub>2</sub>Cl<sub>2</sub>  
19  
20 (100 mL), washed with H<sub>2</sub>O (2 × 50 mL), dried over Na<sub>2</sub>SO<sub>4</sub>, filtered, and concentrated  
21  
22 under reduced pressure to give 4,4-difluoro-1-(4-((1-methyl-1H-1,2,3-triazol-4-  
23  
24 yl)sulfonyl)piperazin-1-yl)cyclohexanecarbonitrile (**52**) as an off-white solid (1.89 g,  
25  
26 34%): ESI MS  $m/z$  375 [M+H]<sup>+</sup>.  
27  
28  
29  
30  
31  
32

33 Step D: To a 0 °C solution of 4,4-difluoro-1-(4-((1-methyl-1H-1,2,3-triazol-4-  
34  
35 yl)sulfonyl)piperazin-1-yl)cyclohexanecarbonitrile (**52**, 2.0 g, 5.34 mmol) in THF (80 mL)  
36  
37 was added LiAlH<sub>4</sub> (0.691 g, 18.2 mmol) portion-wise over 15 min. The mixture stirred at  
38  
39 rt for 5 h then cooled to 0 °C and carefully quenched by with H<sub>2</sub>O (5 mL), 4 N aq NaOH  
40  
41 (1.4 mL). The resulting mixture stirred at rt 15 min followed by addition of Na<sub>2</sub>SO<sub>4</sub> (5 g).  
42  
43  
44 The mixture stirred for an additional 30 min and was filtered. The filtrate concentrated  
45  
46 under reduced pressure and the resulting residue was triturated with hexanes to give a  
47  
48 white solid, which was filtered and dried under reduced pressure to give (4,4-difluoro-1-  
49  
50 (4-((1-methyl-1H-1,2,3-triazol-4-yl)sulfonyl)piperazin-1-yl)cyclohexyl)methanamine (**53**)  
51  
52 as a white foam (1.75 g, 87%): <sup>1</sup>H NMR (300 MHz, CDCl<sub>3</sub>) δ 7.94 (s, 1H), 4.19 (s,  
53  
54  
55  
56  
57  
58  
59  
60

1  
2  
3 3H), 3.22 (s, 4H), 2.79–2.80 (m, 4H), 2.71 (s, 2H), 1.75–1.95 (m, 6H), 1.55–1.65 (m, 2H);  
4  
5  
6 ESI MS  $m/z$  379 [M+H]<sup>+</sup>.  
7

8  
9 Step E: To a 0 °C solution of (4,4-difluoro-1-(4-((1-methyl-1H-1,2,3-triazol-4-  
10  
11 yl)sulfonyl)piperazin-1-yl)cyclohexyl)methanamine (**53**, 0.500 g, 1.32 mmol) in CH<sub>2</sub>Cl<sub>2</sub> (10  
12  
13 mL) was added Et<sub>3</sub>N (0.54 mL, 3.97 mmol) and 2,6-difluorobenzoyl chloride (0.233 g,  
14  
15 1.32 mmol). The resulting mixture stirred at rt for 4 h, was diluted with CH<sub>2</sub>Cl<sub>2</sub>, and then  
16  
17 washed with saturated aqueous NaHCO<sub>3</sub> solution (10 mL). The organic layer was dried  
18  
19 over Na<sub>2</sub>SO<sub>4</sub>, filtered, and concentrated under reduced pressure. The resulting residue  
20  
21 was chromatographed over silica gel (0–50% EtOAc in hexanes) to give *N*-((4,4-difluoro-  
22  
23 1-(4-((1-methyl-1H-1,2,3-triazol-4-yl)sulfonyl)piperazin-1-yl)cyclohexyl)methyl)-2,6-  
24  
25 difluorobenzamide as a white solid (0.465 g, 68%): <sup>1</sup>H NMR (300 MHz, DMSO-*d*<sub>6</sub>) δ 7.96  
26  
27 (s, 1H), 7.39 (m, 1H), 6.96 (m, 2H), 6.08 (m, 1H), 4.19 (s, 3H), 3.55 (d, *J* = 6.2 Hz, 2H), 3.28  
28  
29 (m, 4H), 2.79 (m, 4H), 1.93 (m, 6H), 1.67 (m, 2H), 1.26 (m, 4H); ESI MS  $m/z$  518 [M+H]<sup>+</sup>.  
30  
31  
32  
33  
34  
35

36  
37 Step F: To a 0 °C solution of *N*-((4,4-difluoro-1-(4-(1-methyl-1H-1,2,3-triazol-4-  
38  
39 ylsulfonyl)piperazin-1-yl)cyclohexyl)methyl)-2,6-difluorobenzamide (0.153 g, 0.295  
40  
41 mmol) in CH<sub>3</sub>CN (1 mL) was added a 1.0 M solution of HCl in H<sub>2</sub>O (5 mL). The mixture  
42  
43 stirred at rt for 30 min and was lyophilized to give *N*-((4,4-difluoro-1-(4-(1-methyl-1H-  
44  
45 1,2,3-triazol-4-ylsulfonyl)piperazin-1-yl)cyclohexyl)methyl)-2,6-difluorobenzamide  
46  
47 hydrochloride (**54**) as a white solid (0.163 g, quantitative): mp 202–205 °C; <sup>1</sup>H NMR (300  
48  
49 MHz, DMSO-*d*<sub>6</sub>) δ 9.24 (m, 1H), 8.71 (m, 2H), 7.53 (m, 1H), 7.20 (m, 2H), 4.14 (s, 3H),  
50  
51  
52 3.86 (m, 2H), 3.39 (m, 2H), 3.12 (m, 3H), 2.73 (m, 2H), 2.11 (m, 2H), 1.91 (m, 2H), 1.78  
53  
54  
55  
56  
57  
58  
59  
60

(m, 2H), 1.53 (m, 2H); APCI MS  $m/z$  519  $[M+H]^+$ ; HPLC >99% (AUC), (Method C),  $t_R$  = 18.0 min.

*2,6-Dichloro-N-((4,4-difluoro-1-(4-((1-methyl-1H-1,2,3-triazol-4-yl)sulfonyl)piperazin-1-yl)cyclohexyl)methyl)benzamide Hydrochloride (55)*. Compound **55** was prepared according to a similar procedure described for the synthesis of **54** using 2,6-dichlorobenzoyl chloride. mp 265–270 °C;  $^1\text{H}$  NMR (300 MHz, DMSO- $d_6$ )  $\delta$  10.13 (bs, 1H), 8.70 (bs, 1H), 8.95–8.55 (m, 1H), 7.67–7.37 (m, 3H), 4.13 (s, 3H), 3.80–3.75 (m, 2H), 3.73–3.33 (m, 2H), 3.33–2.89 (m, 4H), 2.78 (m, 2H), 2.44–1.51 (m, 8H); ESI MS  $m/z$  551  $[M+H]^+$ ; HPLC 97.8% (AUC), (Method C),  $t_R$  = 18.5 min.

*2-Chloro-N-((4,4-difluoro-1-(4-((1-methyl-1H-1,2,3-triazol-4-yl)sulfonyl)piperazin-1-yl)cyclohexyl)methyl)-6-(trifluoromethoxy)benzamide Hydrochloride (56)*. Step A: A mixture of (4,4-difluoro-1-(4-(1-methyl-1H-1,2,3-triazol-4-yl)sulfonyl)piperazin-1-yl)cyclohexyl)methanamine (**53**, 0.150 g, 0.39 mmol), 2-chloro-6-(trifluoromethoxy)benzoic acid (0.09 g, 0.39 mmol), EDCI•HCl (0.07 g, 0.39 mmol), HOBT (0.050 g, 0.39 mmol), and Et<sub>3</sub>N (0.37 mL, 1.93 mmol) in DMF (10 mL) stirred at rt for 16 h. The mixture was diluted with H<sub>2</sub>O (20) mL and extracted with EtOAc (3 × 20 mL). The combined organic extracts were washed with H<sub>2</sub>O (3 × 20 mL), and brine (20 mL). The organic layers were then dried over Na<sub>2</sub>SO<sub>4</sub>, filtered, and concentrated under reduced pressure. The resulting residue was chromatographed over silica gel (0–50% EtOAc in hexanes) to give 2-chloro-N-((4,4-difluoro-1-(4-(1-methyl-1H-1,2,3-triazol-4-yl)sulfonyl)piperazin-1-yl)cyclohexyl)methyl)-6-(trifluoromethoxy)benzamide as a white solid (0.051 g, 20%):  $^1\text{H}$  NMR (300 MHz, CDCl<sub>3</sub>)  $\delta$  8.12 (s, 1H), 7.95 (s, 1H), 7.36–7.39 (m,

2H), 5.82–5.89 (m, 1H), 4.19 (s, 3H), 3.56 (d,  $J = 6.2$  Hz, 2H), 3.25–3.33 (m, 4H), 2.74–2.82 (m, 4H), 1.81–1.99 (m, 6H), 1.72–1.80 (m, 2H); ESI MS  $m/z$  601  $[M+H]^+$ .

Step B: To a 0 °C solution of 2-chloro-*N*-((4,4-difluoro-1-(4-(1-methyl-1H-1,2,3-triazol-4-ylsulfonyl)piperazin-1-yl)cyclohexyl)methyl)-6-(trifluoromethoxy)benzamide (0.051 g, 0.08 mmol) in CH<sub>3</sub>CN was added a 1.0 M solution of HCl in H<sub>2</sub>O (1.0 mL, 1.0 mmol). The mixture stirred at rt for 30 min and was lyophilized to give 2-chloro-*N*-((4,4-difluoro-1-(4-(1-methyl-1H-1,2,3-triazol-4-ylsulfonyl)piperazin-1-yl)cyclohexyl)methyl)-6-(trifluoromethoxy)benzamide hydrochloride (**56**) as a white solid (0.021 g, 50%): mp 260–265 °C; <sup>1</sup>H NMR (300 MHz, DMSO-*d*<sub>6</sub>)  $\delta$  10.30 (bs, 1H), 9.15 (bs, 1H), 8.95–8.55 (m, 1H), 7.77–7.32 (m, 3H), 4.13 (s, 3H), 3.80–3.75 (m, 2H), 3.73–3.33 (m, 2H), 3.32–2.89 (m, 4H), 2.87–2.74 (m, 2H), 2.44–1.51 (m, 8H); ESI MS  $m/z$  601  $[M+H]^+$ ; HPLC 98.3% (AUC), (Method C),  $t_R = 20.1$  min.

*2,4-Dichloro-N*-((4,4-difluoro-1-(4-((1-methyl-1H-1,2,3-triazol-4-yl)sulfonyl)piperazin-1-yl)cyclohexyl)methyl)benzamide Hydrochloride (**57**). Compound **57** was prepared according to a similar procedure described for the synthesis of **55** using 2,4-dichlorobenzoyl chloride. mp 175–180 °C; <sup>1</sup>H NMR (300 MHz, DMSO-*d*<sub>6</sub>)  $\delta$  10.31 (bs, 1H), 8.70–8.92 (m, 1H), 8.33–8.45 (m, 1H), 7.62–7.71 (m, 1H), 7.32–7.57 (m, 2H), 4.13 (s, 3H), 3.75–3.80 (m, 2H), 3.33–3.73 (m, 2H), 2.89–3.33 (m, 4H), 2.78–2.89 (m, 2H), 1.51–2.44 (m, 8H); ESI MS  $m/z$  551  $[M+H]^+$ ; HPLC 97.4% purity (Method A).

*2-Chloro-N*-((4,4-difluoro-1-(4-((1-methyl-1H-1,2,3-triazol-4-yl)sulfonyl)piperazin-1-yl)cyclohexyl)methyl)-4-fluorobenzamide Hydrochloride (**58**). Compound **58** was prepared according to a similar procedure described for the synthesis of **56** using 2-

1  
2  
3  
4  
5  
6  
7  
8  
9  
10  
11  
12  
13  
14  
15  
16  
17  
18  
19  
20  
21  
22  
23  
24  
25  
26  
27  
28  
29  
30  
31  
32  
33  
34  
35  
36  
37  
38  
39  
40  
41  
42  
43  
44  
45  
46  
47  
48  
49  
50  
51  
52  
53  
54  
55  
56  
57  
58  
59  
60

chloro-4-fluorobenzoic acid. mp 230–232 °C; <sup>1</sup>H NMR (300 MHz, DMSO-*d*<sub>6</sub>) δ 10.13 (bs, 0.4H), 8.91 (bs, 0.6H), 9.95 (bs, 1H), 8.35–8.51 (m, 1H), 7.21–7.67 (m, 3H), 4.13 (s, 3H), 3.75–3.80 (m, 2H), 3.33–3.73 (m, 3H), 2.89–3.33 (m, 4H), 2.78–2.89 (m, 2H), 1.51–2.44 (m, 8H); ESI MS *m/z* 535 [M+H]<sup>+</sup>; HPLC 98.7% (AUC), (Method C), *t*<sub>R</sub> = 18.4 min.

*2-Chloro-N-((4,4-difluoro-1-(4-((1-methyl-1H-1,2,3-triazol-4-yl)sulfonyl)piperazin-1-yl)cyclohexyl)methyl)-4-(trifluoromethyl)benzamide Hydrochloride (59)*. Compound **59** was prepared according to a similar procedure described for the synthesis of **56** using 2-chloro-4-(trifluoromethyl)benzoic acid. mp 190–192 °C; <sup>1</sup>H NMR (300 MHz, DMSO-*d*<sub>6</sub>) δ 10.31 (bs, 1H), 9.15 (bs, 1H), 8.55–8.95 (m, 1H), 7.52–8.05 (m, 3H), 4.13 (s, 3H), 3.75–3.80 (m, 2H), 3.33–3.73 (m, 2H), 2.89–3.33 (m, 4H), 2.78–2.89 (m, 2H), 1.51–2.44 (m, 8H); ESI MS *m/z* 585 [M+H]<sup>+</sup>; %CHNCl for C<sub>22</sub>H<sub>26</sub>ClF<sub>5</sub>N<sub>6</sub>O<sub>3</sub>S•HCl: calcd %C = 42.52, %H = 4.38, %N = 13.52, %Cl = 11.41; found %C = 42.38, %H = 4.31, %N = 13.37, %Cl = 11.24; HPLC 98.0% (AUC), (Method C), *t*<sub>R</sub> = 20.2 min.

*N-((4,4-Difluoro-1-(4-((1-methyl-1H-1,2,3-triazol-4-yl)sulfonyl)piperazin-1-yl)cyclohexyl)methyl)-2,4-bis(trifluoromethyl)benzamide Hydrochloride (60)*. Compound **60** was prepared according to a similar procedure described for the synthesis of **56** using 2,4-bis(trifluoromethyl)benzoic acid. mp 180–182 °C; <sup>1</sup>H NMR (300 MHz, DMSO-*d*<sub>6</sub>) δ 8.75 (s, 1H), 8.62 (s, 1H), 8.18–8.12 (m, 2H), 7.74–7.71 (m, 1H), 4.15 (s, 3H), 3.31–3.30 (m, 2H), 3.10–2.90 (m, 4H), 2.85–2.70 (m, 4H), 2.00–1.40 (m, 8H); ESI MS *m/z* 619 [M+H]<sup>+</sup>; HPLC >99% (AUC), (Method C), *t*<sub>R</sub> = 20.9 min.

*2-Chloro-N-(1-(4,4-difluoro-1-(4-((1-methyl-1H-1,2,3-triazol-4-yl)sulfonyl)piperazin-1-yl)cyclohexyl)ethyl)-4-(trifluoromethyl)benzamide Hydrochloride ((-)-66 and (+)-67)*. Step

1  
2  
3 A: ZnI<sub>2</sub> (2.53 g, 7.95 mmol) was added to a solution of 1-benzylpiperazine (**24**, 14.0 g,  
4 79.5 mmol) and 4,4-difluorocyclohexanone (10.6 g, 79.5 mmol) in a 1:1 mixture of  
5 toluene and CH<sub>3</sub>OH (160 mL), and the resulting mixture stirred at rt for 1 h. The reaction  
6 mixture was cooled to 0 °C and TMSCN (11.0 mL, 87.4 mmol) was added dropwise over  
7 a period of 15 min. The reaction mixture stirred at rt for 4 h then at reflux for 12 hr. The  
8 reaction mixture was allowed to cool to rt and was concentrated under reduced  
9 pressure. The resulting residue was dissolved in EtOAc (300 mL) and the organic layer  
10 was washed with H<sub>2</sub>O (2 × 200 mL) and brine (1 × 100 mL). The organic layer was dried  
11 over Na<sub>2</sub>SO<sub>4</sub>, filtered, and concentrated under reduced pressure, and the resulting  
12 residue was chromatographed over silica gel (0–10% EtOAc in hexanes) to give 1-(4-  
13 benzylpiperazin-1-yl)-4,4-difluorocyclohexanecarbonitrile (**61**) as white amorphous solid  
14 (24.6 g, 97 %): <sup>1</sup>H NMR (300 MHz, CDCl<sub>3</sub>) δ 7.37–7.27 (m, 5H), 3.50 (s, 2H), 2.72 (m, 4H),  
15 2.53 (m, 4H), 2.21–1.93 (m, 8H).

16  
17  
18  
19  
20  
21  
22  
23  
24  
25  
26  
27  
28  
29  
30  
31  
32  
33  
34  
35  
36 Step B: To a 0 °C solution of 1-(4-benzylpiperazin-1-yl)-4,4-  
37 difluorocyclohexanecarbonitrile (**61**, 16.0 g, 50.14 mmol) in anhydrous Et<sub>2</sub>O (160 mL)  
38 was added a 3.0 M solution of CH<sub>3</sub>Li in DME (25 mL, 75.2 mmol) dropwise. The mixture  
39 was then heated at reflux for 6 h, and then cooled to 0 °C. To this mixture was added  
40 NaBH<sub>4</sub> (5.68 g, 15.0 mmol) followed by dropwise addition of CH<sub>3</sub>OH (160 mL). The  
41 mixture stirred at rt for 2 h, followed by dropwise addition H<sub>2</sub>O (25 mL). The mixture  
42 was concentrated under reduced pressure and the resulting residue was dissolved in  
43 EtOAc (300 mL). The organic layer was washed with H<sub>2</sub>O (100 mL), brine (100 mL), dried  
44 over Na<sub>2</sub>SO<sub>4</sub>, filtered, and concentrated to afford 1-(1-(4-benzylpiperazin-1-yl)-4,4-



1  
2  
3 difluorocyclohexyl)ethanamine as an oil (17.8 g, crude, >99%). To a 0 °C solution of 1-(1-  
4 (4-benzylpiperazin-1-yl)-4,4-difluorocyclohexyl)ethanamine (17.8 g, crude, 52.9 mmol)  
5 and Et<sub>3</sub>N (14.8 mL, 105 mmol) in CH<sub>2</sub>Cl<sub>2</sub> (100 mL) was added a solution of di-*tert*-butyl  
6 dicarbonate (12.71 g, 58.2 mmol) in CH<sub>2</sub>Cl<sub>2</sub> (80 mL) dropwise over a period of 15 min.  
7  
8 The mixture stirred at rt for 5 h and was washed with H<sub>2</sub>O (2 × 150 mL) and brine (150  
9 mL). The organic layer was dried over Na<sub>2</sub>SO<sub>4</sub>, filtered, and concentrated under reduced  
10 pressure. The resulting residue was chromatographed over silica gel (0–30% EtOAc in  
11 hexanes) to afford (*±*)-*tert*-butyl (1-(1-(4-benzylpiperazin-1-yl)-4,4-  
12 difluorocyclohexyl)ethyl)carbamate ((*±*)-**62**) as white solid (18.4 g, 80 %): <sup>1</sup>H NMR (300  
13 MHz, CDCl<sub>3</sub>) δ 7.35–7.28 (m, 5H), 4.35 (m, 1H), 3.87 (m, 1H), 3.48 (s, 2H), 2.78 (m, 4H),  
14 2.41 (m, 4H), 1.77 (m, 5H), 1.42 (m, 10 H), 1.05 (d, *J* = 4.2 Hz, 3H).  
15  
16  
17  
18  
19  
20  
21  
22  
23  
24  
25  
26  
27  
28  
29  
30

31 Step C: A mixture of (*±*)-*tert*-butyl (1-(1-(4-benzylpiperazin-1-yl)-4,4-  
32 difluorocyclohexyl)ethyl)carbamate ((*±*)-**62**, 11.3 g, 25.8 mmol), 10% Pd/C (10% wt/wt  
33 loading, 2.26 g), and ammonium formate (16.2 g, 258 mmol) in CH<sub>3</sub>OH (180 mL) was  
34 heated at reflux for 4 h. The mixture was allowed to cool to rt and was filtered through a  
35 pad of Celite. The filtrate was concentrated under reduced pressure to afford (*±*)-*tert*-  
36 butyl (1-(4,4-difluoro-1-(piperazin-1-yl)cyclohexyl)ethyl)carbamate ((*±*)-**63**) (8.0 g, crude)  
37 as colorless foam, which was used as is in the next step.  
38  
39  
40  
41  
42  
43  
44  
45  
46  
47

48 Step D: Crude (*±*)-*tert*-butyl (1-(4,4-difluoro-1-(piperazin-1-  
49 yl)cyclohexyl)ethyl)carbamate ((*±*)-**63**, 8.0 g, 23.0 mmol) was dissolved in CH<sub>2</sub>Cl<sub>2</sub> (50 mL)  
50 and cooled to 0 °C. To this solution was added Et<sub>3</sub>N (16.2 mL, 115.2 mmol) followed by  
51 dropwise addition of a solution of 1-methyl-1H-1,2,3-triazole-4-sulfonyl chloride (6.25 g,  
52  
53  
54  
55  
56  
57  
58  
59  
60

1  
2  
3 34.5 mmol) in CH<sub>2</sub>Cl<sub>2</sub> (50 mL). The mixture was stirred at rt for 2 h and was diluted with  
4  
5 CH<sub>2</sub>Cl<sub>2</sub> (250 mL) and washed with saturated aqueous NaHCO<sub>3</sub> (100 mL). The organic  
6  
7 layer was washed with brine (100 mL), dried over Na<sub>2</sub>SO<sub>4</sub>, filtered, and concentrated  
8  
9 under reduced pressure to afford (±)-*tert*-butyl (1-(4,4-difluoro-1-(4-((1-methyl-1H-  
10  
11 1,2,3-triazol-4-yl)sulfonyl)piperazin-1-yl)cyclohexyl)ethyl)carbamate ((±)-**64**) as off white  
12  
13 solid (8.1 g, over two steps 71%): <sup>1</sup>H NMR (300 MHz, CDCl<sub>3</sub>) δ 8.00 (s, 1H), 4.41 (m, 1H),  
14  
15 3.89 (m, 1H), 3.21 (m, 3H), 2.85 (m, 4H), 1.90–1.71 (m, 6H), 1.42 (m, 10 H), 1.05 (d, *J* =  
16  
17 4.2 Hz, 3H).

18  
19  
20  
21  
22  
23 Step E: To a to 0 °C solution of (±)-*tert*-butyl (1-(4,4-difluoro-1-(4-((1-methyl-1H-  
24  
25 1,2,3-triazol-4-yl)sulfonyl)piperazin-1-yl)cyclohexyl)ethyl)carbamate ((±)-**64**, 8.0 g, 16.2  
26  
27 mmol) in CH<sub>3</sub>OH (40 mL), was slowly added 12 N aq HCl (40 mL) over a period of 30 min.  
28  
29 The mixture stirred at rt for 5 h, and was concentrated under reduced pressure. The  
30  
31 resulting residue was dissolved in H<sub>2</sub>O (50 mL) and neutralized with solid NaHCO<sub>3</sub>. The  
32  
33 aqueous mixture was extracted with EtOAc (2 × 100 mL), and the combined organic  
34  
35 extracts were washed with brine (100 mL), dried over Na<sub>2</sub>SO<sub>4</sub>, filtered, and concentrated  
36  
37 under reduced pressure to afford (±)-1-(4,4-difluoro-1-(4-((1-methyl-1H-1,2,3-triazol-4-  
38  
39 yl)sulfonyl)piperazin-1-yl)cyclohexyl)ethanamine as white solid ((±)-**64**, 6.2 g, 97 %): ESI  
40  
41 MS *m/z* 393 [M+H]<sup>+</sup>.

42  
43  
44 To a solution of (±)-1-(4,4-difluoro-1-(4-((1-methyl-1H-1,2,3-triazol-4-  
45  
46 yl)sulfonyl)piperazin-1-yl)cyclohexyl)ethanamine ((±)-**64**, 4.7 g, 11.9 mmol ) in DMF (50  
47  
48 ml), was added 2-chloro-4-(trifluoromethyl)benzoic acid (2.95 g, 13.1 mmol), HOBt (2.42  
49  
50 g, 17.9 mmol), EDCl•HCl (3.43 g, 17.9 mmol), and Et<sub>3</sub>N (5.0 ml, 35.9 mmol). The resulting  
51  
52  
53  
54  
55  
56  
57  
58  
59  
60

1  
2  
3 mixture stirred at rt for 16 h and was diluted with H<sub>2</sub>O (300 ml). The aqueous mixture  
4  
5 was extracted with EtOAc (2 × 100 mL), and the combined organic extracts were washed  
6  
7 with H<sub>2</sub>O (3 × 100 mL) and brine (150 mL). The organic layer was dried over Na<sub>2</sub>SO<sub>4</sub>,  
8  
9 filtered, and concentrated under reduced pressure. The resulting residue was  
10  
11 chromatographed over silica gel (0–10% EtOAc in hexanes) to give (±)-2-chloro-*N*-(1-  
12  
13 (4,4-difluoro-1-(4-((1-methyl-1*H*-1,2,3-triazol-4-yl)sulfonyl)piperazin-1-  
14  
15 (4,4-difluoro-1-(4-((1-methyl-1*H*-1,2,3-triazol-4-yl)sulfonyl)piperazin-1-  
16  
17 (yl)cyclohexyl)ethyl)-4-(trifluoromethyl)benzamide as an off-white solid ((±)-**65**, 5.0 g,  
18  
19 69%); <sup>1</sup>H NMR (300 MHz, DMSO-*d*<sub>6</sub>) δ 8.79 (s, 1H), 8.48 (m, 1H), 7.95 (s, 1H), 7.80 (m,  
20  
21 1H), 7.55 (m, 1H), 4.26 (m, 1H), 4.13 (s, 3H), 3.20–2.30 (m, 7H), 2.00–1.51 (m, 9H), 1.10  
22  
23 (m, 3H); APCI MS *m/z* 599 [M+H]<sup>+</sup>.  
24  
25  
26  
27

28  
29 Step F: (±)-2-Chloro-*N*-(1-(4,4-difluoro-1-(4-((1-methyl-1*H*-1,2,3-triazol-4-  
30  
31 (yl)sulfonyl)piperazin-1-yl)cyclohexyl)ethyl)-4-(trifluoromethyl)benzamide ((±)-**65**, 0.289  
32  
33 g) was resolved by preparative chiral HPLC to give (-)-**66** (after treatment with 1.0 M  
34  
35 solution of HCl in H<sub>2</sub>O in CH<sub>3</sub>CN to give the corresponding HCl salt) as a white solid  
36  
37 (0.121 g, 41%) and (+)-**67** (after treatment with 1.0 M solution of HCl in H<sub>2</sub>O in CH<sub>3</sub>CN to  
38  
39 give the corresponding HCl salt) as a white solid (0.112 g, 38%).  
40  
41  
42  
43  
44  
45

46 Spectral data for (-)-**66**: mp 134–136 °C; <sup>1</sup>H NMR (300 MHz, DMSO-*d*<sub>6</sub>) δ 8.79 (s, 1H),  
47  
48 8.48 (m, 1H), 7.95 (s, 1H), 7.80 (m, 1H), 7.55 (m, 1H), 4.26 (m, 1H), 4.13 (s, 3H), 3.20–  
49  
50 2.30 (m, 7H), 2.00–1.51 (m, 9H), 1.10 (m, 3H); APCI MS *m/z* 599 [M+H]<sup>+</sup>; HPLC >99%  
51  
52 (AUC), (Method B), *t*<sub>R</sub> = 26.0 min; [α]<sub>D</sub><sup>20</sup> = -9.78° (*c* = 0.47, CH<sub>3</sub>OH); chiral HPLC >99%  
53  
54 (AUC), (Method E), *t*<sub>R</sub> = 7.45 min.  
55  
56  
57  
58  
59  
60

1  
2  
3  
4  
5  
6 Spectral data for (+)-**67**: mp 134–136 °C; <sup>1</sup>H NMR (300 MHz, DMSO-*d*<sub>6</sub>) δ 8.79 (s, 1H),  
7  
8 8.48 (m, 1H), 7.95 (s, 1H), 7.80 (m, 1H), 7.55 (m, 1H), 4.26 (m, 1H), 4.13 (s, 3H), 3.20–  
9  
10 2.30 (m, 7H), 2.00–1.51 (m, 9H), 1.10 (m, 3H); APCI MS *m/z* 599 [M+H]<sup>+</sup>; %CHNCl for  
11  
12 C<sub>23</sub>H<sub>28</sub>ClF<sub>5</sub>N<sub>6</sub>O<sub>3</sub>S•HCl•0.75H<sub>2</sub>O: calcd %C = 42.57, %H = 4.74, %N = 12.95, %Cl = 10.93;  
13  
14 found %C = 42.48, %H = 5.07, %N = 12.51, %Cl = 11.03; HPLC >99% (AUC), (Method B), *t*<sub>R</sub>  
15  
16 = 26.0 min; [α]<sub>D</sub><sup>20</sup> = +8.0° (*c* = 0.87, CH<sub>3</sub>OH); chiral HPLC >99% (AUC), (Method E), *t*<sub>R</sub> =  
17  
18 16.2 min.  
19  
20  
21  
22  
23  
24  
25  
26  
27

## 28 ■ ABBREVIATIONS USED

29  
30  
31 NMDA receptor, *N*-methyl-D-aspartate receptor; GlyT-1, glycine transporter-1; GlyT-2,  
32  
33 glycine transporter-2; iGluRs, ionotropic glutamate receptors; LTP, long-term  
34  
35 potentiation; LTD, long-term depression; GlyR, glycine receptor; CSF, cerebral spinal  
36  
37 fluid; SAR, structure-activity relationship; SPR, structure-property relationship; ADME,  
38  
39 Absorption, Distribution, Metabolism, Elimination; PPB, plasma protein binding; OCD,  
40  
41 obsessive compulsive disorder; SPA, scintillation proximity assay; HLM, human liver  
42  
43 microsomes; RLM, rat liver microsomes; mPFC, medial prefrontal cortex; *n*-BuLi, *n*-butyl  
44  
45 lithium; THF, tetrahydrofuran; DMF; *N,N*-dimethylformamide; DME, dimethoxyethane;  
46  
47 CH<sub>2</sub>Cl<sub>2</sub>, dichloromethane; CH<sub>3</sub>CN, acetonitrile; Et<sub>2</sub>AlCN, diethylaluminum cyanide; Ti(*i*-  
48  
49 PrO)<sub>4</sub>, titanium isopropoxide; LiAlH<sub>4</sub>, lithium aluminum hydride; PTSA, *para*-toluene  
50  
51 sulfonic acid; Et<sub>2</sub>O, diethyl ether; Boc<sub>2</sub>O, di-*tert*-butyl di-carbonate; TFA, trifluoroacetic  
52  
53  
54  
55  
56  
57  
58  
59  
60

1  
2  
3 acid; TMS, tetramethylsilane; LiHMDS, lithium bis(trimethylsilyl)amide;  $\text{NH}_4\text{HCO}_2$ ,  
4 ammonium formate; *i*-Pr<sub>2</sub>NEt, *N,N*-diisopropylethylamine; KCN, potassium cyanide; Et<sub>3</sub>N,  
5 triethylamine; HBTU, *O*-(benzotriazol-1-yl)-*N,N,N',N'*-tetramethyluronium  
6 hexafluorophosphate; EDCI•HCl, 1-ethyl-3-(3-dimethylaminopropyl)carbodiimide  
7 hydrochloride; HOBt, hydroxybenzotriazole; Gly, glycine; CYP, cytochrome P450;  
8 CYP2C9, cytochrome P450 2C9; CYP2C19, cytochrome P450 2C19; CYP2D6, cytochrome  
9 P450 2D6; CYP3A4, cytochrome P450 3A4; hERG, human ether-à-go-go-related gene; PK,  
10 pharmacokinetics; PD, pharmacodynamics; IV, intravenous; PO, oral; QD, once daily;  
11  $\text{CL}_{\text{int}}$ , intrinsic clearance; Cl, clearance; V<sub>ss</sub>, volume of distribution at steady state; AUC,  
12 area under the curve; %F, % bioavailability  
13  
14  
15  
16  
17  
18  
19  
20  
21  
22  
23  
24  
25  
26  
27

## 28 ■ ASSOCIATED CONTENT

### 29 ☉ Supporting Information

30  
31  
32 *In vivo* protocols. This data is available free of charge via the Internet at  
33  
34 <http://pubs.acs.org>.  
35  
36  
37  
38  
39  
40

## 41 ■ AUTHOR INFORMATION

### 42 Corresponding Authors

43  
44  
45  
46 \*Tel: 518-283-6451. E-mail: [christopher.cioffi@acphs.edu](mailto:christopher.cioffi@acphs.edu)

47  
48 \*Tel: 518-878-6470. E-mail: [shuang@consynance.com](mailto:shuang@consynance.com)

### 49 Current Affiliations

50  
51  
52  
53 &Albany College of Pharmacy and Health Sciences, 106 New Scotland Ave, Albany, NY  
54  
55  
56 12208, USA  
57  
58  
59  
60

1  
2  
3 ‡ConSynance Therapeutics, Inc., Schenectady, NY 12303, USA  
4

5  
6 †Pharma Inventor, Inc. 3800 Wesbrook Mall, Suite # 215 University of British Columbia  
7  
8 Campus, Vancouver, British Columbia Canada, V6S 2L9  
9

10  
11 #Hummingbird Bioscience, PTE, Ltd., 28 Seah Street, #03-01, 188384, Singapore  
12

13  
14 ×Brains On-Line, Inc., 7000 Shoreline Court, South San Francisco, CA 94080, USA  
15

16 †Fred Hutchinson Cancer Research Center, 1100 Fairview Ave N, Seattle, WA 98109, USA  
17

## 18 Notes

19  
20  
21 ConSynance Therapeutics, Inc. has executed an exclusive license with AMRI that covers  
22  
23 the intellectual property for all of the GlyT-1 inhibitors disclosed within.  
24  
25  
26  
27

## 28 ■ ACKNOWLEDGEMENTS

29  
30  
31 The authors acknowledge the following for conducting the various *in vivo* studies  
32  
33 described within: 1) Pharmaron Beijing, Co. Ltd., 6 Taihe Road, BDA, Beijing, 100176,  
34  
35 P.R. China for conducting rat PK studies, 2) Covance Laboratories Inc., 671 South  
36  
37 Meridian Road, Greenfield, Indiana 46140, US, for conducting rat *in vivo* CSF glycine  
38  
39 studies, 3) Maccine Pte Ltd., 10 Science Park Road, #01-05 The Alpha, Singapore Science  
40  
41 Park II, Singapore 117684 for conducting the in life portion of PK and CSF glycine studies  
42  
43 with cynomolgus monkeys, and 4) Brains On-Line LLC., South San Francisco, California,  
44  
45 US, for conducting rat microdialysis experiments.  
46  
47  
48  
49  
50

## 51 ■ REFERENCES

- 1  
2  
3 1) Aprison, M.H. The discovery of the neurotransmitter role of glycine. In: *Glycine*  
4  
5 *Neurotransmission*; Ottersen, O.P.; Storm Mathisen, J. Eds.; John Wiley and Sons:  
6  
7 Chichester, United Kingdom, 1990; pp 1–23.  
8  
9
- 10 2) Betz, H. Ligand-gated ion channels in the brain: the amino acid receptor  
11  
12 superfamily. *Neuron* **1990**, *5*, 383–392.  
13  
14
- 15 3) Betz, H.; Harvey, R. J.; Schloss, P. Structures, diversity and pharmacology of  
16  
17 glycine receptors and transporters. In: *Pharmacology of GABA and Glycine*  
18  
19 *Neurotransmission*. Möhler, H. Ed.; Springer-Verlag; New York, 2000; pp 375–  
20  
21 401.  
22  
23
- 24 4) (a) Wojciech, D.; Parsons, C. G. Glycine and *N*-methyl-D-aspartate receptors:  
25  
26 physiological significance and possible therapeutic applications. *Pharmacol. Rev.*  
27  
28 **1998**, *50*, 597–664; (b) Wolosker, H. NMDA receptor regulation by D-serine: new  
29  
30 findings and perspectives. *Mol. Neurobiol.* **2007**, *36*, 152–164.  
31  
32
- 33 5) (a) Bliss, T. V.; Collingridge, G. L. A synaptic model of memory: long-term  
34  
35 potentiation in the hippocampus. *Nature* **1993**, *361*, 31–39; (b) Bliss, T. V.;  
36  
37 Collingridge, G. L. Memories of NMDA receptors and LTP. *Trends Neurosci.* **1995**,  
38  
39 *18*, 54–56; (c) Traynelis, S. F.; Wollmuth, L. P.; McBain, C. J.; Menniti, F. S.; Vance,  
40  
41 K. M.; Ogden, K. K.; Hansen, K. B.; Yuan, H.; Myers, S. J.; Dingledine, R.; Danysz,  
42  
43 W. Glutamate receptor ion channels: structure, regulation, and function.  
44  
45 *Pharmacol. Rev.* **2010**, 405–496.  
46  
47
- 48 6) Eulenburg, V.; Arnsen, W.; Betz, H.; Gomeza, J. Glycine transporters: essential  
49  
50 regulators of neurotransmission. *Trends Biochem. Sci.* **2005**, *30*, 325–333.  
51  
52  
53  
54  
55  
56  
57  
58  
59  
60

- 1  
2  
3  
4 7) (a) Zafra, F.; Aragón, C.; Olivares, L.; Danbolt, N. C.; Giménez, C.; Strom-  
5  
6 Mathisenm J. Glycine transporters are differentially expressed among CNS cells.  
7  
8 *J. Neurosci.* **1995**, *15*, 3952–3969; (b) Zafra, F.; Gomeza, C.; Olivares, L.; Aragón,  
9  
10 C.; Giménez, C. Regional distribution and developmental variation of the glycine  
11  
12 transporters GLYT1 and GLYT2 in the rat CNS. *Eur. J. Neurosci.* **1995**, *7*, 1342–  
13  
14 1352; (c) Guastella, J.; Brecha, N.; Weigmann, C.; Lester, H. A.; Davidson, N.  
15  
16 Cloning, expression, and localization of a rat brain high-affinity glycine  
17  
18 transporter. *Proc. Natl. Acad. Sci. U.S.A.* **1992**, *89*, 7189–7193; (d) Liu, Q. R.;  
19  
20 Nelson, H.; Mandiyan, S.; Lopez-Corcuera, B.; Nelson, H.; Mandiyan, S.; Nelson,  
21  
22 N. Cloning and expression of a glycine transporter from mouse brain. *FEBS Lett.*  
23  
24 **1992**, *305*, 110–114; (e) Mallorga, P. J.; Williams, J. B.; Jacobson, M.; Marques,  
25  
26 R.; Chauhary, A.; Conn, P. J.; Pettibone, D. J.; Sur, C. Pharmacology and  
27  
28 expression analysis of glycine transporter GlyT1 with [<sup>3</sup>H]-(N-[3-(4'-  
29  
30 fluorophenyl)-3-(4'-phenylphenoxy)propyl])sarcosine. *Neuropharmacology* **2003**,  
31  
32 *45*, 585–593; (f) Zeng, Z.; O'Brien, J. A.; Lemaire, W.; O'Malley, S. S.; Miller, P. J.;  
33  
34 Zhao, Z.; Wallace, M. A.; Raab, C.; Lindsley, C. W.; Sur, C. Williams, D. L. A novel  
35  
36 radioligand for glycine transporter 1: characterization and use in  
37  
38 autoradiographic and in vivo brain occupancy studies. *Nuc. Med. Biol.* **2008**, *35*,  
39  
40 315–325; (g) Hamill, T. G.; Eng, W.; Jennings, A.; Lewis, R.; Thomas, S.; Wood, S.;  
41  
42 Street, L.; Wisnoski, D.; Wolkenberg, S.; Lindsley, C.; Sanabria-Bohorquez, S. M.;  
43  
44 Patel, S.; Riffel, K.; Ryan, C.; Cook, J.; Sur, C.; Burns, H. D.; Hargreaves, R. The  
45  
46 synthesis and preclinical evaluation in rhesus monkey of [<sup>18</sup>F]MK-6577 and  
47  
48  
49  
50  
51  
52  
53  
54  
55  
56  
57  
58  
59  
60



- 1  
2  
3 [11C]CMPyPB glycine transporter 1 positron emission tomography radiotracers.  
4  
5  
6 *Synapse* **2011**, *65*, 261–270; (h) Joshi, A. D.; Sanabria-Bohorquez, S. M.; Bormans,  
7  
8 G.; Koole, M.; De Hoon, J.; Van Hecken, A.; Depre, M.; De Lepeleire, I.; Van Laere,  
9  
10 K.; Sur, C. Hamill, T. G. Characterization of the novel GlyT1 PET tracer [<sup>18</sup>F]MK-  
11  
12 6577 in humans. *Synapse* **2015**, *69*, 33–40; (i) Borroni, E.; Zhou, Y.; Ostrowitzki,  
13  
14 S.; Alberti, D.; Kumar, A.; Hainzl, D.; Hartung, T.; Hilton, J.; Dannals, R. F.; Wong,  
15  
16 D. F. Pre-clinical characterization of [<sup>11</sup>C]RO5013853 as a novel radiotracer for  
17  
18 imaging of the glycine transporter type 1 by positron emission tomography.  
19  
20  
21  
22  
23 *NeuroImage* **2013**, *75*, 291–300.  
24  
25
- 26 8) (a) Pow, D. V.; Hendrickson, A. Distribution of the glycine transporter in  
27  
28 mammalian and non-mammalian retinae. *Vis. Neurosci.* **1999**, *16*, 231–239; (b)  
29  
30 Lee, S.; Zhong, Y.; Yang, X. Expression of glycine receptor and transporter on  
31  
32 bullfrog retinal Muller cells. *Neurosci. Lett.* **2005**, *387*, 75–79.  
33  
34  
35
- 36 9) Gomeza, J.; Hülsmann, S.; Ohno, K.; Eulenburg, V.; Szöke, K.; Richter, D. W.; Betz,  
37  
38 H. Inactivation of the glycine transporter 1 gene discloses a vital role of glial  
39  
40 glycine uptake in glycinergic inhibition. *Neuron* **2003**, *40*, 785–796.  
41  
42  
43
- 44 10) (a) Ceballos, B.; Gimenez, C.; Zafra, F. Localization of the GLYT1 glycine  
45  
46 transporter at glutamatergic synapses in the rat brain. *Cereb. Cortex* **2005**, *15*,  
47  
48 448–459; (b) Raiteri, L.; Raiteri, M. Functional ‘glial’ GLYT1 glycine transporters  
49  
50 expressed in neurons. *J. Neurochem.* **2010**, *114*, 647–653.  
51  
52
- 53 11) (a) Johnson, J. W.; Ascher, P. Glycine potentiates the NMDA response in cultured  
54  
55 mouse brain neurons. *Nature* **1987**, *325*, 529–531; (b) Bergeron, R.; Meyer, T.  
56  
57  
58  
59  
60

- 1  
2  
3 M.; Coyle, J. Y.; Greene, R. W. Modulation of *N*-methyl-D-aspartate receptor  
4 function by glycine transport. *Proc. Natl. Acad. Sci. U. S. A.* **1998**, *95*, 15730–  
5  
6 15374.  
7  
8  
9  
10  
11 12) Hitchcock, S.; Amagadzie, A.; Qian, W.; Xia, X.; Harried, Scott S. Piperazineacetic  
12 acid derivatives as glycine transporter-1 inhibitors and their preparation,  
13 pharmaceutical compositions and use in the treatment of schizophrenia.  
14  
15 WO 2008002583 A1, June 26, **2007**.  
16  
17  
18  
19  
20  
21 21) Atkinson, B. N.; Bell, S. C.; De Vivo, M.; Kowalski, L. R.; Lechner, S. M.; Ognyanov,  
22  
23 V. I.; Tham, C.-S.; Tsai, C.; Jia, J.; Ashton, D.; Klitenick, M. A. ALX 5407: a potent,  
24  
25 selective inhibitor of the hGlyT1 glycine transporter. *Mol. Pharmacol.* **2001**, *60*,  
26  
27 1414-1420.  
28  
29  
30  
31 31) Molander, A.; Soderpalm, B. Glycine reuptake inhibitors for treatment of drug  
32 dependence. WO 2006075011 A2, January 11, **2006**.  
33  
34  
35  
36 36) Jolidon, S.; Narquizian, R.; Nettekoven, M. H.; Norcross, R. D.; Pinard, E.; Stalder,  
37  
38 H. Preparation of alkoxybenzoylpiperazines as inhibitors of glycine transporter 1  
39  
40 (GlyT-1). WO 2005014563 A1, August 2, **2004**.  
41  
42  
43  
44 44) Michardy, S. F.; Lowe, J. A., III. Preparation of bicyclic [3.1.0] heteroaryl amides  
45  
46 as type 1 glycine transport inhibitors. WO 2006106425 A1, March 27, **2006**.  
47  
48  
49 49) Dargazanli, G.; Estenne Bouhtou, G.; Magat, P.; Marabout, B.; Medaisko, F.;  
50  
51 Roger, P.; Sevrin, M.; Veronique, C. Preparation of *N*-[phenyl(piperidin-2-yl)  
52  
53 methyl]benzamides as specific inhibitors of glycine transporters glyt1 and/or  
54  
55 glyt2. FR 2838739 A1, April 19, **2002**.  
56  
57  
58  
59  
60

- 1  
2  
3  
4  
5  
6  
7  
8  
9  
10  
11  
12  
13  
14  
15  
16  
17  
18  
19  
20  
21  
22  
23  
24  
25  
26  
27  
28  
29  
30  
31  
32  
33  
34  
35  
36  
37  
38  
39  
40  
41  
42  
43  
44  
45  
46  
47  
48  
49  
50  
51  
52  
53  
54  
55  
56  
57  
58  
59  
60
- 18) Blackaby, W. P.; Castro P., Jose L.; Lewis, Richard T.; Naylor, E. M.; Street, L. J. Preparation of cyclohexanesulfonyl derivatives as GlyT1 inhibitors to treat schizophrenia. US 20060276655 A1, June 5, **2006**.
- 19) Bradley, D. M.; Branch, C. L.; Chan, W. N.; Coulton, S.; Gilpin, M. L.; Harris, A. J.; Jaxa-Chamiec, A. A.; Lai, Justine Y. Q.; Marshall, H. R.; Macritchie, J. A.; Nash, D. J.; Porter, R. A.; Spada, S.; Thewlis, K. M.; Ward, S. E. Preparation of N-(phenylmethyl) benzamides as glycine transport inhibitors. WO 2006067423 A1, December 21, **2005**.
- 20) (a) Lewis, D. A.; Moghaddam, B. Cognitive dysfunction in schizophrenia: convergence of gamma-aminobutyric acid and glutamate alterations. *Arch. Neurol.* **2006**, *63*, 1372–1376; (b) Houman, H.; Moghaddam, B. NMDA receptor hypofunction produces opposite effects on prefrontal cortex interneurons and pyramidal neurons. *J. Neurosci.* **2007**, *27*, 11496–11500; (c) Lewis, D. A.; Curley, A. A.; Glausier, J. R.; Volk, D. W. Cortical parvalbumin interneurons and cognitive dysfunction in schizophrenia. *Trends Neurosci.* **2012**, *35*, 57–67; (d) Lahti, A. C.; Koffel, B.; LaPorte, D.; Tamminga, C. A. Subanesthetic doses of ketamine stimulate psychosis in schizophrenia. *Neuropsychopharmacology* **1995**, *13*, 9–19; (e) Umbricht, D.; Schmid, L.; Koller, R.; Vollenweider, F. X.; Hell, D.; Javitt, D. C. Ketamine-induced deficits in auditory and visual context-dependent processing in healthy volunteers: implications for models of cognitive deficits in schizophrenia. *Arch. Gen. Psychiatry* **2000**, *57*, 1139–1147; (f) Javitt, D. C.; Zukin, S. R. Recent advances in the phencyclidine model of schizophrenia. *Am. J.*

- 1  
2  
3 *Psychiatry* **1991**, *148*, 1301–1308; (g) Kirov, G.; O'Donovan, M. C.; Owen, M. J.  
4  
5 Finding schizophrenia genes. *J. Clin. Invest.* **2005**, *115*, 1440–1448; (h) Allen, N.  
6  
7 C.; Bagade, S.; McQueen, M. B.; Ioannidis, J. P.; Kavvoura, F. K.; Khoury, M. J.;  
8  
9 Tanzi, R. E.; Bertram, L. Systematic meta-analyses and field synopsis of genetic  
10  
11 association studies in schizophrenia: The SzGene database. *Nat. Genet.* **2008**, *40*,  
12  
13 827–834; (i) Deutsch, S. I.; Mastropaolo, J.; Schwartz, B. L.; Rosse, R. B.; Morisha,  
14  
15 J. M. A “glutamate hypothesis” of schizophrenia. *Clin. Neuropharm.* **1989**, *12*, 1–  
16  
17 13; (j) Olney, J. W.; Farber, N. B. Glutamate receptor dysfunction and  
18  
19 schizophrenia. *Arch. Gen. Psychiatry* **1995**, *52*, 998–1007; (k) Tamminga, C. A.  
20  
21 Schizophrenia and glutamatergic transmission. *Crit. Rev. Neurobiol.* **1998**, *12*, 21–  
22  
23 36; (l) Moghaddam, B. Bringing order to the glutamate chaos in schizophrenia.  
24  
25 *Neuron* **2003**, *40*, 881–884; (m) Javitt, D. C. Glutamatergic theories of  
26  
27 schizophrenia. *Isr. J. Psychiatry Relat. Sci.* **2010**, *47*, 4–16.  
28  
29  
30  
31  
32  
33  
34  
35  
36 21) (a) Cioffi, C. L.; Guzzo, P. R. Inhibitors of glycine transporter-1: potential  
37  
38 therapeutics for the treatment of CNS disorders. *Curr. Top. Med. Chem.* [Online  
39  
40 early access]. DOI: 10.2174/1568026616666160405113340. Published Online:  
41  
42 April 6, 2016; (b) Porter, R. A.; Dawson, L. A. GlyT-1 inhibitors: from hits to  
43  
44 clinical candidates. *Top. Med. Chem.* **2015**, *13*, 51–100; (c) Harsing, L. G. An  
45  
46 overview on GlyT-1 inhibitors under evaluation for the treatment of  
47  
48 schizophrenia. *Drugs Future* **2013**, *38*, 545–558; (d) Hashimoto, K. Glycine  
49  
50 transporter inhibitors for the treatment of schizophrenia. *Open Med. Chem. J.*  
51  
52 **2010**, *4*, 10–19; (e) Thomsen, C. Glycine transporter inhibitors as novel  
53  
54  
55  
56  
57  
58  
59  
60

- 1  
2  
3 antipsychotics. *Drug Discovery Today Ther. Strateg.* **2006**, *3*, 539–545; (f)  
4  
5  
6 Harsing, L. G.; Juranyi, Z.; Gacsalyi, I.; Tapolcsanyi, P.; Czompa, A.; Matyus, P.  
7  
8 Glycine transporter type-1 and its inhibitors. *Curr. Med. Chem.* **2006**, *13*, 1017–  
9  
10 1044; (g) Hashimoto, K. Glycine transporter inhibitors as therapeutic agents for  
11  
12 schizophrenia. *Recent Pat. CNS Drug Discovery* **2006**, *1*, 43–53; (h) Kinney, G. G.;  
13  
14 Sur, C. Glycine site modulators and glycine transporter-1 inhibitors as novel  
15  
16 therapeutic targets for the treatment of schizophrenia. *Curr. Neuropharmacol.*  
17  
18 **2005**, *3*, 35–43; (i) Cioffi, C. L.; Liu, S.; Wolf, M.A. Recent developments in glycine  
19  
20 transporter-1 inhibitors. *Annual Reports in Medicinal Chemistry*; Academic Press,  
21  
22 Cambridge, MA, 2010, Vol. 45, Chapter 2, pp 19–35.  
23  
24  
25  
26  
27  
28 22) (a) Javitt, D. C.; Zylberman, I.; Zukin, S. R.; Heresco-Levy, U.; Lindenmayer, J. P.  
29  
30 Amelioration of negative symptoms in schizophrenia by glycine. *Am. J. Psychiatry*  
31  
32 **1994**, *151*, 1234–1236; (b) Heresco-Levy, U.; Javitt, D. C.; Ermilov, M.; Mordel, C.;  
33  
34 Silipo, G.; Lichtenstein, M. Efficacy of high-dose glycine in the treatment of  
35  
36 enduring negative symptoms of schizophrenia, *Arch. Gen. Psychiatry* **1999**, *56*,  
37  
38 29–36; (c) Heresco-Levy, U.; Ermilov, M.; Lichtenberg, P.; Bar, G.; Javitt, D. C.  
39  
40 High-dose glycine added to olanzapine and risperidone for the treatment of  
41  
42 schizophrenia. *Biol. Psychiatry* **2004**, *55*, 165–171; (d) Heresco-Levy, U.; Javitt, D.  
43  
44 C.; Ermilov, M.; Mordel, C.; Horowitz, A.; Kelly, D. Double-blind, placebo-  
45  
46 controlled, crossover trial of glycine adjuvant therapy for treatment-resistant  
47  
48 schizophrenia. *Br. J. Psychiatry* **1996**, *169*, 610–617; (e) Tsai, G.; Lane, H.; Young,  
49  
50 P. J.; Lane, N.; Chong, M. Glycine transporter 1 inhibitor, N-methylglycine  
51  
52  
53  
54  
55  
56  
57  
58  
59  
60

1  
2  
3 (sarcosine) added to antipsychotics for the treatment of schizophrenia. *Biol.*  
4  
5  
6 *Psychiatry* **2004**, *155*, 452–456; (f) Lane, H.; Huang, C.; Wu, P.; Liu, Y.; Lin, P.;  
7  
8 Chen, P.; Tsai, G. Glycine transporter 1 inhibitor, N-methylglycine (sarcosine),  
9  
10 added to clozapine for the treatment of schizophrenia. *Biol. Psychiatry* **2006**, *60*,  
11  
12 645–649; (g) Umbricht, D.; Alberati, D.; Martin-Facklam, M.; Borroni, E.; Youssef,  
13  
14 E. A.; Ostland, M.; Wallace, T. L.; Knoflach, F.; Dorflinger, E.; Wettstein, J. G.;  
15  
16 Bausch, A.; Garibaldi, G.; Santarelli, L. Effect of bitopertin, a glycine reuptake  
17  
18 inhibitor, on negative symptoms of schizophrenia. A randomized, double-blind,  
19  
20 proof-of-concept study. *JAMA Psychiatry* **2014**, *71*, 637–646.

21  
22  
23  
24  
25  
26 23) Bitopertin disappoints as schizophrenia treatment.  
27  
28 <http://www.medscape.com/viewarticle/826805> (accessed June 15, 2016).  
29

30  
31 24) (a) Huang, C-C.; Wei, I-H.; Huang, C-L.; Chen, K-T.; Tsai, M-H.; Tsai, P.; Tun, R.;  
32  
33 Huang, K-H.; Chang, Y-C.; Lane, H-Y.; Tsai, G. E. Inhibition of glycine transporter-1  
34  
35 as a novel mechanism for the treatment of depression. *Biol. Psychiatry* **2013**, *74*,  
36  
37 734–741; (b) Mathew, S. J. Glycine transporter-1 inhibitors: a new class of  
38  
39 antidepressant? *Biol. Psychiatry* **2013**, *74*, 710–711; (c) Huang, C.-C.; Wei, I.-H.;  
40  
41 Huang, C.-L.; Chen, K.-T.; Tsai, M.-H.; Tsai, P.; Tun, R.; Huang, K.-H.; Chang, Y.-C.;  
42  
43 Lane, H.-Y.; Tsai, G. E. Inhibition of glycine transporter-1 as a novel mechanism for  
44  
45 the treatment of depression. *Biol. Psychiatry* **2013**, *74*, 734–741; (d) Depoortère,  
46  
47 R.; Dargazanli, G.; Estenne-Bouhtou, G.; Coste, A.; Lanneau, C.; Desvignes, C.;  
48  
49 Poncelet, M.; Heulme, M.; Santucci, V.; Decobert, M.; Cudennec, A.; Voltz, C.;  
50  
51 Bouley, D.; Terranova, J. P.; Stemmelin, J.; Roger, P.; Marabout, B.; Sevrin, M.;  
52  
53  
54  
55  
56  
57  
58  
59  
60

1  
2  
3 Vigé, X.; Biton, B.; Steinberg, R.; Francon, D.; Alonso, R.; Avenet, P.; Oury-Donat,  
4  
5  
6 F.; Perrault, G.; Griebel, G.; George, P.; Soubrié, P.; Scatton, B. Neurochemical,  
7  
8 electrophysiological and pharmacological profiles of the selective inhibitor of the  
9  
10 glycine transporter-1 SSR504734, a potential new type of antipsychotic.  
11  
12 *Neuropsychopharmacology* **2005**, *30*, 1963–1985; (e) Bouley, D.; Pichat, P.;  
13  
14 Dargazanli, G.; Estenne-Bouhtou, G.; Terranova, J. P.; Rogacki, N.; Stemmelin, J.;  
15  
16 Coste, A.; Lanneau, C.; Desvignes, C.; Cohen, C.; Alonso, R.; Vigé, X.; Biton, B.;  
17  
18 Steinberg, R.; Sevrin, M.; Oury-Donat, F.; George, P.; Bergis, O.; Griebel, G.;  
19  
20 Avenet, P.; Scatton, B. Characterization of SSR103800, a selective inhibitor of the  
21  
22 glycine transporter-1 in models predictive of therapeutic activity in  
23  
24 schizophrenia. *Pharmacol. Biochem. Behav.* **2008**, *91*, 47–58.  
25  
26  
27  
28  
29

30  
31 25) Clinicaltrials.gov. <https://www.clinicaltrials.gov/ct2/show/NCT01674361>

32  
33 (Accessed June 8, 2016).  
34  
35

36 26) Harvey, R. J.; Yee, B. K. Glycine transporters as novel therapeutic targets in  
37  
38 schizophrenia, alcohol dependence and pain. *Nat. Rev. Drug Discovery* **2013**, *12*,  
39  
40 866–885.  
41  
42

43 27) (a) Molander, A.; Lido, H. H.; Lof, E.; Ericson, M.; Soderpalm, B. The glycine  
44  
45 reuptake inhibitor Org 25935 decreases ethanol intake and preference in male  
46  
47 Wistar rats. *Alcohol Alcohol.* **2007**, *42*, 11–18; (b) Vengeliene, V.; Leonardi-  
48  
49 Essman, F.; Sommer, W. H.; Marstone, H. M.; Spanagel, R. Glycine transporter-1  
50  
51 blockade leads to persistently reduced relapse-like alcohol drinking in rats. *Biol.*  
52  
53 *Psychiatry* **2010**, *68*, 704–711; (c) Lido, H. H.; Marston, H.; Ericson, M.;  
54  
55  
56  
57  
58  
59  
60

1  
2  
3 Soderpalm, B. The glycine reuptake inhibitor Org24598 and acamprosate reduce  
4 ethanol intake in the rat; tolerance development to acamprosate but not to  
5  
6  
7  
8 Org24598. *Addict. Biol.* **2011**, *17*, 897–907; (d) Lido, H. H.; Ericson, M.; Marston,  
9  
10  
11 H.; Soderpalm, B. A role for accumbal glycine receptors in modulation of  
12  
13  
14 dopamine release by the glycine transporter-1 inhibitor Org25935. *Front.*  
15  
16  
17 *Psychiatry* **2011**, *2*, 1–9; (e) de Bejczy, A.; Nations, K. R.; Szegedi, A.; Schoemaker,  
18  
19  
20 J.; Ruwe, F.; Soderpalm, B. Efficacy and safety of the glycine transporter-1  
21  
22  
23 inhibitor Org 25935 for the prevention of relapse in alcohol-dependent patients:  
24  
25  
26 a randomized, double-blind, placebo-controlled trial. *Alcohol Clin. Exp. Res.* **2014**,  
27  
28  
29 *38*, 2427–2435; (f) Uslaner, J. M.; Drott, J. T.; Sharik, S. S.; Theberge, C. R.; Sur, C.;  
30  
31  
32 Zeng, Z.; Williams, D. L.; Hutson, P. H. Inhibition of glycine transporter 1  
33  
34  
35 attenuates nicotine-but not food-induced cue-potentiated reinstatement for a  
36  
37  
38 response previously paired with sucrose. *Behav. Brain. Res.* **2010**, *207*, 37–43; (g)  
39  
40  
41 Cervo, L.; Di Clemente, A.; Orru, A.; Moro, F.; Cassina, C.; Pich, E. M.; Corsi, M.;  
42  
43  
44 Gozzi, A.; Bifone, A. Inhibition of glycine transporter-1 reduces cue-induced  
45  
46  
47 nicotine-seeking, but does not promote extinction of conditioned nicotine cue  
48  
49  
50 responding in the rat. *Addict. Biol.* **2013**, *18*, 800–811; (h) Nic Dhonnchadha, B.  
51  
52  
53 A.; Pinard, E.; Alberti, D.; Wettstein, J. G.; Spealman, R. D.; Kantak, K. M.  
54  
55  
56 Inhibiting glycine transporter-1 facilitates cocaine-cue extinction and attenuates  
57  
58  
59 reacquisition of cocaine-seeking behavior. *Drug Alcohol Depend.* **2012**, 119–126.  
60

28) (a) Barthel, F.; Urban, A.; Sclosser, L.; Eulenburg, V.; Wederhausen, R.;  
Brandenburger, T.; Aragon, C.; Bauer, I.; Hermanns, H. Long-term application of



1  
2  
3 glycine transporter inhibitors acts antineuropathic and modulates spinal *N*-  
4 methyl-D-aspartate receptor subunit NR-1 expression in rats. *Anesthesiology*  
5  
6 **2014**, *121*, 160–169; (b) Morita, K.; Motoyama, N.; Kitayama, T.; Morioka, N.;  
7  
8 Kifune, K.; Dohi, T. Spinal Antiallodynia action of glycine transporter inhibitors in  
9  
10 neuropathic pain models in mice. *J. Pharm. Exp. Ther.* **2008**, *326*, 633–645; (c)  
11  
12 Gilron, I.; Dickenson, A. H. Emerging drugs for neuropathic pain *Expert Opin.*  
13  
14 *Emerging Drugs* **2014**, *19*, 329–341; (d) Vandenberg, R. J.; Ryan, R. M.; Carland, J.  
15  
16 E.; Imlach, W. L.; Christie, M. J. Glycine transport inhibitors for the treatment of  
17  
18 pain. *Trends Pharm. Sci.* **2014**, *35*, 423–430; (e) Centeno, M. V.; Mutso, A.;  
19  
20 Millecamps, M.; Apkarian, A. V. Prefrontal cortex and spinal cord mediated anti-  
21  
22 neuropathy and analgesia induces by sarcosine, a glycine-T1 transporter  
23  
24 inhibitor. *Pain* **2009**, *145*, 176–183; (f) Dohi, T.; Morita, K.; Kitayama, T.;  
25  
26 Motoyama, N.; Morioka, N. Glycine transporter inhibitors as a novel drug  
27  
28 discovery strategy for neuropathic pain. *Pharmacol. Ther.* **2009**, *123*, 54–79; (g)  
29  
30 Tanabe, M.; Takasu, K.; Yamaguchi, S.; Kodama, D.; Ono, H. Glycine transporter  
31  
32 inhibitors as a potential therapeutic strategy for chronic pain with memory  
33  
34 impairment. *Anesthesiology* **2008**, *108*, 929–937.

- 35  
36  
37  
38  
39  
40  
41  
42  
43  
44  
45  
46 29) Komatsu, H.; Furuya, Y.; Sawada, K.; Asada, T. Involvement of the strychnine-  
47  
48 sensitive glycine receptor in the anxiolytic effects of GlyT-1 inhibitors on  
49  
50 maternal separation-induced ultrasonic vocalization in rat pups. *Eur. J.*  
51  
52 *Pharmacol.* **2015**, *746*, 252–257.  
53  
54  
55  
56  
57  
58  
59  
60

- 1  
2  
3  
4  
5  
6  
7  
8  
9  
10  
11  
12  
13  
14  
15  
16  
17  
18  
19  
20  
21  
22  
23  
24  
25  
26  
27  
28  
29  
30  
31  
32  
33  
34  
35  
36  
37  
38  
39  
40  
41  
42  
43  
44  
45  
46  
47  
48  
49  
50  
51  
52  
53  
54  
55  
56  
57  
58  
59  
60
- 30) (a) Shen, H.-Y.; van Vliet, E. A.; Bright, K.-A.; Hanthorn, M.; Lyte, N. K.; Gorter, J.; Aronica, E.; Boison, D. Glycine transporter 1 is a target for the treatment of epilepsy. *Neuropharmacology* **2015**, *99*, 554–565; (b) Socala, K.; Nieoczym, D.; Runfeldt, C.; Wlaz, P. Effects of sarcosine, a glycine transport type 1 inhibitor, in two mouse seizure models. *Pharmacol. Rep.* **2010**, *62*, 392–397; (c) Kalinichev, M.; Starr, K. R.; Teague, S.; Bradford, A. M.; Porter, R. A.; Herdon, H. J. Glycine transporter 1 (GlyT1) inhibitors exhibit anticonvulsant properties in the rat maximal electroshock threshold (MEST) test. *Brain Res.* **2010**, *1331*, 105–113; (d) Shen, H.-Y.; van Vliet, E. A.; Bright, K.-A.; Hanthorn, M.; Lytle, N. K.; Gorter, J.; Aronica, E.; Boison, D. Glycine transporter 1 is a target for the treatment of epilepsy. *Neuropharmacology* **2015**, *99*, 554–565.
- 31) Pinto, M. C. X.; de Assis Lima, I. V.; da Costa, F. L. P.; Rosa, D. V.; Mendes-Goulart, V. A.; Resende, R. R.; Romano-Silva, M. A.; de Oiverira, A. C. P.; Gomez, M. V.; Gomez, R. S. Glycine transporters type 1 inhibitor promotes brain preconditioning against NMDA-induced excitotoxicity. *Neuropharmacology* **2015**, *89*, 274–281.
- 32) Burket, J. A.; Benson, A. D.; Green, T. L.; Rook, J. M.; Lindsley, C. W.; Conn, P. J.; Deutsch, S. I. Effects of VU0410120, a novel GlyT1 inhibitor, on measures of sociability, cognition and stereotypic behaviors in a mouse model of autism. *Prog. Neuro-Psychopharmacol. Biol. Psychiatry* **2015**, *3*, 10–17.
- 33) (a) Heresco-Levy, U.; Shoham, S.; Javitt, D. C. Glycine site agonists of the N-methyl-D-aspartate receptor and Parkinson's disease: a hypothesis. *Mov. Disord.*

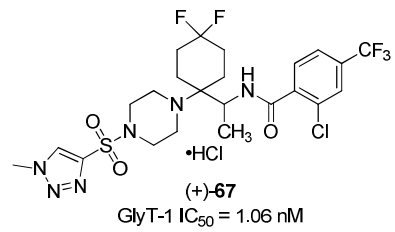
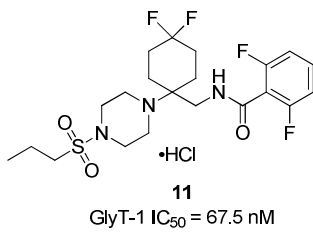
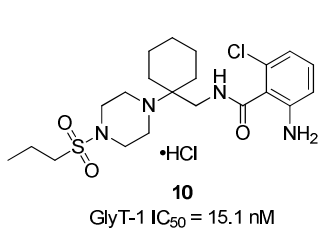
- 1  
2  
3 **2013**, 28, 419–424; (b) Tsai, C-H.; Huang, H-C; Liu, B. L.; Li C. I.; Lu, M. K.; Chen, S.;  
4  
5  
6 Tsai, M. C.; Yang, Y. W.; Lane, H. Y. Activation of *N*-methyl-D-aspartate receptor  
7  
8 glycine site temporally ameliorates neuropsychiatric symptoms of Parkinson's  
9  
10 disease with dementia. *Psychiatry Clin. Neurosci.* **2014**, 68, 692–700; (c) Schmitz,  
11  
12 Y.; Castagna, C.; Mrejeru, A. Lizardi-Ortiz, J. E.; Lindsley, C. W.; Sulzer, D. Glycine  
13  
14 transporter-1 inhibition promotes striatal axon sprouting via NMDA receptors in  
15  
16 dopamine neurons. *J. Neurosci.* **2013**, 33, 16778–16789.  
17  
18  
19  
20  
21 34) Hanuska, A.; Szenasi, G.; Albert, M.; Koles, L.; Varga, A.; Szabo, A.; Matyus, P.;  
22  
23 Harsing Jr., L. G. Some operational characteristics of glycine release in rat retina:  
24  
25 the role of reverse mode operation of glycine transporter type-1 (GlyT-1) in  
26  
27 ischemic conditions. *Neurochem. Res.* **2016**, 41, 73–85.  
28  
29  
30  
31 35) Alberati, D.; Koerner, A.; Pinard, E.; Winter, M. GLYT1 inhibitors for the use in the  
32  
33 treatment of hematological disorders. WO 2015/165842 A1, November 5, **2015**.  
34  
35  
36 36) Cioffi, C. L.; Wolf, M. A.; Guzzo, P. R.; Sadalpure, K.; Parthasarathy, V.; Dethe, D.;  
37  
38 Maeng, J.-H.; Carulli, E.; Loong, D. T.; Fang, X.; Hu, M.; Gupta, P.; Chung, M.; Bai,  
39  
40 M.; Moore, N.; Luche, M.; Khmel'nitski, Y.; Love, P. L.; Watson, M. A.; Mhyre, A.  
41  
42 J.; Liu, S. Design, synthesis, and SAR of *N*-((1-(4-(propylsulfonyl)piperazine-1-  
43  
44 yl)cycloalkyl)methyl)benzamide inhibitors of glycine transporter-1. *Bioorg. Med.*  
45  
46 *Chem. Lett.* **2013**, 23, 1257–1261.  
47  
48  
49  
50  
51 37) Cioffi, C. L.; Wolf, M. A.; Guzzo, P. R.; Liu, S.; Sadalpure, K.; Parthasarathy, V.;  
52  
53 Maeng, J.-H.; Glycine transporter-1 inhibitors, methods of making them, and  
54  
55 uses thereof. US 9045445 B2, June 5, **2015**.  
56  
57  
58  
59  
60

- 1  
2  
3 38) Coulton, S.; Gilpin, M. L.; Porter, R. A. Glycine transporter inhibiting compounds  
4  
5 and uses in medicine. PCT Int. Appl. WO 2007/147839 A1, December 27, **2007**.  
6  
7
- 8 39) Thomson, J. L.; Blackaby, W. P.; Jennings, A, S. R.; Goodacre, S. C.; Pike, A.;  
9  
10 Thomas, S.; Brown, T. A.; Smith, A.; Pillai, G.; Street, L. J.; Lewis, R. T.  
11  
12 Optimisation of a series of potent, selective and orally bioavailable GlyT1  
13  
14 inhibitors. *Bioorg. Med. Chem. Lett.* **2009**, *19*, 2235–2239.  
15  
16
- 17 40) (a) Walter, M. W.; Hoffman, B. J.; Gordon, K.; Johnson, K.; Love, P.; Jones, M.;  
18  
19 Man, T.; Phebus, L.; Reel, J. K.; Rudyk, H. C.; Shannon, H.; Svensson, K.; Yu, H.;  
20  
21 Valli, M. J.; Porter, W. J. Discovery and SAR studies of novel GlyT1 inhibitors.  
22  
23 *Bioorg. Med. Chem. Lett.* **2007**, *17*, 5233–5238; (b) Lowe, J. A.; Hou, X.; Schmidt,  
24  
25 C.; Tingley, F. D.; McHardy, S.; Kalman, M.; DeNinno, S.; Sanner, M.; Ward, K.;  
26  
27 Lebel, L.; Tunucci, D.; Valentine, J. the discovery of a structurally novel class of  
28  
29 inhibitors of the type 1 glycine transporter. *Bioorg. Med. Chem. Lett.* **2009**, *19*,  
30  
31 2974–2976.  
32  
33
- 34 41) (a) Lin, J. H.; CSF as a surrogate for assessing CNS exposure: and industrial  
35  
36 perspective. *Curr. Drug Met.* **2008**, *9*, 45–59; (b) Schaffer, C. L. Defining  
37  
38 neuropharmacokinetic parameters in CNS drug discovery to determine cross-  
39  
40 species pharmacologic exposure-response relationships. *Annual Reports in*  
41  
42 *Medicinal Chemistry*; Academic Press, Cambridge, MA, 2010, Vol. 45, Chapter 4,  
43  
44 pp 55–70; (c) Rankovic, Z. CNS drug design: balancing physicochemical properties  
45  
46 for optimal brain exposure. *J. Med. Chem.* **2015**, *58*, 2584–2608.  
47  
48  
49  
50  
51  
52  
53  
54  
55  
56  
57  
58  
59  
60

- 1  
2  
3  
4  
5  
6  
7  
8  
9  
10  
11  
12  
13  
14  
15  
16  
17  
18  
19  
20  
21  
22  
23  
24  
25  
26  
27  
28  
29  
30  
31  
32  
33  
34  
35  
36  
37  
38  
39  
40  
41  
42  
43  
44  
45  
46  
47  
48  
49  
50  
51  
52  
53  
54  
55  
56  
57  
58  
59  
60
- 42) Kopec, K.; Flood, D. G.; Gasiior, M.; McKenna, B. A. W.; Zuvich, E.; Schreiber, J.; Salvino, J. M.; Durkin, J. T.; Ator, M. A.; Marino, M. J. Glycine transporter inhibitors with reduced residence time increase prepulse inhibition without inducing hyperlocomotion in DBA/2 mice. *Biochem. Pharmacol.* **2010**, *80*, 1407–1417.
- 43) Mezler, M.; Hornberger, W.; Mueller, R.; Schmidt, M.; Amberg, W.; Braje, W.; Ochse, M.; Scoemaker, H.; Behl, B. Inhibitors of GlyT1 affect glycine transport via discrete binding sites. *Mol. Pharmacol.* **2008**, *74*, 1705–1715.
- 44) Perry, K. W.; Falcone, J. F.; Fell, M. J.; Ryder, J. W.; Yu, H.; Love, P. L.; Katner, J.; Gordon, K. D.; Wade, M. R.; Man, T.; Nomikos, G. G.; Phebus, L. A.; Cauvin, A. J.; Johnson, K. W.; Jones, C. K.; Hoffmann, B. J.; Sandusky, G. E.; Walter, M. W.; Porter, W. J.; Yang, L.; Merchant, K. M.; Shannon, H. E.; Svensson, K. A. Neurochemical and behavioral profiling of the selective GlyT1 inhibitors ALX5407 and LY2365109 indicate a preferential action in caudal vs. cortical brain areas. *Neuropharmacology* **2008**, *55*, 743–754.

1  
2  
3  
4  
5  
6  
7  
8  
9  
10  
11  
12  
13  
14  
15  
16  
17  
18  
19  
20  
21  
22  
23  
24  
25  
26  
27  
28  
29  
30  
31  
32  
33  
34  
35  
36  
37  
38  
39  
40  
41  
42  
43  
44  
45  
46  
47  
48  
49  
50  
51  
52  
53  
54  
55  
56  
57  
58  
59  
60

### Table of Content Graphic



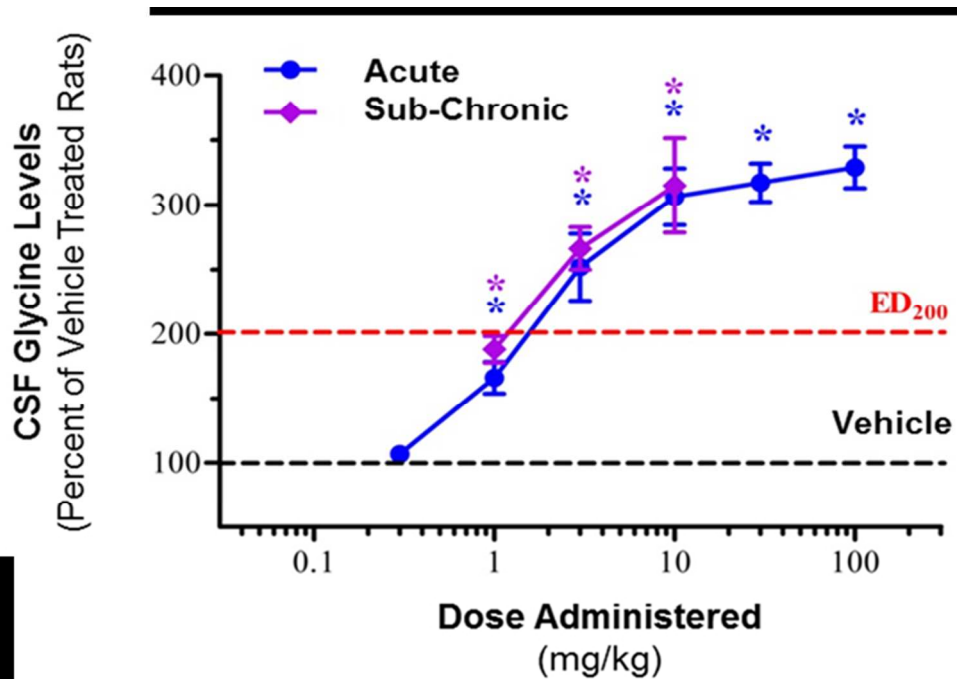


Figure 3

137x95mm (150 x 150 DPI)

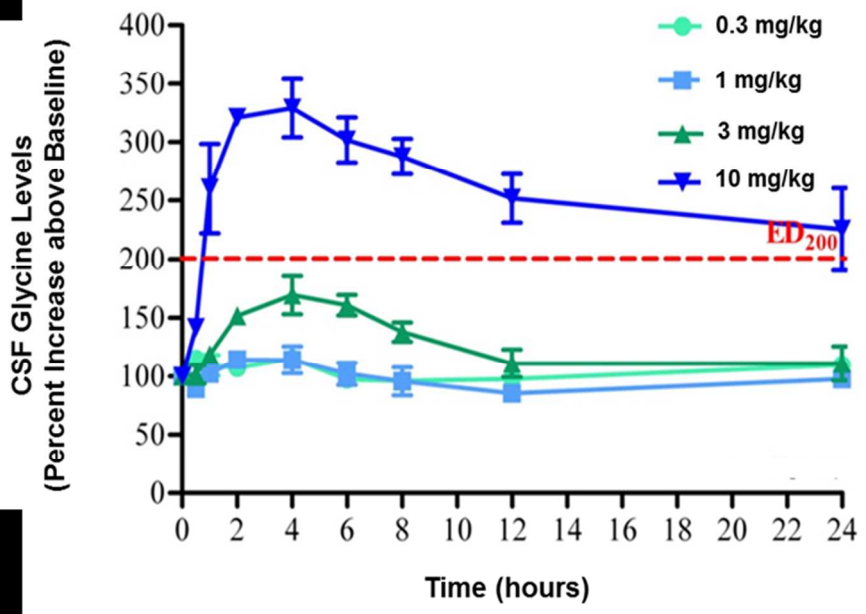


Figure 4

137x93mm (150 x 150 DPI)



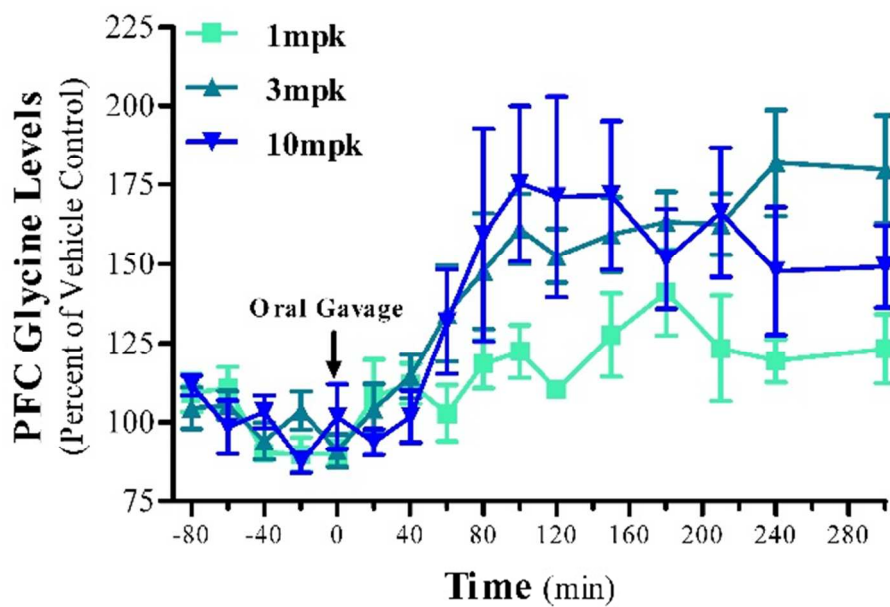


Figure 5

84x57mm (220 x 220 DPI)

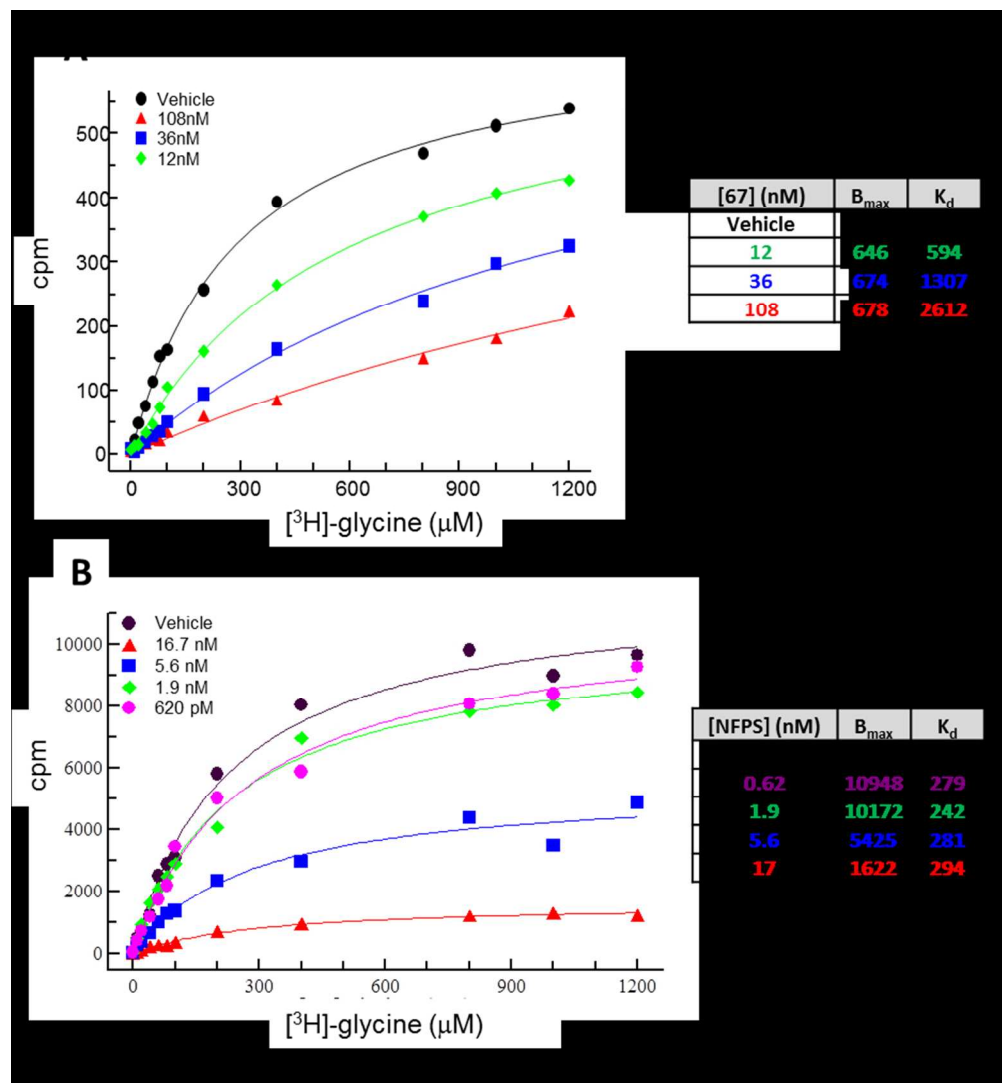


Figure 6

158x171mm (150 x 150 DPI)